Water−Splitting Chemistry of Photosystem II

ARTICLE *in* CHEMICAL REVIEWS · DECEMBER 2006

Impact Factor: 46.57 · DOI: 10.1021/cr0204294 · Source: PubMed

CHEMICAL REVIEWS

Volume 106, Number 11

Water-Splitting Chemistry of Photosystem II

James P. McEvoy† and Gary W. Brudvig*

Department of Chemistry, Yale University, P.O. Box 208107, New Haven, Connecticut 06520-8107

Received January 30, 2006

Contents

* Telephone 203 432 5202; fax 203 432 6144; e-mail gary.brudvig@yale.edu.
† Present address: Department of Chemistry, Regis University, Mail Stop D4, 3333 Regis Blvd., Denver, CO 80221.

1. Introduction

Life on earth is almost entirely solar-powered. We can get some idea of the enormous quantity of energy received from the sun by noting that during daylight hours, the sun provides several thousand times more power to the surface of the U.S.A. than is produced by all of the nation's electrical power stations.[1,2] Around 50% of the radiation that reaches the earth's surface, roughly the visible region, is of a frequency useful to photosynthetic organisms. Oxygenic photosynthetic organisms convert this radiation into chemical energy, in the form of carbohydrate and dioxygen, at an optimal efficiency of something like 25%.[3] These products together sustain the rest of aerobic life, with carbohydrate acting as a source of high-energy electrons and dioxygen providing a lower-energy destination for these electrons.

The overall equation of oxygenic photosynthesis is given in eq 1, where (CH_2O) represents carbohydrate:

$$CO_2 + 2H_2\mathbf{O} \xrightarrow{h\nu} (CH_2O) + \mathbf{O}_2 + H_2O \qquad (1)$$

The atoms of the product dioxygen molecule are derived entirely from water, which is oxidatively split into dioxygen

10.1021/cr0204294 CCC: $59.00
Published on Web 11/08/2006

James P. McEvoy read Chemistry at Merton College, Oxford, obtaining his M. Chem. degree in 1998. He moved to Linacre College for his doctoral work, developing variable-temperature protein film voltammetry under the supervision of Fraser A. Armstrong. Having earned his D. Phil. in 2002, he spent a year working with John S. Foord, also at Oxford, investigating the use of diamond electrodes in protein electrochemistry. In 2003, he joined Gary W. Brudvig at Yale University as a postdoctoral associate and has since worked on photosystem II and developed his interests in bioinorganic redox chemistry.

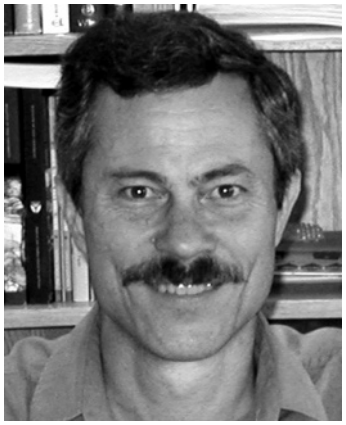

Gary W. Brudvig received his bachelor's degree in Chemistry from the University of Minnesota in 1976 and in 1980 gained his Ph.D. in Chemistry from the California Institute of Technology, where he investigated the metal centers in cytochrome *c* oxidase under the direction of Sunney I. Chan. After two years as a Miller Fellow at the University of California, Berkeley, studying with Kenneth Sauer, he joined the faculty at Yale University, where he is now Professor and Chair of Chemistry and where he applies both biophysical and bioinorganic techniques to the study of photosystem II.

and protons by the enzyme photosystem II (PSII). PSII is a large protein complex found in the thylakoid membranes of oxygenic photosynthetic organisms, which are cyanobacteria, algae, and higher green plants. It exists as a homodimer whose total molecular weight is around 650 kDa. Each monomer comprises around 20 polypeptide subunits and many cofactors (Figure 1). Some of these (most of the chlorophylls and carotenoids) are primarily involved in the transfer of photonic energy and are concentrated in peripheral PSII subunits, such as CP43 and CP47. Other cofactors, with which we are presently concerned, are involved in the transfer of energy in the form of electrons. Most of the protein's electron transfer (ET) cofactors (Figure 1B) are coordinated by the two subunits D1 and D2, which are approximately symmetrical transmembrane subunits in the center of each monomer (Figure 1A). The whole PSII dimer is itself surrounded by further chlorophyll- and carotenoid-containing light-harvesting proteins (or phycobilisomes, in

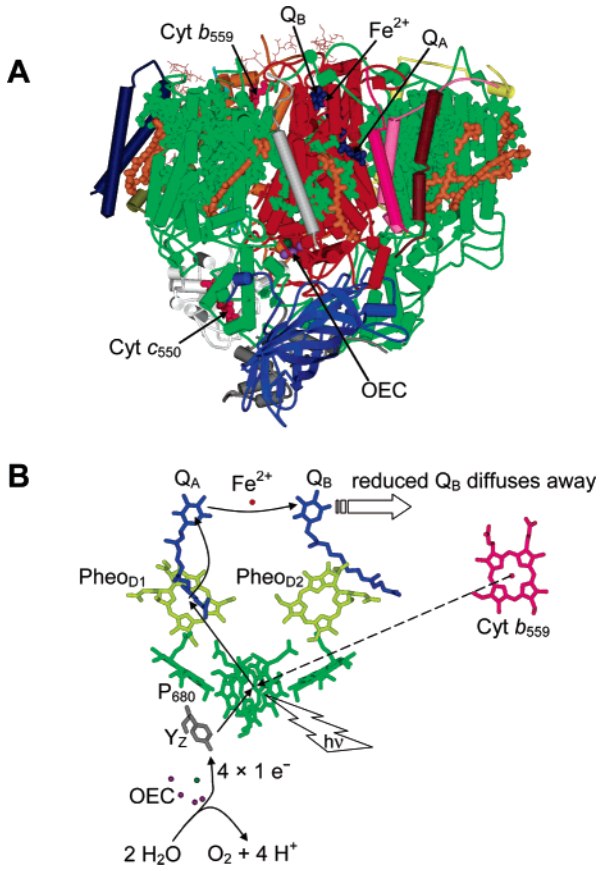

Figure 1. Structure of photosystem II. Panel A shows a schematic view of the polypeptide subunits and cofactors of a PSII monomer, and panel B shows the principal electron transfer (ET) cofactors. In panel A, for the protein backbone (tubes and strands), D1 and D2 are in red, CP43 and CP47 are in green, α-cyt b_{559} and β-cyt b_{559} are in light orange, H protein is in yellow, I protein is in light gray, J protein is in light blue (mostly hidden), K protein is in olive green, L protein is in light pink, M protein is in dark brown, manganese stabilizing protein is in royal blue, T_C protein is in dark pink, U protein is in dark gray, cyt c_{550} is in white, and Z protein is in dark blue. The three unassigned transmembrane helices (visible top left) are shown by thin burgundy lines. For the cofactors (spheres), chlorophylls and pheophytins are in green, carotenoids are in orange, cytochromes (cyt b_{559} and cyt c_{550}) and non-heme Fe^{2+} are in salmon pink, quinones (Q_A and Q_B) are in dark blue, OEC Mn atoms are in purple, and Ca is in dark green. In panel B, the cofactor colors are the same as those in panel A, and D1-Tyr161 (Y_Z) is in gray. Solid arrows indicate the primary catalytic ET pathway; the dashed arrow indicates a secondary nonturnover ET pathway from cyt b_{559} to P_{680}^+. Atomic coordinates for panels A and B were taken from ref 52, PDB accession number 2AXT.

the case of cyanobacteria), which absorb photons and pass their energy to PSII. The enzyme collects this photonic energy and transduces it to redox energy by creating a primary charge separation within the central D1 + D2 subunits, oxidizing a chlorophyll center (called P_{680}) and reducing a pheophytin molecule. Electrons are extracted from water and eventually passed to plastoquinone, a membrane-soluble redox mediator. The overall reaction catalyzed by PSII is given in eq 2.

$$2H_2O + 2\text{plastoquinones} + 4H^+_{\text{stroma}} \xrightarrow{h\nu} O_2 + 4H^+_{\text{lumen}} + 2\text{plastoquinols} \quad (2)$$

The electron-transfer reactions of PSII may be divided into those (on the "acceptor" side), which receive electrons from

P_{680}, and those that provide electrons to the oxidized P_{680}^+. We concentrate in this review on the "donor side" pathway, in which a tetramanganese cluster is oxidized to reduce P_{680}^+, readying the primary electron donor for another photochemical charge separation and building up oxidizing equivalents, which are used to oxidize water. There have recently been excellent reviews on other aspects of PSII, including its primary photochemistry;[4,5] its composition;[6−11] the biogenesis, assembly, photodamage, and turnover of its subunits;[12−16] the design of artificial manganese clusters for water oxidation;[17] and PSII-inspired artificial photosynthesis.[18] Many of these reviews form part of a book on photosystem II, which has recently been published[19] and which includes a chapter on the subject of photosynthetic oxygen production.[20] Special issues of several journals have also been published in the past few years, each containing valuable articles and reviews.[21−24]

2. The Function of Photosystem II

2.1. The Acceptor Side

Upon obtaining a certain amount of collected light energy (optimally, a photon of 680 nm wavelength light and of 1.82 eV energy), P_{680} is oxidized to produce a charge separation. This gives a cation radical, P_{680}^+, and a pheophytin anion radical, $Pheo^-$ (Figure 1B). P_{680}^+ is the most oxidizing species known in biology, with two recent estimates putting its reduction potential at about 1.25 V.[25,26] The electron embarks upon a complicated journey within the PSII monomer, on the acceptor side of the ET chain. It passes first to a pheophytin molecule and goes on to reduce a tightly bound quinone cofactor, Q_A. By now, 200 ps after the initial charge separation, the electron is separated by about 26 Å from the highly oxidizing P_{680}^+. The charge separation $P_{680}^+\cdots Q_A^-$ is physiologically stable for several hundred microseconds[27] and is easily studied either at low temperatures or in the presence of an inhibitor, both treatments blocking the further progress of the electron. Under normal physiological conditions, however, the electron continues to a second quinone molecule, the weakly bound Q_B, which, after it has been reduced by two electrons, diffuses out into the membrane to continue the photosynthetic ET chain at the cytochrome b_6f complex.

2.2. The Donor Side: The Oxygen-Evolving Complex (OEC), the S-State Cycle, and Tyrosine Z

Water oxidation is catalyzed by a center containing manganese, calcium, and (probably) chloride. This is known both as the oxygen-evolving complex (OEC) and as the water-oxidizing complex (WOC), although for the sake of consistency, we will always use the former name. It is the job of the OEC to couple successive one-electron reductions of P_{680}^+ to four-electron oxidations of water to dioxygen (eq 3).

$$2H_2O \rightarrow O_2 + 4H^+ + 4e^- \quad (3)$$

The OEC acts as an electrical accumulator. It is repeatedly oxidized (one electron at a time) by P_{680}^+ until, when the OEC has been oxidized four times, it converts water to dioxygen and resets itself to its most reduced state.[28] Each oxidation state of the OEC is known as an "S-state" ("S" may stand for "storage"), with S_0 being the most reduced state and S_4 the most oxidized state in the catalytic cycle (Figure 2). The S_1 state is dark-stable. All of the S-state transitions, apart from $S_4 \rightarrow S_0$, are induced by the photochemical oxidation of P_{680}^+, which in turn oxidizes the OEC via a redox-active tyrosine. The $S_4 \rightarrow S_0$ transition is spontaneous and light-independent, and as a result, the $S_3 \rightarrow [S_4] \rightarrow S_0$ step happens so quickly that it has largely resisted investigation until very recently.[29,30] These new experiments have apparently illuminated different intermediates in the overall $S_3 \rightarrow [S_4] \rightarrow S_0$ transition but not the S_4 state itself.[31−33] The intermediate revealed by Haumann et al.,[29] for instance, appears to be the $S_3Y_Z^\bullet$ state in our terminology, while that seen by Clausen and Junge[30] is probably S_4' (see below).

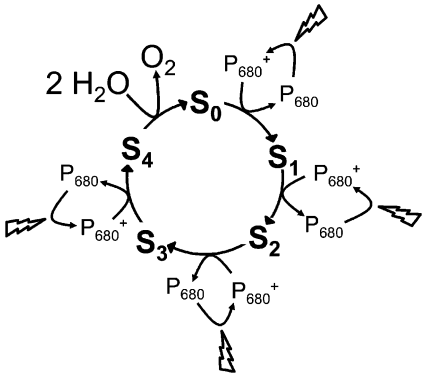

Figure 2. The catalytic cycle of the OEC. In the $S_0 \rightarrow S_1$, $S_1 \rightarrow S_2$, $S_2 \rightarrow S_3$, and $S_3 \rightarrow S_4$ transitions, light energy is used to oxidize P_{680} to P_{680}^+, which in turn oxidizes the metal−oxo cluster of the OEC (via Y_Z, not shown). The $S_4 \rightarrow S_0$ transition is light-independent and releases O_2. This transition is particularly complicated, and intermediates (such as S_4', see Figure 19) have been postulated.

The OEC is electrically linked to P_{680} by a redox-active tyrosine residue of the D1 subunit, which is called tyrosine Z or Y_Z.[34−36] The oxidized form of Y_Z is the radical species $Y_Z^{+\bullet}$, which is usually taken to exist in the neutral, deprotonated form $Y_Z^\bullet$ (see section 4.5). Y_Z is close enough to the OEC that it might be intimately involved in the chemical catalysis of water oxidation, rather than simply act as the immediate oxidant of the OEC. A useful review of the properties both of Y_Z and the analogous tyrosine in the D2 subunit, Y_D,[37,38] has been recently published.[34]

When we refer to a state S_n in this review, n refers solely to the oxidation state of the ligated metal cluster of the OEC. Every $S_n \rightarrow S_{n+1}$ transition (a set that excludes the spontaneous $[S_4] \rightarrow S_0$ step) passes through an intermediate $S_nY_Z^\bullet$, in which the oxidized tyrosine is poised to oxidize the metal cluster of the OEC. The $[S_4] \rightarrow S_0$ transition may pass through several intermediates, but we will assume for the sake of simplicity that there is only one, which we term S_4'. In this intermediate, two ligated oxide species are oxidized to a peroxide level, while the metal cluster is correspondingly reduced by two units. Since there is no change in the overall oxidation state of the hydrated metal cluster, the subscript remains 4. (If the subscript were to refer to the oxidation state of the Mn_4Ca metal cluster alone, one might call this intermediate S_2'.) Some have postulated peroxide formation at the S_3 level,[39,40] in which case there would be no distinct S_4 state but an $S_3'Y_Z^\bullet$ state that directly yields O_2 and the S_0 state.[41]

3. The Structure of the Oxygen-Evolving Complex (OEC)

3.1. Introduction

The structure of PSII has, until recently, been inferred from spectroscopic data obtained alongside biochemical and molecular biological manipulations. This information has been combined with our knowledge of the structure of the bacterial photosynthetic reaction center, whose X-ray crystal structure was solved to 3 Å resolution 20 years ago[42] and is now available at better than 2.3 Å resolution.[43−45] The similarity between the central regions of PSII and the bacterial reaction center was revealed with the isolation of a PSII reaction center (D1, D2, and cyt b_{559} subunits)[46] and by analysis of sequence homology.[47] However, the bacterial reaction center does not oxidize water (it obtains electrons instead from a soluble cytochrome), so researchers interested in the OEC have been denied this important structural guide. They have instead relied largely on X-ray absorption spectroscopy (XAS),[48] electron paramagnetic resonance (EPR) spectroscopy,[49,50] and vibrational spectroscopy.[51] More recently, crystallographic X-ray diffraction structures of PSII have been obtained at increasing resolutions,[52−56] and these have begun to play an important part in illuminating the OEC.

3.2. The Components of the OEC

3.2.1. Manganese

Manganese has long been known to be essential for photosynthetic oxygen evolution, and it was eventually established that the OEC contains four manganese ions.[57−59] EPR spectroscopy was important in confirming this result, following the discovery that the S_2 state of the OEC is paramagnetic and yields a distinct multiline signal.[60] Although it was initially unclear whether this signal was produced by a manganese dimer or a tetramer,[60] later analysis of the continuous wave (cw) EPR data indicated a tetrameric origin.[61−63] Pulsed EPR experiments have shown this unequivocally.[64−67]

3.2.2. Calcium

Calcium was found in the 1980s to be an essential cofactor in oxygen evolution.[68] One calcium is required per OEC.[69,70] The metal's proximity to the Mn_4 unit was established with the discovery that its binding depends on the S-state[71] and of a long-lived, modified EPR multiline signal produced by the S_2-state of the Ca^{2+}-depleted OEC.[72−74] XAS[75,76] and pulsed EPR[77] evidence for the location of Ca^{2+} within the OEC is detailed in section 3.3. It has been hypothesized both that calcium acts in water splitting by binding a substrate water molecule[78−81] and that it modifies the redox potential of the OEC, perhaps by controlling proton transfer.[82−84] Direct evidence for the former hypothesis comes from mass spectroscopic measurements of ^{18}O-labeled dioxygen release from OECs in which calcium has been replaced with strontium.[85] A review of calcium's role in the OEC has recently been published.[86]

Removing calcium from the OEC blocks the S-state cycle at the $S_2Y_Z^{\bullet}$ state.[72−74,87−90] Under normal catalytic conditions, $Y_Z^{\bullet}$ oxidizes S_2 to give the S_3Y_Z state, but calcium depletion blocks this reaction. The effect was early proposed to be essentially electrostatic in origin.[91] Recent EPR results indicate that the blockage may be overcome at low pH, suggesting that calcium depletion might disrupt the delivery of protons to $Y_Z^{\bullet}$ upon its reduction.[92] UV/vis spectroscopy and proton-release measurements likewise indicate that calcium is involved in maintaining a hydrogen-bonding network around Y_Z.[84]

3.2.3. Chloride

Chloride has been long known to affect photosynthetic oxygen-evolution rates in PSII (see refs 86, 93, and 94 for reviews), but its presence in the OEC remains less well established than that of calcium, and there is no firm evidence that chloride is bound to the Mn_4Ca cluster. Chloride's binding site has been found to be at, or near, the site of water splitting.[95] That conclusion was confirmed by experiments showing that its binding and effect depend on the S-state of the OEC[96,97] and by S_2/S_1 FTIR difference spectroscopy in the presence and absence of the Cl^- ion.[98,99] Radioisotope labeling studies have suggested that approximately one Cl^- ion binds at the OEC.[100] Acetate binding competes with that of chloride[101] and acetate has been shown by pulsed EPR spectroscopy to bind close to Y_Z.[102] Pulsed EPR experiments have also demonstrated that azide binds competitively with chloride and close to the OEC,[103] but there remains no good evidence for the exact location of chloride within the OEC. There is evidence that chloride depletion blocks OEC turnover at the $S_2Y_Z^{\bullet}$ state, just as calcium depletion does.[89,91,96,104] (Earlier work had indicated that chloride depletion blocks the S_2 to S_3 transition[105−108]). On the basis of oxygen-evolution activity measurements and EPR spectroscopy, chloride, like calcium, has been proposed to influence proton-transfer away from the OEC as part of a hydrogen-bonding network.[109] However, recent evidence suggests that chloride (unlike calcium) is not absolutely required for water splitting but that catalysis (possibly at the $S_2 \rightarrow S_3$ step) is only slowed in the absence of chloride, when care is taken to avoid damaging the protein during chloride depletion.[109] Indeed, chloride may be substituted by different anions (possibly Br^-, NO_3^-, NO_2^-, and I^-), which maintain water-splitting activity to varying extents,[110−113] although the $S_3 \rightarrow [S_4] \rightarrow S_0$ transition is always slower than that with chloride.[114,115]

3.2.4. Water

It is clear that, at some point in the S-state cycle, substrate water must bind to the OEC. The first attempts to measure directly the interaction between manganese in the OEC and isotope-labeled water using pulsed EPR were unsuccessful,[116] but subsequent efforts have distinguished magnetic coupling interactions in the S_2 state,[117−119] as well as in the S_0 and S_1 states.[119] Several ^2H_2O molecules (about three) have been modeled in close proximity to manganese in the S_2 state, but the overall deuteron modulation depth is comparable to that seen in fully solvated Mn^{II}, indicating that the OEC is in contact with numerous exchangeable hydrogens.[119] Similar results are obtained in the S_1 and S_0 states, although the S_0 state was modeled with three water ligands and the S_1 and S_2 states with two water ligands and one nearby but unligated water.[119] Substrate analogues such as alcohols and ammonia have also been seen to bind to the OEC using EPR methods,[66,120−123] spectroscopic assignments being backed up by model compound investigations.[124]

Techniques besides EPR have confirmed the presence of water at the OEC. Near-infrared Raman spectroscopy

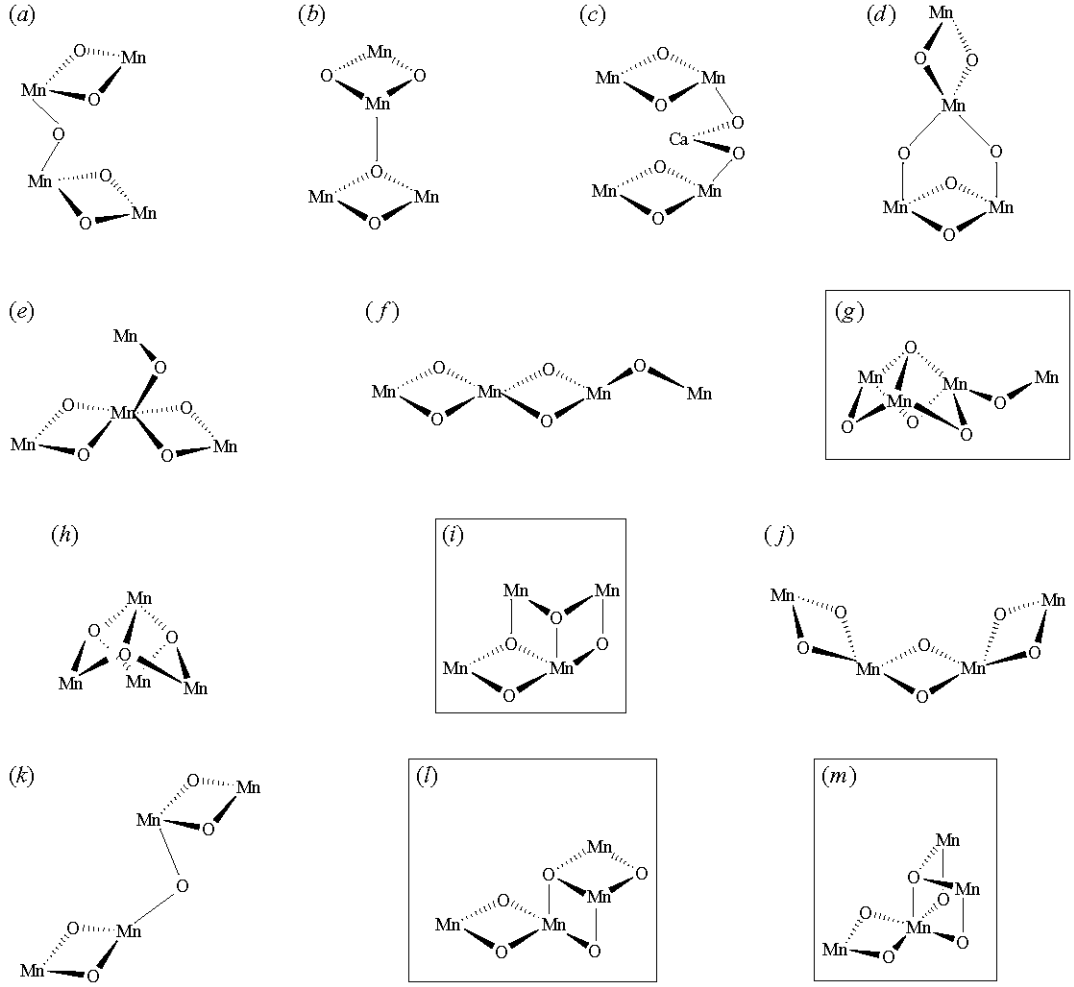

Figure 3. Possible arrangements of the four Mn ions of the OEC, based on the EXAFS measurements of Yachandra, Sauer, and coworkers. All models comprise two or three di-μ-oxo-bridged Mn_2O_4 moieties. The most recent work of this group[136] favors those models (*g*, *i*, *l*, and *m*) shown in boxes. Model *i* is most similar to the structure suggested by the crystallography of Ferreira et al.[53] Adapted with permission from ref 330. Copyright 2002 Royal Society.

indicates that at least two waters (or hydroxides) are bound to the OEC in the S_1 state,[125] and FTIR spectroscopy reveals S-state-dependent ligand−water vibrations.[126−128] Mass spectrometric measurements of ^{18}O-labeled dioxygen evolution have been used to estimate that the OEC is available to a pool of about 12 water molecules,[129,130] although other isotope fractionation data stand in contradiction to this work.[174,441] Time-resolved mass spectrometric measurements have been particularly useful in characterizing water binding to the different S-states of the OEC, and these data will be addressed later (see especially section 5.2.3).

3.3. The Arrangement of Manganese and Calcium in the OEC and Proximity of Tyrosine Z

Manganese EXAFS (extended X-ray absorption fine structure) spectroscopy is the variety of XAS that has proved most useful in defining the structure of the OEC (work reviewed recently in refs 48, 131, and 132). It provides information about short-range electron scattering to give accurate bond distances in the first and second coordination spheres. Mn EXAFS reveals the following set of distances from Mn within the OEC in the S_1 state:[83,133,134] a first coordination shell of O or N atoms at 1.8−2.0 Å, two or three (but see below) Mn···Mn distances of ca. 2.7 Å, and one or two distances of 3.3−3.5 Å.[135] Recent experiments, using improved instrumentation, indicate that the "ca. 2.7 Å distances" comprise two 2.7 Å distances and one 2.8 Å distance.[136] This result seems to settle the argument as to whether there are two or three such "short" Mn···Mn distances in the S_1 state. The 3.3−3.5 Å shell appears to comprise both Mn···Ca and Mn···Mn contributions.[75,76,137,138] Results obtained from calcium EXAFS have established most convincingly that the intact OEC comprises a cluster containing both manganese and calcium.[75] The 2.7 Å Mn···Mn distances[139,140] are consistent with the presence of di-μ-oxo linkages between Mn^{III} or Mn^{IV} ions.[141] A family of possible OEC structures based on these EXAFS results (but omitting calcium) has strongly influenced research in this area and is shown in Figure 3.

EXAFS has also been used to study the OEC in states other than S_1. The $S_1 \rightarrow S_2$ transition is apparently unaccompanied by significant changes in the OEC structure,[142] a conclusion confirmed by the recent high-resolution measurements.[136] The $S_0 \rightarrow S_1$ transition, though, does involve some change in EXAFS-detected interatomic distances: according to two groups, one of the 2.7 Å distances present in the S_1 state is longer in the S_0 state, at around 2.85 Å.[143,144] Structural changes in the $S_2 \rightarrow S_3$ transition are more marked and have been variously interpreted, either as the creation of a new 2.7 Å Mn···Mn distance[144] or as the inequivalent

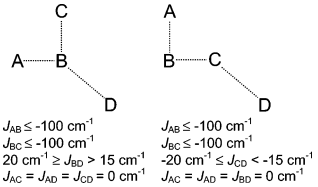

Figure 4. The "3 + 1" or "dangler" model of Mn arrangement in the OEC proposed by Peloquin et al.[64] on the basis of electron spin−echo ENDOR (ESE-ENDOR) measurements. J_{XY} is the exchange coupling constant between Mn(X) and Mn(Y). Two arrangements of the four Mn ions are shown, each with magnetic couplings (2 strong, 1 weak) that are compatible with these experiments. Adapted from ref 64. Copyright 2000 American Chemical Society.

lengthening of two 2.7 Å distances to 2.8 and 3.0 Å.[145] The surprisingly low reactivity of the S_3 state to certain exogenous reductants has been interpreted as additional evidence for some structural reorganization in the $S_2 \rightarrow S_3$ step.[146]

Indeed there are a variety of data to suggest that the $S_2 \rightarrow S_3$ transition is unique in the catalytic cycle. Most crucially, it is the $S_2 \rightarrow S_3$ transition that is blocked by calcium and chloride depletion (see sections 3.2.2 and 3.2.3), as well as by a variety of inhibitors. These include fluoride,[104,109,112,147,148] acetate,[89,149−153] and amines.[121,148] In all cases, the catalytic cycle stops at the $S_2Y_Z^{\bullet}$ state. $S_2 \rightarrow S_3$ exhibits the highest activation energy of all the steps,[154] and its reorganization energy is the highest besides that of the oxygen-evolving $S_3 \rightarrow [S_4] \rightarrow S_0$ step.[155,156] The effect of pH on the rate of $S_2 \rightarrow S_3$, although not large, is the greatest among all the transitions.[157] The $S_2 \rightarrow S_3$ H/D kinetic isotope effect has been found to be the largest in the catalytic cycle,[154,157] although that result is not universally obtained.[158]

EPR spectroscopy has been important in establishing the structure of the OEC, as recently reviewed in refs 50 and 119. Most notably, ^{55}Mn ENDOR (electron−nuclear double resonance) spectroscopy has been used to propose a "3 + 1" arrangement of the four Mn ions on the basis of magnetic coupling tensors,[64] with one manganese ion weakly coupled to a strongly coupled trinuclear core (Figure 4). The linear 3 + 1 arrangement originally suggested on the basis of this work[64] (model *f* in Figure 3) is incompatible with current EXAFS models comprising three 2.7−2.8 Å Mn···Mn distances (see above).[136,143] Instead, attention has shifted toward such models as *g*, *i*, *l*, and *m* in Figure 3, as suggested earlier by Hasegawa and co-workers on the basis of cw EPR analysis and EXAFS constraints.[159]

The associated hyperfine coupling constants have recently been independently confirmed,[160] and several groups have found that a 3 + 1 manganese arrangement is compatible with their EPR data.[161,162] ^{88}Sr ESEEM (electron spin−echo envelope modulation) spectroscopy has recently been used to establish, in confirmation of EXAFS results, that the (Sr^{2+}-occupied) Ca^{2+}-binding site is less than 5 Å from the manganese ions of the OEC.[77] EPR spectroscopy has repeatedly been used to measure the dipolar distance between Y_Z and the OEC metal−oxo cluster. An early analysis gave a distance of less than 5 Å,[88] but further analyses have given distances closer to 8 Å,[163−166] in good agreement with the X-ray crystallographic models.[52,53,55,56]

3.4. Amino Acids Nearby and Ligating the OEC

The short first coordination sphere distances revealed by EXAFS indicate that the manganese ions of the OEC are principally coordinated by oxygen or nitrogen atoms (data reviewed in refs 83 and 133). Many experiments, often involving site-directed mutagenesis, have been performed to identify the ligating amino acid residues.[11,167−169] ESEEM spectroscopy has revealed the presence of a ligating histidine,[170,171] which is probably D1-His332.[172,173] Consistent with histidine ligation is the finding that the vibrational frequencies of one or more histidines are sensitive to S-state transitions.[175] The remaining proteinaceous metal ligands have largely been assumed to be carboxylates, with attention focused on conserved aspartate and glutamate residues in the D1 subunit, as well as on the D1 carboxyl terminus. It is well-established that the free carboxyl group of D1-Ala344 is required for proper assembly and function of the OEC.[176] The X-ray crystallographic data of Ferreira et al. (see section 3.5) place it bound to or very near the calcium ion;[52] however, FTIR spectroscopy indicates that it is not a ligand to this metal.[177−179] For example, Strickler et al. observed no change in the symmetric stretching mode of the carboxyl terminus of D1-Ala344 upon replacement of calcium by strontium in the OEC, although the IR frequencies of several other carboxylate groups were affected by the substitution.[178] The vibrational frequencies of the carboxylate terminus are sensitive to the changing S-state of the OEC, with a notable S_2/S_1 response,[179,180] indicating that the carboxyl terminus does bind to the OEC in some fashion. The S_2/S_1 response has been shown to be reversed in the $S_3 \rightarrow S_0$ transition.[180] The authors of these studies, therefore, conclude that D1-Ala344 binds to a redox-active Mn ion rather than to Ca^{2+}.[178] This conclusion is compatible with the most recent crystal structure, which assigns the residue more confidently as a ligand to manganese than to calcium.[52] It is nonetheless possible, in our view, that D1-Ala344 does ligate calcium and that the electrostatic effect of the $S_1 \rightarrow S_2$ transition is transmitted through calcium from the OEC to the carboxylate terminus. We have carried out a quantum mechanical analysis that supports this hypothesis.[181] Our calculations also indicate that the symmetric stretching mode of D1-Ala344 is insensitive to an in silico substitution of calcium by strontium in the OEC.[181]

Another residue that has recently been under scrutiny is D1-Asp170, a residue with a well-established role in Mn^{2+} binding in the first stage of OEC cluster assembly.[182,183] X-ray crystallographic data[52,53] indicate that it also binds the assembled OEC (see section 3.5), but EPR and ESEEM spectroscopy of a D1-D170H mutant recently failed to demonstrate ligation of the substituted histidine to the cluster.[184] The authors concluded that three explanations are plausible: (1) that D1-Asp170 does not ligate the OEC, (2) that it does but that the substituted histidine does not replace aspartate as a ligand, or (3) that both D1-Asp170 and D1-His170 ligate the OEC but that the hyperfine couplings to the ligating nitrogen of the histidine are too large or anisotropic to have been seen. FTIR spectroscopy does indicate that D1-Asp170 is at least near to the cluster,[185] although its vibrational frequencies seem unaffected by any of the S-state transitions up to the S_3 state.[186] The authors of the latter study conclude that if D1-Asp170 does ligate manganese in the OEC (as it probably does, especially given that it binds the first Mn ion during assembly of the OEC),[183] it is a manganese whose redox state does not change up to the S_3 state. One might expect that the electrostatic effects of the oxidation of one manganese ion in the OEC would be delocalized sufficiently to be detected at all of the metal

ions. There is evidence that, at least in the $S_1 \rightarrow S_2$ transition, the electron is indeed lost from a strongly delocalized orbital.[187] It is possible, however, that changes in formal oxidation state of the manganese bound to D1-Asp170 are not accompanied by significant changes in the metal's electrostatic charge[188] (due to charge-compensating effects) and are, therefore, not sensed by D1-Asp170.[189] Because the "dangler" Mn of the OEC (Mn(4) in Figure 5) is so closely linked to the proton exit pathway beginning at D1-Asp61 and less closely associated with the remaining three Mn ions, facile proton loss from its coordinated waters upon its oxidation may make a carboxylate ligand to this metal insensitive to changes in its formal oxidation state. Residues asscciated with other parts of the OEC, more electrostatically affected by changes in electron density, may be more affected. For this explanation to be tenable, we must also suppose that the structural rearrangements of the OEC (seen by EXAFS) in the $S_0 \rightarrow S_1$ and $S_2 \rightarrow S_3$ transitions do not affect the D1-Asp170 vibrations examined in the FTIR experiment, even when D1-Asp170 ligates the Mn ion that undergoes oxidation. If D1-Asp170 ligates the "dangler" Mn of the OEC (see section 3.5), the structural changes might be confined to the other three manganese ions, or if Mn(4) does move, the FTIR experiments might not be sensitive enough to detect this. Further experiments and calculations will be needed to establish that the manganese ligated by D1-Asp170 is redox inactive up to the S_3 state, as indicated by the FTIR data.

3.5. Crystallographic Data

The first crystallographic studies of PSII used electron cryomicroscopy to obtain an outline of the various subunits at 8 Å resolution.[190] The first X-ray crystal structure of *Thermosynechococcus elongatus* PSII, at 3.8 Å resolution,[56] revealed the locations of several cofactors but resolved neither the individual amino acid side chains nor the locations of the individual metal ions within the OEC, which was represented by a single pear-shaped region of electron density. The 3.7 Å structure from *T. vulcanus*[55] revealed a similarly shaped electron density for the OEC, although the authors favored a different arrangement of metal ions within this region. Furthermore, they tentatively proposed some of the ligating amino acid residues, all of which belonged to the D1 subunit. The next published structure, from *T. elongatus* again, at 3.5 Å resolution,[53] was a considerable improvement. It assigned nearly all of the 19 subunits to specific gene products, as well as most of the individual amino acid residues of the protein. An anomalous difference X-ray map was used for the first time to construct a model of the OEC, using different radiation wavelengths to establish separately the locations of manganese and calcium within the cluster. The site was thus modeled as a Mn_3CaO_4 cuboid with a "dangler" Mn atom attached to the outside of the cuboid via a corner μ_4-oxide (Figure 5). The amino acid residues found to ligate the manganese ions of the cluster were as follows: D1-Asp342, D1-Asp170, D1-Glu333, D1-Glu189, D1-His332, and CP43-Glu354. D1-Ala344, the carboxy terminus, was found very close to the calcium ion but not to be a ligand. All of these residues, with the exception of CP43-Glu354, had been previously proposed to be ligands to the OEC.[168,169] Of all these ligands, biochemical (mutational) evidence for ligation is weakest in the case of D1-Glu189,[167] and it is possible that Mn(2) is ligated by D1-His332 alone. Recent FTIR experiments

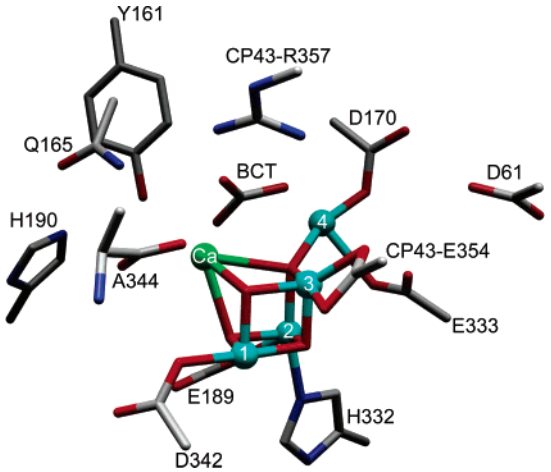

Figure 5. Crystallographic model of the OEC and its surroundings offered by Ferreira et al.,[53] PDB accession number 1S5L. Mn ions (numbered as in ref 53) are shown in cyan, calcium is in green, oxygen is in red, carbon is in gray, and nitrogen is in blue. BCT denotes bicarbonate, which was modeled in the X-ray structure, but its presence in the OEC is uncertain (see text). For clarity, only the side chains of the amino acids are shown, except in the case of D1-Ala344, whose terminal carboxylate portion is thought to be important (see text). Unless otherwise indicated, amino acid residues belong to the D1 subunit.

strengthen the case that D1-Glu189 is not a ligand of the OEC.[191]

It is important to note that the modeled μ-oxide coordination was constructed in part according to the EXAFS and model compound information outlined in section 3.3. The X-ray structure is not of atomic resolution, so the electron density map of the OEC does not explicitly reveal the position of every atom within the cluster. The atomic arrangement of the OEC put forward by the authors of this paper would not be justifiable solely on the basis of the crystallographic data. Nevertheless, the modeled structure is consistent both with the electron density and with a variety of other data. In particular, the 3 + 1 arrangement of Mn ions resembles that of model *i* in Figure 3, making the crystallographic model broadly compatible with EXAFS and EPR data (see section 3.3).

A 3.2 Å resolution structure of PSII from *T. elongatus* has been published,[54] but the OEC region was little better-defined than in the 3.8 and 3.7 Å structures, and an atomic model was not offered. Most recently, Loll et al. have published a 3.0 Å resolution structure of PSII from the same organism.[52] This is of particular interest in assigning more accurately the positions of carotenoids and bound lipids. An anomalous difference X-ray map was used (as in the 3.5 Å resolution structure) to distinguish between calcium and manganese electron density in the OEC. Although a full atomic model of the OEC was not offered in this work, the arrangement of the manganese and calcium atoms (again restrained by EXAFS data) is rather similar to that seen in the 3.5 Å resolution structure. Loll et al. also find a 3 + 1 arrangement of the manganese ions, although it is more like model *g* in Figure 3 than model *i*. The mean difference in the absolute position of each metal ion in the OEC between the 3.5 and 3.0 Å resolution structures is 2.9 Å. More relevant, however, are the *relative* positions of the metal ions in the two structures, a comparison that addresses the shapes of the two OEC models. The mean difference in distance between equivalent pairs of metals in the two crystal structures is less than 0.5 Å, far below the resolution of either

structure. Furthermore, 86% of the total intermodel discrepancy in these intermetal distances is found in just three of them: Mn(2)−Mn(4) (5.8 Å in the 3.0 Å resolution structure, vs 3.2 Å in the 3.5 Å structure), Ca−Mn(4) (4.6 Å vs 3.9 Å), and Mn(1)−Mn(3) (3.3 Å vs 2.7 Å). The mean intermodel discrepancy in the remaining seven intermetal bonds is less than 0.1 Å. If we now compare bond angles, we find that the mean intermodel difference between the four bond angles in the Ca, Mn(1), Mn(2), and Mn(3) atomic set is 7°, whereas the mean intermodel difference between the six angles involving Mn(4) is 30°. Again, though, 78% of this total angular discrepancy is found in just two angles: Mn(4)−Mn(3)−Mn(2) (154° in the 3.0 Å resolution structure vs 65° in the 3.5 Å resolution structure) and Mn(1)−Mn(2)−Mn(4) (69° vs 121°). The same amino acids were identified as ligands to the cluster, although they are oriented quite differently in the two models (see below).

The two principal differences between the 3.0 Å resolution and the 3.5 Å resolution OEC structures are that (1) the 3.0 Å resolution structure finds the dangler Mn ion rather further away from the other four metal ions, implying that it may not be linked to the others by a single μ_4-oxo atom and (2) all of the amino acid carboxylate ligands in the 3.0 Å resolution structure are modeled to bind to the metal ions as μ,η^2 bridging ligands. With regards to the first point, Loll et al. found, by obtaining some data at 20 K rather than 100 K, that the dangler Mn is most prone to temperature-dependent radiation damage and subsequent disorder so its position is difficult to determine accurately.[52]

Indeed,Yano et al. have issued an important warning concerning the reliability of X-ray crystallography of the OEC.[192] It appears from their XAS results that the X-ray fluxes commonly used to obtain crystallographic data are sufficient to reduce the Mn ions of the OEC considerably, perhaps even to an all-Mn^{II} state.[192] The same conclusion has been reached by Dau and co-workers.[193,194] EXAFS spectroscopy shows that this is accompanied by changes in the metal coordination spheres even at 100 K, the temperature typically used for PSII crystallography.[192,194] Although reduction of the manganese ions is, therefore, likely in all of the crystallographic experiments, it remains unclear to what extent structural change has been mitigated by data collection at low temperature, from various positions of the same crystal, and from several different crystals. The authors of the most recent 3.0 Å resolution structure[52] used an X-ray wavelength of 1.91 Å, which has been found[192] to cause less radiation damage than the 2.25 Å wavelength used previously.[53]

The similarity of the 3.5 Å and the 3.0 Å resolution OEC structures give grounds for hope that radiation-induced damage to the cluster is not an insurmountable problem in crystallographic studies of the complex. Nevertheless, it must be emphasized that radiation-induced reduction and deterioration of the structure is a real problem in the crystallography of the OEC. As higher-resolution data are obtained, it is expected that reduction-induced structural shifts will become an even more significant source of error. We have made the decision in this review to emphasize the OEC structure presented by the authors of the 3.5 Å crystal structure,[53] rather than that of Loll et al.,[52] because the former is a more chemically complete and credible structure. It is widely accepted, for instance, that the ca. 2.7 Å Mn···Mn distances obtained from EXAFS experiments are due to di-μ-oxo-bridged Mn units (see section 3.3),[141] but no such bridging oxides are included in the model of Loll et al.[52] It, therefore, seems to us that the model of Loll et al.[52] is less realistic than the model of Ferreira et al.,[53] which some think goes too far in the direction of conjecture.[192]

An interesting aspect of the 3.5 Å resolution structure is the appearance of electron density between the dangler manganese and the calcium ion. This was taken to indicate the presence of a complex anion such as nitrate, sulfate, or bicarbonate. Bicarbonate is well-known to be involved on the acceptor side of the PSII ET chain,[195,196] but its role on the donor side is controversial.[197] It has intermittently been suggested (recently, for instance, in ref 198) to be a substrate for the OEC oxygen-evolving reaction, but mass spectrometric measurements have indicated that ^{18}O from $HC^{18}O_3^-$ is not quickly incorporated into product O_2.[199−202] These results show that water, not bicarbonate, is the substrate for the OEC. There is evidence that bicarbonate is involved in the assembly of the OEC,[203,204] suggesting that it may be retained as a ligand of the assembled OEC. However, we follow the authors of the 3.5 Å resolution structure[53] in concluding that any anion ligand between Mn(4) and Ca^{2+} is likely to be adventitious, blocking the water-binding site. This is supported by the higher-resolution X-ray data, which do not show bicarbonate in this position.[52,54] Loll et al. plausibly interpret electron density between Mn(4) and Ca^{2+} as belonging to D1-Asp170.[52] Owing to the lack of any direct evidence for both the presence and activity of bicarbonate in the assembled, functional OEC, it seems very unlikely that bicarbonate plays a role in the water-splitting chemistry of PSII.

Work is under way to test the validity of the OEC model of Barber, Iwata, and co-workers.[53] Inorganic model chemistry and quantum mechanical calculations both will play important roles in augmenting experimental studies of the PSII protein. A Mn_4O_4 cuboidal structure was proposed for the OEC some time ago,[61,205] and many tetrameric manganese clusters have been synthesized since then as speculative structural models (reviewed recently along with other Mn complexes in refs 141 and 206). There is no model complex as yet that replicates the discrete Mn_3CaO_4 motif, with or without the fourth (dangler) manganese, but a polynuclear complex that comprises a $Mn^{II}Mn^{III}_2Mn^{IV}CaO_4$ moiety (with a Mn^{IV} dangling from a μ_4-oxide) has been synthesized,[207] and density functional calculations have indicated that the arrangement is energetically plausible in isolation from the protein.[208,209]

4. Proton-Coupled Electron Transfer (PCET) in the OEC

4.1. Introduction

Splitting a molecule of water releases eight charged particles: four negatively charged electrons and four positively charged protons. Because they are so much more massive, protons can rapidly tunnel over only a fraction of the distance that an electron is able to (<1 Å vs ca. 20 Å),[210] and proton movements within a protein are, therefore, usually thermally activated. This means that when electron transfer is coupled to proton transfer, as it is in the OEC, proton transfer may be rate-determining. We can expect the OEC and its environment to have been specifically designed to transfer protons rapidly away from the active site and to the lumenal surface of the protein.

In our examination of the movement of protons and electrons away from the OEC, we will first look at how the oxidation state of the OEC changes with S-state and then review the proton release pattern. Finally, we will ask how the movements of the two types of particles are coupled together. This matter has been illuminatingly examined, from different perspectives, in two recent reviews.[39,211]

4.2. Oxidation State Changes in the OEC

It is widely assumed that the oxidation state changes in the OEC are largely, or entirely, manganese-based. Early, arguable evidence of this came from NMR measurements of proton relaxation rates around the OEC, which change according to the changing magnetic properties of the manganese ions in different oxidation states.[212−214] Optical spectroscopy has also played an important role in characterizing the S-state transitions.[215] However, EPR and XAS spectroscopies have yielded more detailed insights, and we will concentrate on these results here.

There is most consensus concerning the S_1 and S_2 states. Since the S_2 state is paramagnetic (an $S = {}^1/_2$ form yielding the multiline EPR signal and an $S = {}^5/_2$ form the $g = 4.1$ signal),[216−218] it must be that the cluster giving rise to these signals contains an odd number of half-integer spin ions. Therefore, the S_2 state must have an odd number of Mn^{II} or Mn^{IV} ions or both, which are the only common Mn oxidation states with half-integer spin. EXAFS spectroscopy (see section 3.3) indicates the presence of $Mn(\mu\text{-}O)_2Mn$ units, which are only found in the +3 and +4 oxidation states.[219] Indeed, a survey of the Cambridge Crystallographic Database reveals that 90% of manganese complexes with a Mn···Mn distance between 2.65 and 2.75 Å have at least one of these Mn ions in the +4 oxidation state. These facts, together with XAS data (see below), have led researchers to the conclusion that the S_2 state contains either one or three Mn^{IV} ions, the remainder being Mn^{III}. Thus, the S_2 tetramer oxidation states may be either III, III, III, IV or III, IV, IV, IV. It is worth noting that Thorp has used the method of "bond valence sum analysis", empirically relating EXAFS-measured bond lengths to metal oxidation states, to argue for the latter option.[220]

Most researchers believe that this III, IV, IV, IV assignment is correct, largely on the basis of three types of experiment: XAS, X-ray emission spectroscopy (XES), and EPR spectroscopy. The principal XAS technique in this context is X-ray absorption near-edge structure, or XANES. Whereas Mn EXAFS examines short-range scattering of a manganese photoelectron, giving information about its surroundings, XANES uses a lower X-ray energy. Instead of being ejected, the manganese electron is promoted from a core shell (usually 1s) to an outer shell (usually 4p). These "X-ray edge" data give information about the oxidation state of the manganese ion and have been important in monitoring changes in manganese oxidation states through the S-state cycle. (reviewed in refs 48, 131, and 132) However, it is not so useful for assigning *absolute* oxidation states in the OEC. Even in simple model compounds, it is difficult to distinguish between Mn^{III} and Mn^{IV} XANES spectra, and as a result it has been estimated that there is a 25% uncertainty in absolute oxidation state assignments.[221] Some argue that the technique's uncertainty in the OEC is even higher; if (as is likely) metal ligation changes accompany at least some of the S-state transitions, XAS results might be so much affected that the method becomes unreliable as a probe of manganese oxidation states.[162] However, XES is less affected by metal ligation and has also been used to measure oxidation state changes in the OEC[222,223] with reference to model compounds.[224] All of these results suggest a III, IV, IV, IV assignment for S_2, a conclusion generally consistent with EPR spectroscopy. The EPR data, though, are open to different interpretations, because hyperfine coupling tensors may be modeled in different ways. Zheng and Dismukes have modeled cw EPR data as arising from a III, III, III, IV configuration,[225] although other investigators obtain a better match with III, IV, IV, IV.[161] Good evidence for the latter assignment comes not from spectroscopy but from careful stoichiometric chemical reductions of the OEC, which eventually release Mn^{II} from the protein.[226] XAS investigations of the chemically reduced S_{-1} state indicate a III, III, III, III configuration,[227] and oxygen-evolution and reactivity studies of the stable S_{-3}, as well as the labile S_{-4} and S_{-5} states, are consistent with this analysis.[228]

Changes in manganese oxidation states are more confidently inferred from XANES and XES data than absolute oxidation states, and there is considerable agreement that at least three of the S-state transitions involve manganese oxidation. Early XANES[229] and UV/vis[230] experiments indicated manganese-based ($Mn^{III} \rightarrow Mn^{IV}$) oxidation in the $S_1 \rightarrow S_2$ transition, and this result has been confirmed several times since.[142,144,223,231−235] (These and other XAS results are reviewed in refs 48, 131−134, and 236). This implies a III, III, IV, IV oxidation state for S_1, if one takes the consensus assignment of III, IV, IV, IV for S_2. XANES and XES likewise indicate Mn-centered oxidation in the $S_0 \rightarrow S_1$ state,[144,223,233−235,237] so S_0 is presumably either II, III, IV, IV or III, III, III, IV. XANES of the S_{-1} state produced by treatment of the S_1 state with NH_2OH has been interpreted as indicating a III, III, III, III state,[221] which would imply a III, III, III, IV assignment for S_0. Recent ^{55}Mn ENDOR spectroscopy of the S_0 state leads to the same conclusion, with a notable absence of Mn^{II}.[65] However, some XAS and XES measurements have been taken to imply the presence of Mn^{II} in S_0.[222,232,235,237] Although there is mounting evidence for a III, III, III, IV formulation for S_0, it is too soon to announce a consensus. It is, indeed, possible that the two S_0 redox states are very near to one another in energy, so that one or the other predominates under different conditions.

The nature of the oxidation in the $S_2 \rightarrow S_3$ transition is hotly contested. Some XAS researchers contend that Mn is not oxidized in this step,[48,223,234] others the opposite.[144,235] Reference 132 and the appendix of ref 223 contain useful discussions of the experimental, data-analysis, and interpretative issues in this controversy. EPR spectroscopy indicates that the OEC is converted from a half-integer-spin to an integer-spin state, but this observation alone does not clinch the argument for manganese oxidation, because it is possible that a nearby oxygen or nitrogen radical couples to the manganese ions in the cluster to produce an overall integer-spin state. We think that manganese-based oxidations are most likely in all of the S-state transitions, giving a IV, IV, IV, IV oxidation state for S_3. Pecoraro has presented a thorough argument for this position based largely on an analysis of XANES edge energies from different groups, as well as by analogy with manganese model complex chemistry.[141] The all-IV S_3 assignment would explain the unusually low reactivity of S_3 with some exogenous reductants,[146] because the d^3 Mn(IV) ions are expected to be inert to ligand substitution reactions in an octahedral coordination geometry. In any case, it should be noted that there is unlikely to be

much (if any) correlation between the assigned formal manganese oxidation states and actual charge densities in the OEC. As recent results from resonant inelastic X-ray scattering have indicated, the electron lost in the $S_1 \rightarrow S_2$ step may be lost from a delocalized molecular orbital.[187]

4.3. The Proton-Release Pattern

Several groups have made accurate measurements of the proton-release stoichiometries in each of the S-state transitions. Indeed, the measured proton release stoichiometries in solution are non-integer and pH-dependent.[238−241,244,258,259,442] Many of the experiments have been performed on different protein preparations and at different pHs, both factors that cause substantial variation in results. The protons released are a combination of the protons derived from water itself and other indirect proton releases. These are presumed to be due to pH-dependent, electrostatically induced pK_a shifts in ionizable species in and around the OEC.[238] The intrinsic proton release pattern from the OEC in the four observable S-state transitions ($S_0 \rightarrow S_1$, $S_1 \rightarrow S_2$, $S_2 \rightarrow S_3$, and $S_3 \rightarrow [S_4] \rightarrow S_0$) appears to be around 1,1,1,1 in spinach PSII core preparations and around 1,0,1,2 in preparations that include more protein subunits.[238] These variations make interpretation a little difficult.[238,239] Broadly speaking, there have been those who consider that the results from the core preparations reveal more clearly the intimate workings of the OEC without complication by extraneous subunits and those who consider that the more complete, physiologically realistic preparations are reliable because they avoid the structural deformities of the core preparations.[211] This latter view is supported by the observations that (1) adding glycerol (a protein-stabilizing agent) to a core preparation restores the approximate 1,0,1,2 proton release pattern[240] and (2) a crystallizable core preparation, presumably highly homogeneous, exhibits the same pattern.[241]

As well as measuring the protons released by the protein, researchers have examined the changing electrostatic charge at the OEC by measuring electrochromic band shifts in chlorophyll UV/vis spectra.[242,243] Some work has confirmed a correlation, albeit imperfect, between these spectral shifts and the numbers of protons released from PSII-enriched membranes.[244,245] The yield and rate of production of the S_2 EPR multiline signal were early found to be independent of pH,[246] and although more precise experiments later found a marked pH dependence in the multiline intensity,[247] this does not reflect a pH dependence in the $S_1 \rightarrow S_2$ transition efficiency, which is unchanged between pH 4 and 8.[248] FTIR spectroscopy likewise discerns no effect of pH on the $S_1 \rightarrow S_2$ efficiency.[249] These studies point to a close link between the S-state transition proton-release stoichiometry and the charge developed at the OEC. Specifically, a positive charge appears to arise as a result of the $S_1 \rightarrow S_2$ transition, which correlates with the removal from the OEC of an electron but not a proton. Although other interpretations have been offered,[250] the charge-change interpretation of the chlorophyll UV/vis spectral data is strengthened by noting that the reduction of P_{680}^+ (i.e., oxidation of Y_Z) is slower in the $S_2 \rightarrow S_3$ and $S_3 \rightarrow [S_4] \rightarrow S_0$ transitions than in the two earlier transitions.[40,251,252] Still more notable is the increase in activation and reorganization energies in the latter two transitions, obtained by measuring the temperature-dependences of P_{680}^+ reduction.[156,253,254] As a consequence, the $S_1 \rightarrow S_2$ transition proceeds at temperatures as low as 140 K,[147] whereas the $S_0 \rightarrow S_1$ and $S_2 \rightarrow S_3$ steps proceed only above 220 K.[255,256] Additionally, Y_Z is not oxidizable at 5 K when the OEC is in the S_2 or the S_3 states, although it is in the lower S-states.[257] These observations are consistent with the development of a positive charge near the tyrosine in the second half of the catalytic cycle.

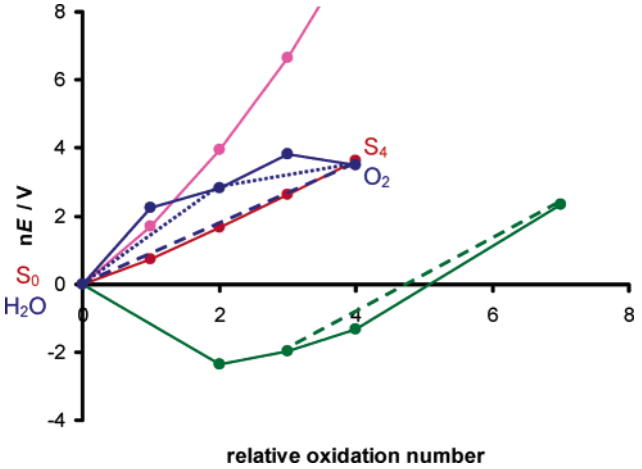

Figure 6. Frost diagram (*nE* vs relative oxidation number) showing the cumulative reduction potentials of four species: the OEC[307,383] in red (pH = 6, referenced to S_0); a single manganese ion[437] in green (pH = 6, referenced to Mn^0); a hypothetical manganese tetramer, without PCET, in magenta (see text for details, referenced to $Mn^{III}_3Mn^{IV}$); oxygen[437−439] in blue (pH = 6, referenced to $2H_2O$; the species shown on the solid blue line are $2H_2O$ (0), $H_2O + OH^\bullet$ (1), H_2O_2 (2), $O_2^{-\bullet}$ (3), and O_2 (4)). The blue long-dashed line represents the four-electron S_4/S_0 couple. The two blue short-dashed lines represent the two two-electron couples, S_4/S_2 and S_2/S_0. The green dashed line represents the Mn^{VII}/Mn^{III} couple. All reduction potentials are given versus the standard hydrogen electrode (SHE).

4.4. Thermodynamic Analysis of Water Splitting

Experimental efforts to understand the complicated redox chemistry of the OEC have been accompanied by theoretical considerations of the thermodynamics of water splitting. The OEC must precisely couple its redox chemistry to that of its substrate to ensure that a four-electron oxidation of water occurs, with little or no production of intermediate oxidized products (i.e., hydroxyl radicals, hydrogen peroxide, or superoxide). To put the problem more quantitatively, a Frost diagram of some important species is given in Figure 6.

In interpreting a Frost diagram, it is the *gradient* of a line connecting two oxidation states that is the important quantity, because this corresponds to the free energy of the redox reaction. The steeper the gradient, the greater the driving force ($-\Delta G$) for the conversion of the redox species higher in the diagram to the one lower in the diagram. With this in mind, we can immediately see that the four-electron oxidation of water to dioxygen (dashed blue line) is an energetically favorable path for the oxidation of water. It is certainly easier than four sequential one-electron oxidations, because in that case the first step (H_2O to $OH^\bullet$) is very endergonic. Two sequential two-electron oxidations (the dotted blue lines) look at first glance a more plausible route, and as we shall see below, this is actually the case.

The second fact highlighted by Figure 6 is that the one-electron reduction potentials of the OEC are controlled in such a way that by the time the S_4 state is attained, its four-electron accumulated oxidizing power is only just enough to oxidize water to oxygen. Experimental evidence has recently been obtained that the free energy change in the $S_4 \rightarrow S_0$ transition, with accompanying oxygen evolution, is a

mere −7 kJ mol^{-1}.[30] Even though the $S_3 \rightarrow S_4$ potential has not been measured, we can infer that the overpotential for water splitting is low by summing the potentials of the other transitions, which are approximately known, and remembering that the maximum potential available for the $S_3 \rightarrow S_4$ step is that of the $Y_Z^{\bullet}/Y_Z$ potential. This has been found to be ca. 100 mV below that of P_{680},[36] which in turn has been recently estimated to be about 1.25 V,[25,26] making the $Y_Z^{\bullet}/Y_Z$ potential somewhere around 1.0−1.2 V.

If the earlier S-state transitions were higher in potential, then there might be a risk of oxidizing water too soon in the S-state cycle, producing H_2O_2. However, as the potentials stand, this short-circuit reaction is unfeasible under normal catalytic conditions, because the S_2/S_0 two-electron couple (ca. 0.85 V) is considerably lower than the H_2O_2/H_2O couple (1.48 V). The OEC has been designed to increase its oxidizing power steadily, without the large successive increases in oxidation that one might expect if positive charges were constantly accumulating at the center (see below).

If we now turn our attention to the green data in Figure 6, representing free manganese, we see that a single ion of this element would be most ill-suited to the task of oxidizing water to dioxygen. The only suitable four-electron couple available would be Mn^{VII}/Mn^{III} (dashed green line), but it would be difficult to prevent the ion from being further reduced to Mn^{II}, which is a notable thermodynamic sink in the redox chemistry of isolated manganese. More comparable to the OEC are the magenta data in Figure 6, which show the estimated reduction potentials of a hypothetical manganese tetramer, which loses four electrons but no protons in its successive oxidations. We have used two pieces of experimental data to produce these estimates. The first is the reported reduction potential of ca. 1.7 V vs SHE for the $Mn_4^{III,III,IV,IV}/Mn_4^{III,III,III,IV}$ couple in an OEC model compound synthesized by Christou and co-workers.[260] We have used this as a rough estimate for the S_0/S_1 couple if proton transfer did not occur. The second experimental result that we have used is the successive ca. 0.54 V increase in reduction potentials of a dimeric manganese model compound undergoing three oxidations, from $Mn_2^{II,II}$ to $Mn_2^{III,IV}$.[261] (In contrast, PCET has been found to reduce the increase in successive reduction potentials in Mn complexes to a little over 0.1 V).[262] We see that the increases of these estimated "electron-only" reduction potentials of the OEC are extremely large, far higher than that of P_{680}^{+}. Indeed, this hypothetical S_2 state is high enough in energy that if it were attainable, it would certainly oxidize water to H_2O_2.

Careful and quantitative analysis of the thermodynamics of water splitting at the OEC has been carried out by Krishtalik.[263,264] He concluded that although the concerted four-electron process is the most energetically favorable (this is apparent from examining the reduction potentials), the reorganization energy for a true concerted four-electron oxidation is prohibitively high and a more likely reaction pathway is that of two two-electron reactions. Furthermore, this pathway (or any other pathway) would not be favored by strongly binding the partially oxidized intermediate(s), because whatever energetic advantage one thus gains in a certain step is lost in the succeeding step. Krishtalik reasoned that the reaction would instead be favored by strongly binding product protons throughout the cycle to a species whose pK_a varies according to the oxidation state of the manganese cluster. Such a base would be able to accept a proton from the OEC/water complex as it is oxidized and lose the proton before the next S-state transition, in preparation for the next proton-coupled electron transfer.

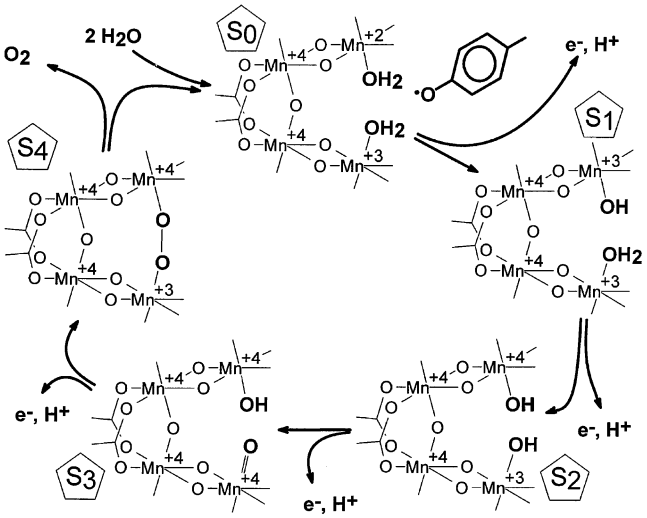

Figure 7. The Y_Z hydrogen-abstraction hypothesis advanced by Babcock and co-workers.[265] Note that this figure makes use of a "2 + 2" or "dimer-of-dimers" Mn arrangement, but the theory does not depend on this. Reprinted with permission from *Science* (http://www.aaas.org), ref 265. Copyright 1997 American Association for the Advancement of Science.

4.5. Tyrosine Z and the Hydrogen Abstraction Model

The immediate oxidant of the OEC Mn cluster, itself oxidized by P_{680}^{+}, is tyrosine-161 of the D1 subunit, Y_Z.[35,36] Babcock and co-workers,[265−268] along with Britt and co-workers,[88] were the first to suggest that this tyrosine might act as the redox-coupled base whose existence had been previously postulated by Krishtalik (Figure 7). These authors used several lines of evidence to reach this conclusion. First, they noted that ENDOR spectroscopy had shown that Y_Z was very close to the manganese cluster, at a distance of less than 5 Å.[88] (Later EPR work gave longer distances, see section 3.3). Second, they noted that EPR spectroscopy indicated that the hydrogen-bonding environment of Y_Z is disordered and complex,[269−273] which would be consistent with the mobility required if Y_Z were to dispose of its acquired proton to bulk. (This work was, however, conducted using OEC-depleted PSII particles, and degradation of the OEC has been found to affect its environment substantially).[84,156,274,275] Third, they noted that the O−H bond energy in the phenolic tyrosine side chain (362 kJ mol^{-1})[276] is similar to that measured in model manganese compounds. For instance, the bridging hydroxide ligand has a bond dissociation energy of 318 kJ mol^{-1} in $Mn^{III}Mn^{IV}$(μ-O, μ-OH)salpn$_2$, where salpn = *N*,*N*′-bis(salicylidene)-1,3-propanediamine.[277] This correspondence makes it plausible that the $Y_Z^{\bullet}$ radical might remove a hydrogen atom from water or hydroxide that is coordinated to high-valent manganese.

It is important to stress that the pK_a's of the reduced and oxidized forms of tyrosine are very different (ca. 10 and −2, respectively),[278] so it is likely that the residue will both gain a proton upon reduction and lose a proton upon oxidation. There is, indeed, experimental evidence for this in the case of Y_Z, from pH and isotope effects examined by UV/vis and EPR spectroscopy.[270,275,279−281] (Some optical spectroscopic studies have suggested that reduced Y_Z exists as a tyro-

sinate[282]—see, though, ref 211. Nugent and co-workers have argued that Y_Z exists as a tyrosinate, for example in ref 283). A concerted electron/proton-transfer mechanism has been indicated by a recent thermodynamic analysis in manganese-depleted PSII.[284] It is particularly revealing that the nanosecond H/D kinetic isotope effect of Y_Z oxidation in the intact OEC is almost unity,[154,157,270,285−287] a result that is consistent with the presence of a hydrogen-bonding network stabilized by the complete cluster, which would facilitate proton movement around Y_Z.[288−292] D1-His190 is widely believed to be the immediate proton-exchange partner for Y_Z, on the basis of experiments conducted on site-directed mutants[168,169,280,281,293] and, now, on the basis of the PSII crystallographic structure.[52,53] Since Y_Z may be photooxidized at very low temperatures (5 K), at least in the lower S-states, it has been suggested that the side chain accepts and releases its proton via a short hydrogen bond,[257,294] as the analogous tyrosine, Y_D, is proposed to do in the D2 subunit.[295−298] The debate as to whether Y_Z^- is really protonated or not is to some extent semantic; it may be that the proton, both in the oxidized and in the reduced states of Y_Z, is located somewhere between the phenolic oxygen and its hydrogen-bonding partner. It has been suggested[252] and subsequently discussed[39,286] that Y_Z (or Y_D or both) might be linked to its histidine proton acceptor via symmetric "low-barrier hydrogen bonds".[299] If such a bond existed, it would imply that the pK_a's of the paired tyrosines and histidines were the same. The proton-coupled redox chemistry of Y_Z and Y_D is discussed in a recent review.[34]

Although the precise location of the Y_Z proton may not be crucial, the source and destination of the proton are certainly important. Contrary to the hydrogen-abstraction hypothesis, during the S-state transition the *same* proton might remain near Y_Z, moving only the small distance between Y_Z and D1-His190 according to the redox state of Y_Z. This "proton-rocking" hypothesis has been notably espoused by Junge, Rappaport, and Renger, along with their respective co-workers, largely on the basis of time-resolved optical spectroscopy and proton release measurements.[252,275,286,300−302] Additional evidence for this theory comes from the observation that proton release coupled to Y_Z oxidation is found (albeit in Mn-depleted protein) to be pH-independent below pH 5, whereas the pK_a of $Y_Z^{+\bullet}$ is −2.[300] According to the proton-rocking hypothesis, oxidation and reduction of Y_Z exerts a variable electrostatic effect on the OEC through the constrained movement of this proton. This hypothesis has been more recently adopted to explain results obtained from EPR spectroscopy,[285,303−305] with Petrouleas and co-workers describing Y_Z as an electron abstractor (when it oxidizes the OEC) and proton repeller (when it is itself oxidized by P_{680}^+).[303] Styring and co-workers have also published detailed models of the reactions of Y_Z in different S-states and protonation states of the OEC,[92,247,248,257,306−308] paying particular attention to the pH-dependent redox equilibria between the states $S_nY_Z^\bullet$ and $S_{n+1}Y_Z$.

5. Proposed Mechanisms of Oxygen Evolution

5.1. Historical Overview

There have been many proposals for the mechanism of water oxidation over the years. The first substantial efforts came in the late 1970s (see, for instance, ref 309), although these were hampered by the scanty experimental data available at the time (reviewed in refs 58 and 310). The 1980s saw the first structural proposals for oxygen evolution from the OEC.[205,311] These made use of advances in inorganic model chemistry[312] and postulated that the O−O bond of dioxygen formed between two manganese-bridging μ-oxide ions. This reaction was suggested to occur either in an adamantane-like Mn_4O_6 cluster[205] or in a cubane-like Mn_4O_4 cluster,[311] both structures being formed late in the S-state cycle. Reviews of the state of opinion in this period may be found in refs 80, 298, and 313−316. A selection of more recent reviews and proposals are to be found in refs 20, 39−41, 78, 79, 83, 131, 134, 162, 211, 265, 278, 283, 315, and 317−326. Because there are so many mechanistic proposals, it is impossible to examine or even to mention them all. We have chosen a few of the more prominent hypotheses that we think demonstrate important topics in the field.

5.2. Some Current Proposals for Water Oxidation Categorized by the Method of O–O Bond Formation

5.2.1. Coupling Reactions Involving an Oxyl Radical

As noted in section 4.2, there is some XANES evidence that the $S_2 \rightarrow S_3$ transition involves the oxidation of a species other than a manganese ion. This observation has inspired a number of mechanistic proposals in which the S_3 state of the OEC comprises an oxyl radical, which goes on to react with another oxygen atom in the S_4 state to produce dioxygen.

Yachandra and Co-workers. Yachandra and co-workers have proposed[48,83,236] that the oxidations in both the $S_2 \rightarrow S_3$ and $S_3 \rightarrow S_4$ transitions are centered on manganese-bound oxygen atoms, rather than on the manganese ions themselves. The resulting radicals are then suggested to couple together, forming the O−O bond of dioxygen (Figure 8). If both of the oxyl radicals are manganese-bridging μ-oxos, this implies a μ-η^2:η^2-peroxo intermediate.[83,236] This reaction has a precedent in dimeric copper chemistry, where under some circumstances there is a finely balanced equilibrium between the bis(μ-oxo)dicopper(III) and the (μ-η^2:η^2-peroxo)dicopper(II) form (Figure 9).[327−329]

The oxidation of a manganese-bridging oxide in the $S_2 \rightarrow S_3$ transition is compatible with the increase in the average Mn−Mn distance seen by EXAFS,[145] as well as with the view that XANES data do not support a manganese-centered oxidation in this step.[223] The second oxyl radical, formed in the $S_3 \rightarrow S_4$ transition, has been suggested to be a bridging, terminal, or exogenous oxygen.[48,330] The shortening of what seems to be a 2.85 Å Mn···Mn distance in the S_0 state to a 2.7 Å distance in S_1[143,331] inspired the suggestion that a μ-oxo bridge is deprotonated in the $S_0 \rightarrow S_1$ step.[236,332]

The proposal of Yachandra and co-workers was originally incorporated into the then-prevailing 2 + 2 "dimer-of-dimers" structural model of the manganese cluster, which was mostly based on EXAFS measurements.[135,333] This structure was later found to be incompatible with ^{55}Mn ENDOR results,[64] which indicated instead a 3 + 1 arrangement of Mn ions (see section 3.3). The proposal that bridging oxyl radicals couple to form dioxygen is, however, compatible with more recent structural proposals, as shown in Figure 8.[48] These are consistent with both EXAFS and pulsed EPR data and can incorporate calcium into the OEC.[131,330,332]

Messinger and Co-workers. Messinger has recently formulated a detailed mechanistic cycle[334] using a slight

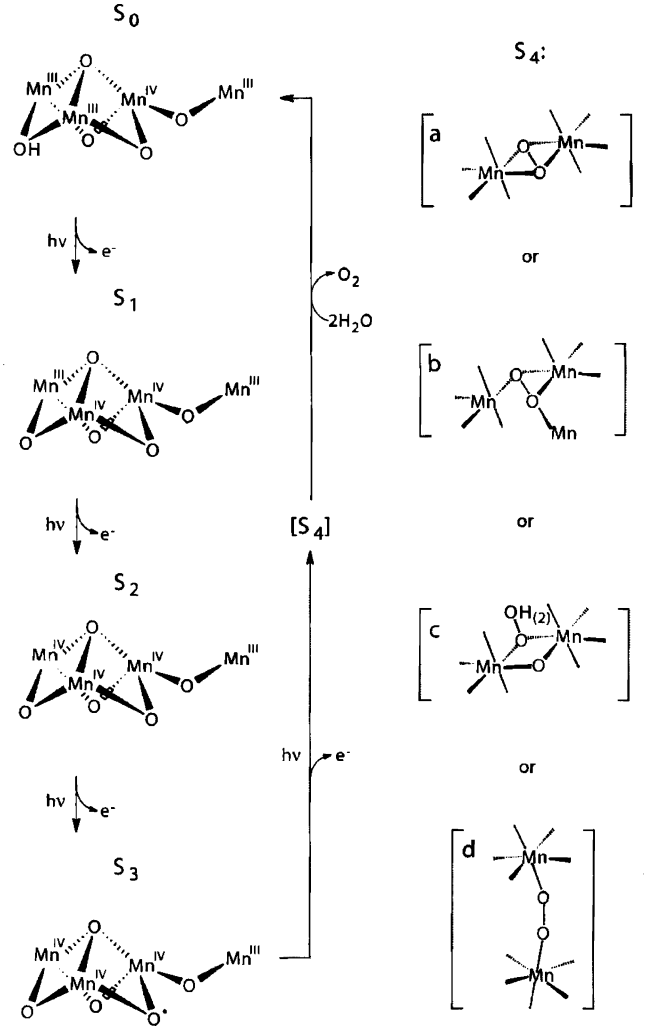

Figure 8. Recent mechanistic proposal of Yachandra and co-workers. Reprinted from ref 48. Copyright 2005 Springer.

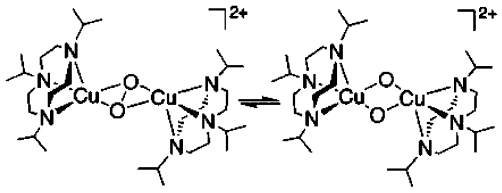

Figure 9. Characterized equilibrium between bis(μ-oxo)dicopper(III) and (μ-η^2:η^2-peroxo)dicopper(II) from the work of Tolman and co-workers. Reprinted from ref 329. Copyright 2004 American Chemical Society.

modification of the 3.5 Å resolution crystallographic model of the OEC.[53] Although a "nucleophilic attack" mechanism (see section 5.2.3) was seriously considered, the author ultimately favored a radical mechanism, in which the O−O bond is formed by the radical coupling of a terminal O atom (bound to Mn(4)) with a μ_3-oxide ligand of the cuboidal cluster (see Figure 10).

A major advantage of this scheme is that it provides a clear rationale for the shortening of a Mn···Mn distance from 2.85 to 2.7 Å in the $S_0 \rightarrow S_1$ transition[29] by proposing in this step the deprotonation of a Mn-bridging μ-oxo ligand in the cuboidal cluster. The surprising mass spectrometric finding that the substrate water molecule with the slower rate of exchange with bulk water (k_{ex}) is associated with calcium[85] is explained by including this water as a μ_3-bridging oxide ligand between calcium, Mn(2), and Mn(3). Furthermore, this substrate μ_3-oxide is somewhat disconnected from Mn(4) by modifying the crystallographic model of Ferreira et al.,[53] linking Mn(4) to the cuboidal cluster not via the substrate oxide but by a μ_2-oxo bridge to Mn(3). This was done to accommodate a second mass spectrometric finding, that the slower-exchanging substrate water increases its k_{ex} roughly 100-fold in the $S_1 \rightarrow S_2$ transition, that is, upon the oxidation of Mn(4). It was furthermore found necessary to suggest a change in the hydrogen bonding of this substrate oxygen (the formation of a new hydrogen bond with the other substrate water) in order to comprehend the *increase* in k_{ex} upon manganese oxidation.

Siegbahn and Co-workers. Siegbahn and co-workers have used density functional calculations to examine the mechanism of water splitting. Previous results from this group suggested the likelihood of oxyl radical formation in the S_3 or S_4 state.[322] They have applied their methods most recently to the 3.5 Å resolution crystallographic structure of the OEC.[208,335] Their results indicate that a structural change is required in order to attain the S_3 state, a change suggested to be induced by the oxidation of Mn(4) (see Figure 5) and the associated deprotonation of a water ligand of Mn(3) in the $S_2 \rightarrow S_3$ transition. Calculations indicate that this newly formed hydroxide now ligates Mn(4), forming a new μ-oxo bridge between the two manganese atoms. This result is in agreement with the EXAFS experiments of Dau and co-workers[134] (see below), which were interpreted by the authors to indicate the formation of a new 2.7 Å Mn···Mn distance in this step. It is suggested that this bridging hydroxyl provides one of the dioxygen oxygen atoms, the other coming from external water.[322,335] However, analysis of this final O−O bond-forming step has not been completed.

Dau and Co-workers. Dau and co-workers[134] have suggested that the O−O bond is formed by the reaction of a hydroxyl radical with a terminal oxyl radical species in the S_4 state (Figure 11A). An important feature of this model is that the Mn−μ-oxide moieties act as redox-active bases in the water-splitting reaction, a role previously suggested by Messinger, Wydrzynski, and co-workers.[336] They are suggested to abstract hydrogen atoms from the substrate water molecules late in the S-state cycle, with the manganese ion accepting an electron and the μ-oxide accepting a proton. The first such hydrogen abstraction, from an exogenous water molecule, gives a hydrogen-bonded hydroxyl radical. After this has reacted with a terminal oxyl ligand to form a manganese-bound peroxo intermediate, another Mn−μ-oxide moiety abstracts a hydrogen atom to induce dioxygen loss.

The authors account for their EXAFS data in all four accessible S-states[134,144,193,337] by proposing the following: (a) the deprotonation of a μ-oxide ligand in the $S_0 \rightarrow S_1$ step, resulting in the shortening of this Mn···Mn distance from 2.85 to 2.7 Å and (b) the formation of a new μ-oxide bridge in the $S_2 \rightarrow S_3$ transition (Figure 11B). The latter accounts for the appearance of a new 2.7 Å Mn···Mn vector in the S_3 state and is also compatible with the idea that the $S_2 \rightarrow S_3$ transition involves some structural reorganization (see section 3.3). Dau and co-workers further hypothesize that the formation of this new μ-oxo bridge is induced by the oxidation of a five-coordinate, Jahn−Teller-stabilized Mn^{III} ion in the S_2 state to the Mn^{IV} oxidation state in S_3.[134]

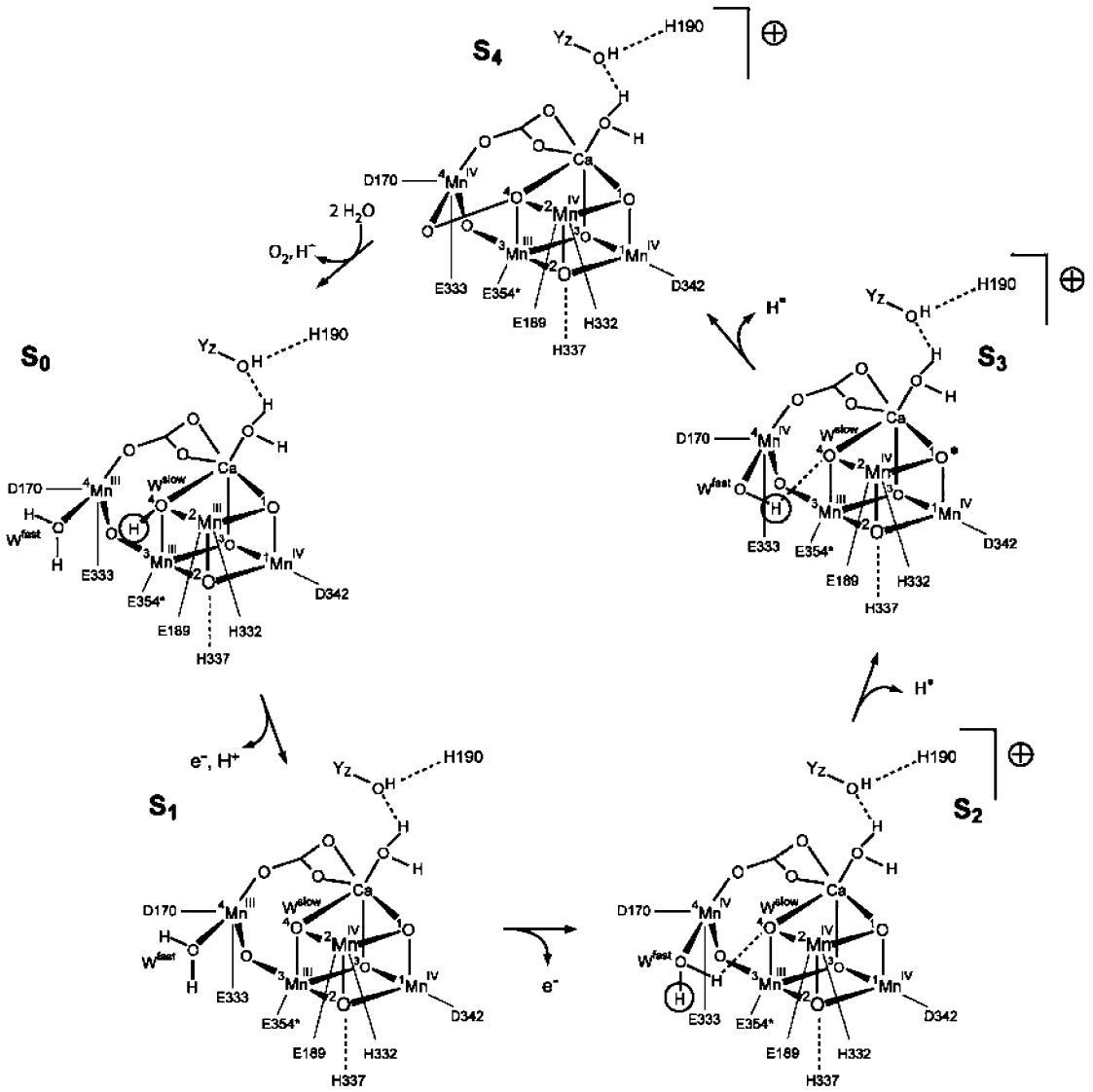

Figure 10. Recent mechanistic proposal of Messinger, based in part upon the crystallographic model of Ferreira et al.[53] Reprinted with permission of the PCCP Owner Societies from ref 334. Copyright 2004 Royal Society of Chemistry.

5.2.2. Coupling of Two Mn-Bridging Oxo Ligands across the Face of a Cuboidal Cluster

Dismukes and co-workers have advanced the "Jack-in-the-Box" hypothesis of dioxygen formation, based on the reactivity of their model tetranuclear Mn_4O_4 complexes.[338] Their proposal is a version of the "double-pivot" mechanism of Vincent and Christou,[311] one of the earliest structural mechanistic proposals for the operation of the OEC (Figure 12). The cuboidal cluster is proposed to convert upon oxidation to a Mn_4O_2 "butterfly" core arrangement, losing two oxygen atoms in the form of dioxygen.

As may be seen from Figure 12, both oxygens of the bound peroxide intermediate are coordinated by three manganese ions. An early theoretical study of the reactivity of an OEC model compound using the extended Hückel method concluded that there was an advantage in coordinating a peroxy intermediate in O_2 evolution (the S_4' state) by three or even four Mn ions.[339] (An alternative, planar geometry for the tetracoordination of this species was proposed earlier by Lippard and co-workers).[340]

There is evidence for this mechanism of dioxygen production in the gas phase[338] where it is stimulated by the absorption of low-wavelength UV radiation. Absorption (even at higher powers) of higher-wavelength radiation did not have the same effect, pointing to a specific photolytic reaction rather than to a thermal origin. (Manganese oxide compounds are known in general to release dioxygen upon heating; see, for example, ref 341). To strengthen this interpretation, other manganese−oxo complexes treated in the same way did not produce dioxygen in significant yield.[342] Dismukes and co-workers have also used their tetrameric compounds, in combination with a peroxide oxidant, to oxidize organic substrates. One proposed mechanism is via a reactive Mn^V═O intermediate.[343] Such intermediates have been characterized in UV-treated Mn-porphyrins.[344,345]

In solution, proton-coupled *reduction* of the inorganic Mn_4O_4 complex has been found to induce the loss of two μ-oxo bridges as water and to form the Mn_4O_2 "butterfly" product. This is the reverse of a hypothesized hydration reaction, constituting *oxidative* formation of the cuboidal cluster, which might then further react oxidatively as it does in the gas phase (see above).[346] Indeed it is on the basis of these reductive experiments in solution that the gas-phase photolyzed product has been assigned, because it has not

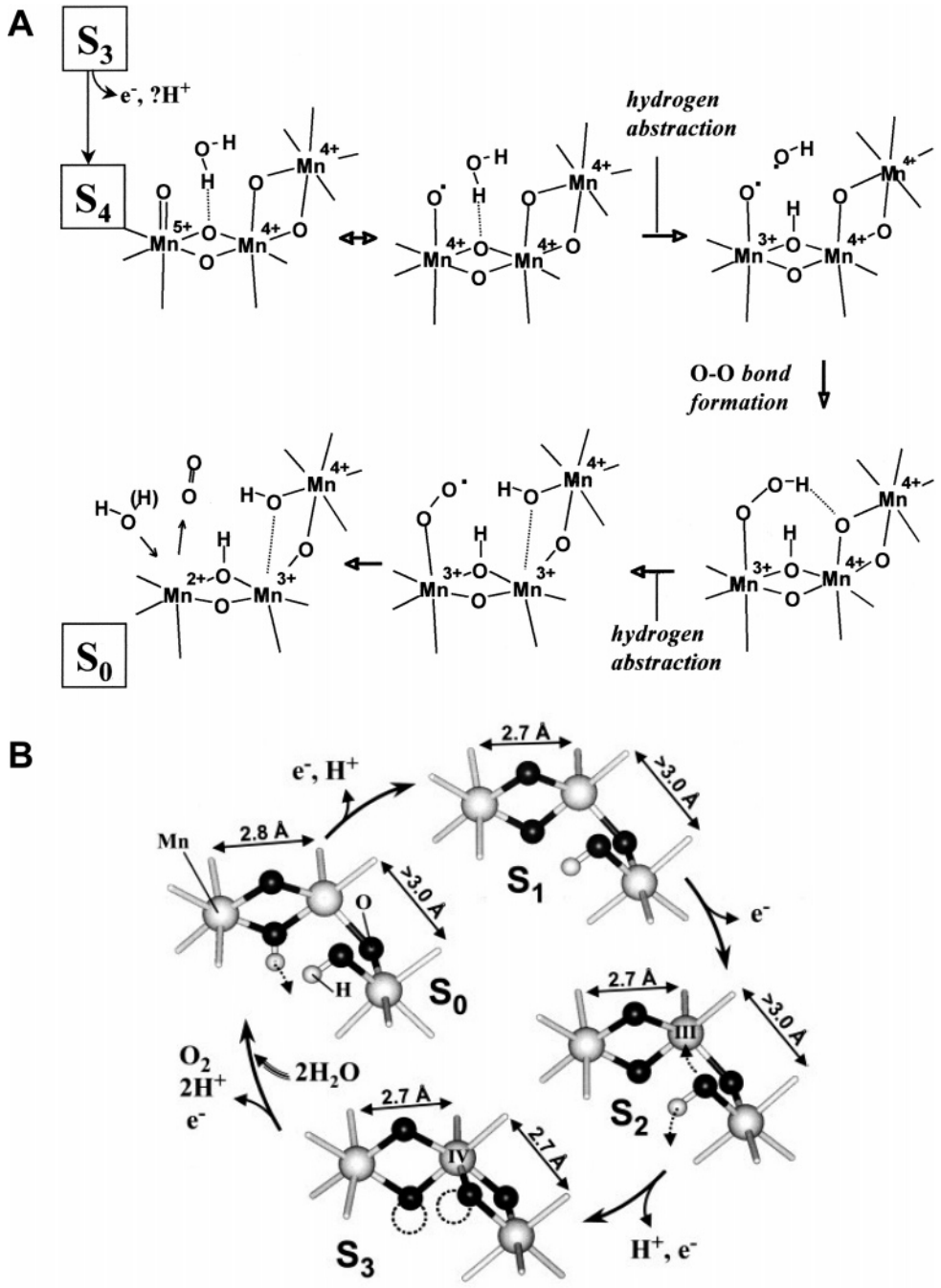

Figure 11. Mechanistic proposal of Dau and co-workers. Part A deals with the O−O bond-forming reaction ($S_3 \rightarrow [S_4] \rightarrow S_0$), while part B assigns OEC structures, based on EXAFS measurements, throughout the S-state cycle. Part A reprinted with permission from ref 134. Copyright 2001 Elsevier. Part B reprinted from ref 144. Copyright 2005 American Chemical Society.

itself been isolated or characterized. The proton-coupled reductions of the tetrameric complexes have been extensively analyzed.[347,348] A particularly interesting result is that the O−H bond at the μ_3 corner oxide in the $Mn_4^{IV,IV,III,III}$ complex is considerably stronger than the tyrosine phenol O−H bond,[348] arguing against the likelihood of hydrogen atom abstraction from this position in the OEC by Y_Z.

5.2.3. Attack of a Terminally Bound Water or Hydroxide upon a Terminal Mn^V═O

Precedents in Model Chemistry. Naruta and co-workers have characterized a dinuclear Mn^V porphyrin complex that oxidizes water to dioxygen, potentially catalytically (see Figure 13).[349]

Oxomanganese(V) porphyrin complexes have been characterized previously (see, for examples, refs 344 and 345) and can perform organic oxidations.[350−352] More stable nonporphyrin Mn^V oxo compounds are also known,[353−356] which may be activated as oxidants by tuning the electron-donating properties of the Mn ligands.[357] A dimeric $Mn_2^{III,IV}$ compound that evolves dioxygen upon chemical oxidation has been postulated to act via a terminal Mn^V═O intermediate.[358,359] The longest-studied catalyst of water oxidation to dioxygen is the Ru_2 dimer family,[360,361] which also appears to operate via a terminal Ru^V═O species.[362,363] The first to suggest a comparable "nucleophilic attack" mechanism of O−O bond formation in the OEC were Messinger, Wydrzynski, and coworkers.[336]

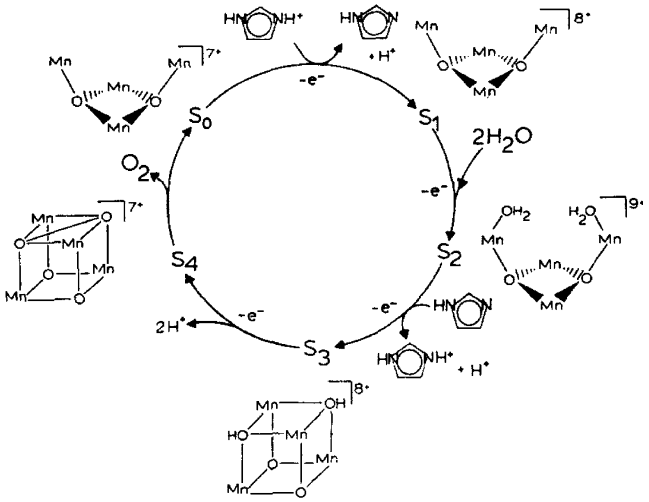

Figure 12. Mechanistic proposal of Christou and co-workers. Dismukes and co-workers also favor a Mn_4 cuboid/butterfly cycle, with O−O presumably formed across the face of the cuboidal form of the OEC. Reprinted with permission from ref 311. Copyright 1987 Elsevier.

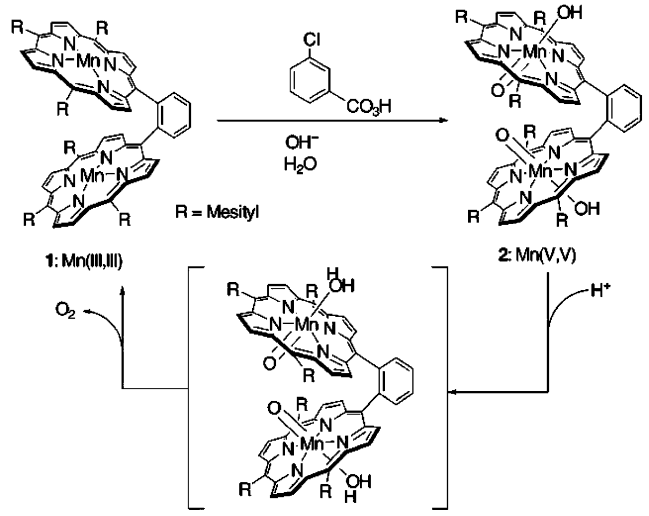

Figure 13. Linked Mn porphyrin complex of Naruta and co-workers, oxidizable to the Mn^V, Mn^V state with subsequent loss of dioxygen. Reprinted with permission from ref 349. Copyright 2004 John Wiley and Sons.

Mn−OH as Attacking Group: Separation of Oxidizing Power from Substrate Waters. Wydrzynski and co-workers have advanced a theory of water splitting in the OEC on the basis of their measurements of the rates of exchange (k_{ex}) of ligand waters in various S-states. These results may be summarized as follows. They have found, first, that at least one substrate water molecule is bound throughout the catalytic cycle, and the other at least by S_2.[364] Each has a distinctly different k_{ex} up to and including the S_3 state, presumably indicating chemically different coordination and, therefore, that O−O bond formation is delayed until the S_4 state (or, perhaps, the $S_3Y_Z^\bullet$ state, see below). Second, these waters (in whatever protonation state) are able to exchange with bulk water on the second time scale up to the S_3 state. Although measurements of manganese μ-oxo ligand exchange rates were not available, Wydrzynski and co-workers proposed, on the basis of comparison with some other metal−oxo complexes, that these OEC exchange rates are too fast to be consistent with manganese−μ-oxo exchange.[365] They conclude from this that the two substrate waters are

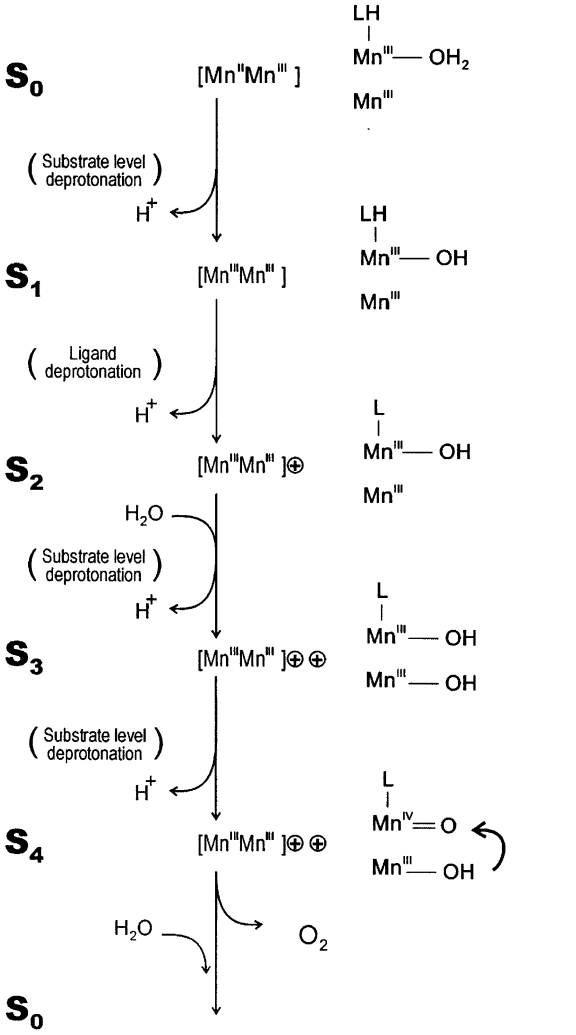

Figure 14. Mechanistic proposal of Wydrzynski and co-workers, based on time-resolved mass-spectrometric measurements tracking ^{18}O. Reprinted from ref 440. Copyright 2000 American Chemical Society.

bound as terminal ligands to manganese. Third, principally because of an *increase* in the slower k_{ex} on going from $S_1 \rightarrow S_2$, which they take to be incompatible with the oxidation of a substrate-water-binding manganese, Wydrzynski and co-workers suggest that the substrate-water-binding manganese ions are separate from those manganese ions that are oxidized in the first three S-state transitions (Figure 14).[365] This is reminiscent of a much earlier proposal by Wydrzynski,[366] as well as a contemporary proposal by Pace and co-workers.[367,368]

Renger and co-workers have proposed that the O−O bond is formed in a bound peroxide redox isomer of S_3, which dominates in the $S_3Y_Z^\bullet$ state.[39,40] In fact, in our nomenclature, this corresponds to an equilibrium between the $S_3Y_Z^\bullet$ and $S_3'Y_Z^\bullet$ states. This proposal accounts for the very quick release of O_2 upon oxidation of the OEC by $Y_Z^\bullet$,[301,369] leading in this proposal not to a distinct S_4 state but directly to $S_0(O_2)$. A longer lag phase has been reported in the $S_3Y_Z^\bullet \rightarrow S_0Y_Z$ step, however,[370] which might more easily accommodate the formation of a discrete S_4 intermediate.

Ca−OH or Ca−OH_2 as Attacking Group. Pecoraro and co-workers (see Figure 15),[78] as well as ourselves,[79,81] have postulated a specific role for calcium in ligating one of the substrate waters. This ligated water[79] or hydroxide[78] forms

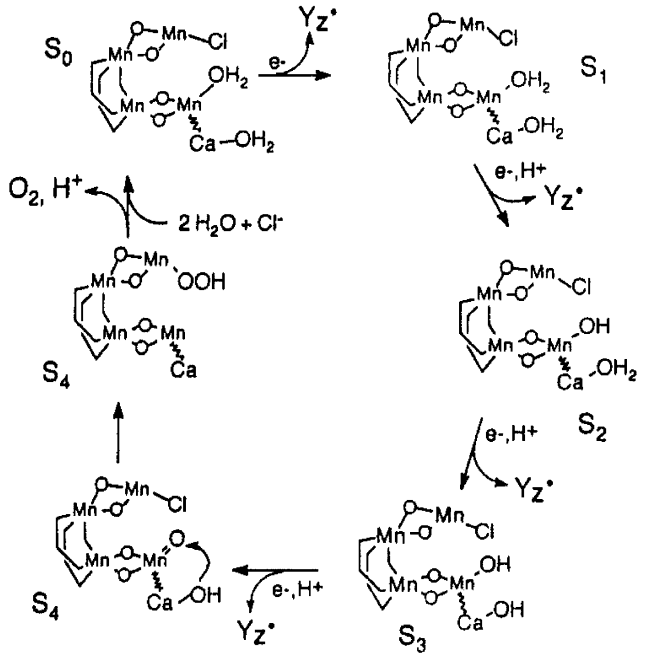

Figure 15. Mechanistic proposal of Pecoraro and co-workers, incorporating a dimer-of-dimers Mn structure along with the Y_Z hydrogen abstraction hypothesis. The O−O bond is formed by the attack of a calcium-bound hydroxide upon a Mn=O group. Reprinted with permission from ref 78. Copyright 1998 IUPAC.

the O−O bond of O_2 by attacking the oxygen of a terminal Mn^{V}=O species in the S_4 state (Figure 15).

Hendry and Wydrzynski have provided direct evidence from ^{18}O-exchange mass spectrometry measurements[85] that calcium is involved in binding one of the substrate waters. Upon calcium depletion and reconstitution of the OEC with strontium, the k_{ex} value of the *slower-exchanging* substrate water increased by around 3−4-fold, while that of the faster-exchanging substrate water was unchanged. The authors of the study noted that one could interpret this result by assuming that calcium (or strontium) ligates the slow-exchanging substrate water, whereas the faster-exchanging water is bound only to manganese.[85] It is important to note that the k_{ex} of the slower-exchanging water was found to be around 10^8 times slower than the k_{ex} value of $\geq 10^8$ s^{-1} found for $[Ca(H_2O)_6]^{2+}$ by acoustic methods.[443] Hendry and Wydrzynski accounted for this discrepancy by hypothesizing that the calcium-bound, slow-exchanging water is bound in one of two ways: either as a bridging ligand between Ca^{2+} and one of the Mn ions or by forming a hydrogen bond to a bridging oxygen atom of a $Mn_2(\mu\text{-}O)_2$ unit.[85] Hendry and Wydrzynski quantified their analysis by applying the Eyring relation to the pK_a's of the two hydrated ions, $[Ca(H_2O)_6]^{2+}$ or $[Sr(H_2O)_6]^{2+}$. This is because both the hydration enthalpies and the pK_a's of hydrated divalent metal ions are proportional to Z^2/r, where Z is the charge of the cation and r is the length of the M−O bond.[371] (Intuitively, we recognize that more acidic hydrated cations, with large Z^2/r values, have stronger M−O bonds, which means that they exhibit low k_{ex} values.) If we assume that the entropies of hydration are similar, one can write $\log(k'/k) \approx \Delta(\Delta G_{hydration}) \approx \Delta pK_a$. The 3−4-fold difference between k_{ex}^{Ca} and k_{ex}^{Sr} matches the 0.51[372] difference between the pK_a's of $[Ca(H_2O)_6]^{2+}$ and $[Sr(H_2O)_6]^{2+}$ ($\log 3.2 = 0.51$). This correlation was surprising, because it implies that Ca^{2+} binds the slow-exchanging water while the fast-exchanging water is presumably bound to Mn^{3+} or Mn^{4+}.[85] As noted above, Hendry and Wydrzynski hypothesized that the slow-exchanging substrate water is associated with both calcium and manganese.[85] However, quantum mechanical calculations indicate that calcium's real electrostatic charge in the OEC is likely to be higher than that of the manganese ions, making possible the terminal ligation of the slow-exchanging substrate water to calcium.[188] Additionally, on the basis of manganese model-compound studies, a metal-bridging water is likely to exchange with bulk very much more slowly than either k_{ex} observed in the OEC.[373] Finally, we must consider not only the intrinsic substitution kinetics of the metal ions in the OEC but also the ease with which water can access each of the metal ions. Both the 3.0 Å and the 3.5 Å resolution crystal structures show that the start of the proton-exit channel (D1-Asp61) is close to Mn(4) and far from Ca^{2+}.[52,53] This channel is probably full of water, serving as the conduit for water exchange.[189] If Mn(4) binds substrate water, then one would expect this water to move in and out of the protein more rapidly than the calcium-bound water, other things being equal. It is possible that the variation of the slow-exchanging substrate water's k_{ex} with S-state (notably a 100-fold increase on going from S_1 to S_2) is due to changes in hydrogen-bonding connections around the OEC that permit or block water movement to calcium.

Evidence that calcium has a mechanistic role also comes from work in which a variety of mono-, di-, and trivalent metal ions were substituted into the calcium site.[374] Results are consistent with a size-selective binding site, preferentially binding those di- and trivalent ions that are similar in size to calcium. Strikingly, however, only Sr^{2+} is found to restore oxygen-evolving activity to a significant extent.[68,374−376] We conclude that it is the similarity in the pK_a of the calcium and strontium metal−aqua complexes that accounts for strontium's restorative ability.[374] Cd^{2+}, although very similar to Ca^{2+} in ionic radius,[276] forms a hexaqua ion with a pK_a almost four units lower than that of Ca^{2+} [372] and does not restore oxygen evolution. This has been interpreted to mean that metal-bound *water*, rather than hydroxide, is the active species in nucleophilic attack of the proposed Mn^{V}=O species.[79] EXAFS spectroscopy has shown that replacing calcium with either Sr^{2+} or Dy^{3+} has little effect on the structure of the OEC.[82,138] Based on the observation that the binding of di- and trivalent cations to the OEC is equivalently dependent on their ionic radii, it was concluded that Dy^{3+} might bind as a divalent Dy^{3+}−OH unit, with a net charge of +2.[374] These results also indicate that Ca^{2+} binds water, giving the moiety an overall charge of +2, rather than hydroxide, which would give a charge of +1. This conclusion is again consistent with the reaction of a calcium-bound water in the O−O bond-forming step.

6. Discussion of Proposed Mechanisms

Such is the size and complexity of the literature on PSII that it is possible to find some experimental support for all of the above ideas. Having said that, we feel that there are some key features that must be included in a useful model and, likewise, some data that definitely weigh against some of the proposals. For instance, models that invoke the incorporation of one or both of the substrate waters as metal-bridging oxo units are disadvantaged by the relatively fast rates of substrate/bulk water exchange measured by time-resolved mass spectrometry.[365] Recent results from our laboratory,[373] as well as examination of other high-valent

metal−oxo complexes,[365] indicate that rates of μ-oxo ligand exchange within the OEC, in any of the S-states, would be several orders of magnitude slower than the observed rates of substrate water exchange. This indicates that the substrate waters are incorporated into the OEC as terminal ligands, not as μ-oxo ligands, up through the S_3 state.

The two mechanistic elements that we feel are particularly important to address are these: the role of calcium in the OEC and the movement of protons away from the OEC. The fact that several metals can replace calcium in the OEC *structurally*[72,74−76,82,137,375,377−380] but that optimal catalytic activity depends principally on the metal's acid/base properties[374] seems to us highly significant. The most recent crystallographic models of the OEC[52,53] are consistent with the reaction of a calcium-bound terminal water with a terminal oxo group on the dangler Mn(4) ion[189,381] and thus with the proposals of Pecoraro and co-workers[78] and ourselves.[79] Oxygen atoms bound to metal ions separated by 4.6 Å (ref 52) or 3.9 Å (ref 53) may come close enough together to react in the S_4 state. As mentioned above (section 5.2.3), the binding of a substrate water to calcium is also supported by ^{18}O mass spectrometry.[85] It should be noted, though, that the crystal structure is not of a sufficiently high resolution to identify water molecules, and their locations must be inferred from simple coordination chemistry[53,382] or, better, from computational modeling.[188,189,381]

On the subject of proton transfer, it is important to note that coupled proton and electron transfers appear to be particularly important in the $S_2 \rightarrow S_3$ and the $S_3 \rightarrow [S_4] \rightarrow S_0$ transitions. It is these transitions, in the latter half of the catalytic cycle, that operate with the lowest driving energies[30,383] and are, therefore, most in need of thermodynamic assistance obtained from strong proton binding.[263] This is corroborated by the fact that in PSII-enriched membranes, only the $S_2 \rightarrow S_3$ and the $S_3 \rightarrow [S_4] \rightarrow S_0$ transitions are blocked at high pH, with apparent pK_a's of deactivation of 9.4 and 8.0, respectively.[248] It is hypothesized that this deactivation is associated with a decrease in the reduction potential of Y_Z so that it is unable to oxidize the OEC in the higher S-states.[248] (*T. elongatus* core complexes reveal no such high-pH block in their $S_2 \rightarrow S_3$ and $S_3 \rightarrow [S_4] \rightarrow S_0$ transitions, an observation that may correspond with the lower reduction potentials of the OEC in the S_2 and S_3 states in *T. elongatus* PSII than in spinach PSII).[249] Furthermore, as previously discussed in section 4.3, ET between the OEC and P_{680}^+ is markedly slower in the S-state transitions beyond S_2 than in the early steps,[40,251,252] and these steps have greater activation and reorganization energies than the previous steps.[156,253,254] We remind the reader that it is the $S_2 \rightarrow S_3$ step that is blocked by the absence of calcium[72−74,87−89] or chloride,[89,96,105,107,108] as well as by the presence of fluoride[104,109,112,147,148] and acetate[89,149−153] inhibitors. The sensitivity of this step to these inhibitory treatments may be related to the transition's peculiar dependence on PCET. There is evidence that calcium[84,92] and chloride[109] are involved in the maintenance of a hydrogen-bonded network around the OEC and that their removal disturbs proton transfer. Acetate, the best-studied of the inhibitors, binds competitively with chloride[101] and, by presenting a methyl group in place of chloride, presumably disrupts the native hydrogen-bonding environment.

These considerations have made it important to understand the precise mechanism of proton transfer away from the OEC during turnover. Both Pecoraro[78] and ourselves[79] adopted the idea of tyrosine Z as a hydrogen atom abstractor,[88,265−267] at least in some of the S-state transitions. The recent X-ray crystal structures[52,53] show the phenolic oxygen of Y_Z to be 5 Å away from calcium, the closest cluster atom, and 8 Å away from the furthest manganese atoms, distances that are consistent with recent EPR measurements.[163−166] Although this distance between the cluster and Y_Z is too long for a Mn-coordinated water to lose its protons directly to Y_Z, it would still be possible to envisage proton transfer through an intermediary water or hydroxide.[384] However, the crystal structure also indicates that there is a proton-exit pathway of acid/base amino acid residues (within a mostly hydrophobic region), which leads away from the OEC cluster to the lumenal surface at roughly 90° to the cluster···Y_Z vector. Y_Z is shown to be within hydrogen-bonding distance of D1-His190, as predicted,[168,169,280,281,293] but neither residue is connected to this proton-exit pathway. While it is possible that future, better-resolved structures will show that Y_Z is, after all, connected to the proton exit channel (perhaps by D1-Gln165), the balance of evidence has significantly shifted away from the idea that Y_Z acts as a catalytic base. What species, then, does extract protons from the OEC/water complex?

7. Development of a Structure-Based Mechanism of Water Splitting

7.1. Proposed Identity of the Redox-Coupled Catalytic Base

Both the 3.5 Å resolution[53] and the 3.0 Å resolution[52] X-ray crystal structures show that the side chain of an arginine residue, CP43-Arg357, approaches close to the proposed "active face" of the OEC cluster, between Ca^{2+} and the dangler Mn(4). Both structures show that the distance between the closest nitrogen of the arginine side chain and Mn(4) is about 5 Å. Molecular-mechanics calculations, based on the 3.5 Å resolution crystallographic structure, show that the guanidinium side chain plausibly makes several hydrogen-bonding contacts with the water or hydroxide ligands or both of Ca^{2+}, Mn(4), and Mn(3).[189] In this way, it is linked to the two proposed substrate water ligands, one of which is bound to Ca^{2+} and the other to Mn(4). Through the latter linkage, as well as perhaps through the Mn(4)-ligating D1-Asp170 residue, CP43-Arg357 is linked to D1-Asp61, which is the start of the proton-exit channel identified crystallographically.[53] The 3.0 Å resolution crystal structure[52] confirms that D1-Asp61 lies less than 5 Å away from Mn(4), on the other side of the cluster from Y_Z. Additionally, FTIR spectroscopic experiments (using ^{15}N-labeling) have been tentatively interpreted in terms of S-state dependent arginine vibrational frequencies,[175] an interpretation consistent with the close proximity of arginine(s) to the OEC.

The highly conserved[385] and functionally important[386] CP430-Arg357, therefore, appears to be uniquely well positioned to abstract protons from the proposed substrate waters of the OEC and to deliver them to the proton-exit pathway. We have recently proposed that CP43-Arg357 indeed acts as the catalytic base in the $S_2 \rightarrow S_3$ and $S_3 \rightarrow [S_4] \rightarrow S_0$ transitions of the OEC.[382] Instead of Y_Z itself abstracting protons from the water/OEC complex, we suggest that, in the later S-states, oxidation of Y_Z decreases the pK_a of CP43-Arg357 so that its guanidinium side chain deprotonates to bulk. This electrostatic effect is achieved by the confinement of positive charge at the Y_Z/D1-His190 pair,

rather than the loss of the phenolic proton to bulk (see following paragraph). Subsequent oxidation of the OEC is accompanied by reduction of Y_Z and concomitant neutralization of the positive charge on the Y_Z/D1-His190 pair. This neutralization causes the pK_a of the CP43-Arg357 side chain to rise to its previous value, and it accepts a proton from the Mn(4)-bound substrate water as Mn(4) is oxidized, causing the pK_a of its bound water to fall. In other words, we propose that *bifurcated PCET* occurs, in which the electron passes to Y_Z (before going on to P_{680}^+) and the proton passes to CP43-Arg357 (before going out to bulk). (The possibility of such a bifurcated mechanism has previously been noted by Renger).[40] CP43-Arg357 plays the role of a redox-coupled base in the reaction, whose presence was predicted by Krishtalik on thermodynamic grounds.[263] The residual oxygen evolution of the CP43-R357S mutant examined by Knoepfle et al.[386] may be explained by postulating that some other nearby residues or even CP43-Ser357 itself may inefficiently accept protons from the Mn(4)-bound substrate water as its pK_a falls. We also note that the relative inactivity of the CP43-R357S mutant may be due to inefficient assembly of the OEC rather than any hypothesized catalytic role of the arginine residue.

It will be appreciated that this proposal for the action of arginine as a redox-active base in water splitting goes hand-in-hand with the "proton-rocking" hypothesis of Junge, Rappaport, and Renger (see section 4.5). It is compatible with the observation by Lavergne and co-workers that, at least in the $S_3 \rightarrow [S_4] \rightarrow S_0$ transition, a rapid (30 μs) phase of electrochromism (presumed to correlate with proton movement in the region of the OEC) is associated with a lag phase of electron transfer.[238,301,387] (No such lag phase has been reported in the $S_2 \rightarrow S_3$ transition). In other words, it appears that a proton is lost from the vicinity of the OEC before the manganese center is oxidized. That has previously been interpreted as the change of the pK_a of a nearby group (we suggest CP43-Arg357) from above 9 to a value of 6.[300] More recently, Dau, Haumann, and co-workers have used time-resolved XAS to establish that there is a kinetically resolvable form of the OEC, produced by illumination of the S_3 state, which does not involve oxidation of the manganese cluster.[29] The temperature dependence of the free energy change associated with this intermediate's formation reveals that the process is largely entropically driven. This is consistent with the movement of a proton from a tightly bound situation to a more weakly bound situation, and the authors of this work tentatively identify this process with the deprotonation of the CP43-Arg357 side chain into bulk solution.[29]

A key part of our proposal is that this bifurcated PCET mechanism is only activated after the attainment of the S_2 state, because it is only then that a positive charge develops on the OEC. It is the combination of the positive charge on the OEC, continuously present in the S_2, S_3, and S_4 states, and the transient positive charge on the oxidized Y_Z/D1-His190 pair that is responsible for the deprotonation of CP43-Arg357 and, thus, its momentary activation as a catalytic base. Figure 16 shows the relative pK_a values that we propose for CP43-Arg357 and the Mn-bound substrate water/hydroxide throughout the S-state cycle, while Figure 17 shows our proposal for OEC oxidation before and after attainment of the S_2 state.

The arginine side chain normally has a high pK_a (above 12)[388] so is not typically considered to be active in enzyme

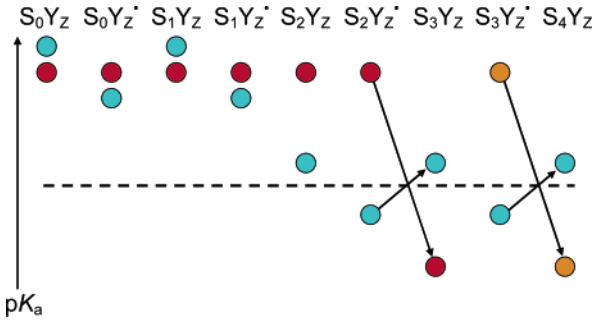

Figure 16. Proposed relative pK_a's of CP43-Arg357 (blue), substrate water bound to the dangler Mn(4) (red), and the same water deprotonated to a hydroxide ligand (orange). The pH of the lumenal bulk solution is indicated by the horizontal dashed line. pK_a changes leading to proton transfers are indicated by solid arrows. Up to the $S_1Y_Z^\bullet$ state, oscillations in the arginine pK_a are caused by the alternating oxidation and reduction of Y_Z. Development of a positive charge on the OEC cluster in the S_2Y_Z state leads to a significant decrease of the arginine's pK_a. Progression to the $S_2Y_Z^\bullet$ state leads to a further decrease, and CP43-Arg357 deprotonates to bulk. Progression to the S_3Y_Z state involves the oxidation of Mn(4), greatly lowering the pK_a of its bound substrate water. Accompanying reduction of Y_Z increases the pK_a of the arginine, and it accordingly gains a proton (along a hydrogen bond) from the acidified Mn(4) water ligand. The same process repeats in the next two steps, except that here a Mn(4) hydroxide ligand is deprotonated to an oxo group by CP43-Arg357.

acid/base catalysis. However, three groups of enzymes are now thought to make use of arginine in this role,[389] and two more have been proposed to do the same. Perhaps the best-established example is fumarate reductase and, by inference, succinate dehydrogenase.[390−393] In the fumarate reductase catalytic reaction, hydride-ion donation to the fumarate C═C bond by a flavin cofactor is accompanied by proton donation to the same moiety by arginine, achieving a two-electron, two-proton reduction of fumarate to succinate (Figure 18). Kinetic and crystallographic data indicate that arginine is important both as a Lewis acid, in stabilizing the developing negative charge at the substrate, and as a general acid catalyst.[391] The proposed mechanism of succinate dehydrogenase is exactly the reverse, with arginine acting as a catalytic base. The pH of maximum catalytic activity is around 6,[394] very similar to that of PSII.[248,395,396] Interestingly, the pK_a of the active arginine is not lowered by sequestering it in a hydrophobic environment. On the contrary, the enzyme's active site is near the protein surface and exposed to water.[389,397,398] L-Aspartate oxidase is closely related to fumarate reductase and has been suggested to work similarly,[399] also using arginine as a general acid/base catalyst.[400,401]

Certain polysaccharide lyases (PLs) have also been found to depend on arginine acid/base catalysis. The PLs in which arginine catalysis is best established are the pectate lyases of PL families 1 and 10.[402,403] The PL-1 pectin lyases also appear to use arginine as a catalytic base and display maximum catalytic activity around pH 6.[404] The PL-1 and PL-10 pectate lyases have activity vs pH maxima at 9 or above,[402,403] a pH dependence that is partly related to the occupancy of a calcium-binding site near the active site.[405] This Ca^{2+} ion has been implicated in lowering the pK_a of the arginine side chain.[405] Both pectate lyases and pectin lyases have active sites that are directly exposed to the solvent.[402,406,407]

The third documented example of an arginine active in acid/base catalysis is in inosine 5′-monophosphate dehydro-

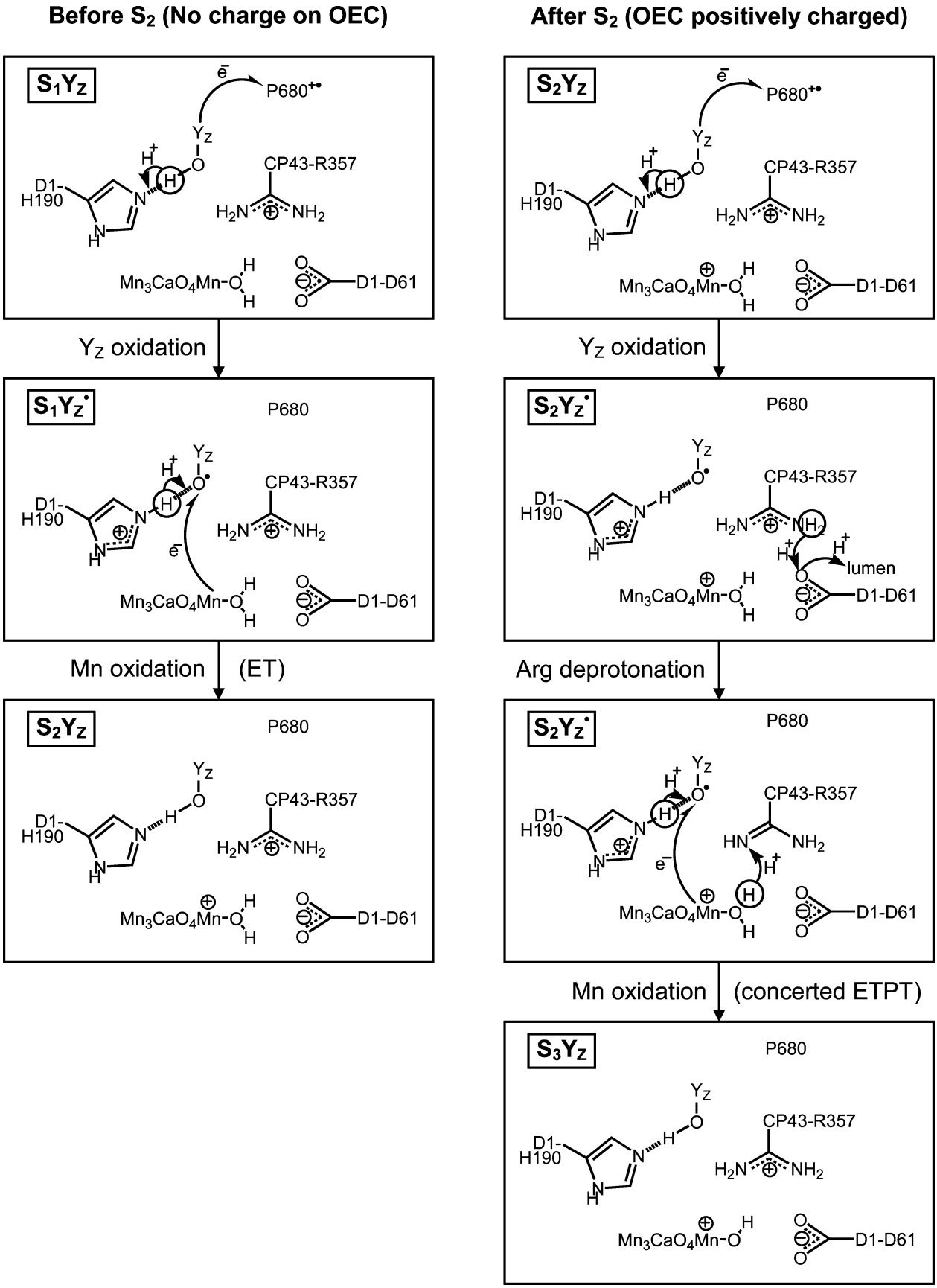

Figure 17. Comparison of proposed PCET reactions before (left) and after (right) attainment of the S_2 state. In the $S_1 \rightarrow S_2$ transition, $Y_Z^{\bullet}$ oxidizes the OEC cluster and reacquires its own proton, previously lost to nearby D1-His190. In the $S_2 \rightarrow S_3$ transition, the $Y_Z^{\bullet}$ PCET reaction is the same, but the neutral CP43-Arg357 side chain simultaneously abstracts a proton from the Mn-bound substrate water. This results in a concerted, bifurcated PCET reaction at the OEC. Reprinted with permission of the PCCP Owner Societies from ref 382. Copyright 2004 Royal Society of Chemistry.

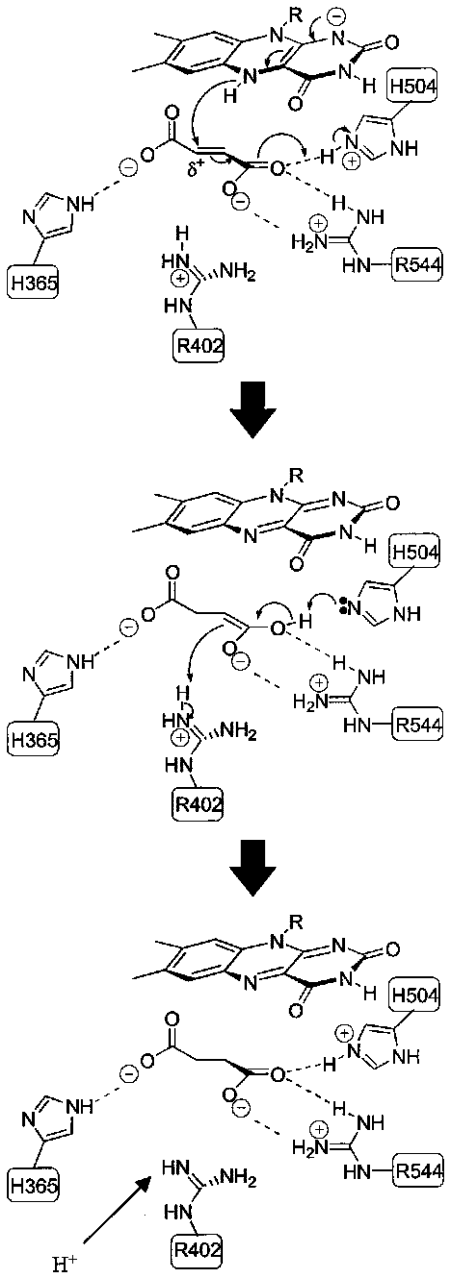

Figure 18. Proposed mechanism of fumarate reduction in the respiratory fumarate reductases. Fumarate accepts a hydride ion from the flavin cofactor and a proton from the nearby (and conserved) Arg402 residue. Arginine is immediately reprotonated from bulk via a proton-transfer pathway. Reprinted from ref 390. Copyright 2000 American Chemical Society.

genase (IMPDH). Here, an arginine side chain is thought to act in its neutral form as a general base to deprotonate water, thus activating it as a nucleophile.[408,409] This enzyme exhibits maximum activity around pH 8,[410] which appears to be equal to the pK_a of the active-site arginine.[408] A water channel connects the buried active site to bulk water.[411]

An active-site arginine is suspected to be involved in tyrosine phenol lyase, in the deprotonation of the phenolic substrate,[412−414] as well as in the plant heme peroxidases. These latter enzymes contain a distal arginine residue at the active site, which was early proposed to be necessary for the protonation of the Fe^{III}−peroxy intermediate and consequent formation of compound I.[415] Site-directed mutagenesis studies have confirmed the importance of the residue.[416−418] Although the original, and still popular, suggestion was that the arginine electrostatically promotes proton transfer from the distal histidine to the peroxy intermediate,[415,419] it is quite possible that arginine itself acts as the proton donor,[420] as suggested by recent molecular dynamics calculations.[421] The plant peroxidase reaction with H_2O_2 is retarded at low pH with an apparent pK_a of less than 6,[422] even below pH 4 in the case of soybean peroxidase,[423] and the heme is solvent-accessible.[424]

Finally, an example exists of a suspected acid/base-active arginine outside the active site of an enzyme: a deprotonated arginine side chain has been observed, with time-resolved FTIR spectroscopy, in the proton-exit pathway of bacteriorhodopsin.[425] This interpretation is controversial, however.[426]

Notably, in most of the above examples the acid/base arginine is either part of an active site that is directly exposed to water, as in fumarate reductase, polysaccharide lyase, and the plant peroxidases, or is involved with a proton-transfer channel, as in IMPDH and bacteriorhodopsin. Only in tyrosine phenol lyase can the suspected acid/base-active arginine be said to reside in a locally hydrophobic environment. Thus, a more common structural motif in these proteins is the location of arginine in a markedly hydrophilic site, adjacent to waters and other polar amino acid residues.[389] This is surprising, because common sense would suggest that the pK_a of an arginine might be best lowered by protecting the side chain from high-dielectric water (see, for example, ref 427). Electrostatic calculations support this idea.[428] It appears that there are a variety of other strategies for pK_a-reduction at work,[389] perhaps including, in the case of pectate lyase, the presence of a nearby Ca^{2+} ion (as in PSII). However, in the case of PSII, we suggest that there is at work an electrostatic effect more potent than the proximity of one anionically ligated dication. We propose that the development of an uncompensated positive charge on the OEC (in the $S_1 \rightarrow S_2$ transition) substantially lowers the pK_a of CP43-Arg357 and that it is lowered even further when a transient positive charge is shared between $Y_Z^{\bullet}$ (ca. 7 Å away) and D1-His190 (ca. 9 Å away). This hypothesis is strengthened by recent theoretical work by Knapp and coworkers, using the linearized Poisson−Boltzmann method along with Monte Carlo sampling of protonation states. They found that the protonation state of CP43-Arg357 in their model is sensitive both to the oxidation state of the OEC[429,430] and that of Y_Z,[430] exactly as we have proposed.

Although direct evidence for a role of CP43−Arg357 as the catalytic base in the OEC is lacking, every element of our proposal for the role of CP43-Arg357 in PSII has a precedent, confirmed or suspected, in other systems. The example of IMPDH shows that neutral arginine may be used to deprotonate a water molecule, which makes chemical sense, because a strong base must be necessary to deprotonate a species with a high pK_a. The examples of fumarate reductase and pectin lyase show that the operation of an acid/base-active arginine is compatible with maximum catalytic activity around pH 6, as is seen in PSII. The example of the plant peroxidases provides a possible precedent for arginine's acid/base role specifically in the redox chemistry of oxygen. Indeed, Renger has recently discussed the parallels between the environment of water in the OEC and that of the peroxide intermediate in the heme peroxidases.[40] It is more difficult to find characterized examples of metalloprotein PCET involving the (de)protonation of a nearby species that is neither a metal ligand nor itself redox-active. However, such a bifurcated PCET reaction has been observed recently in a

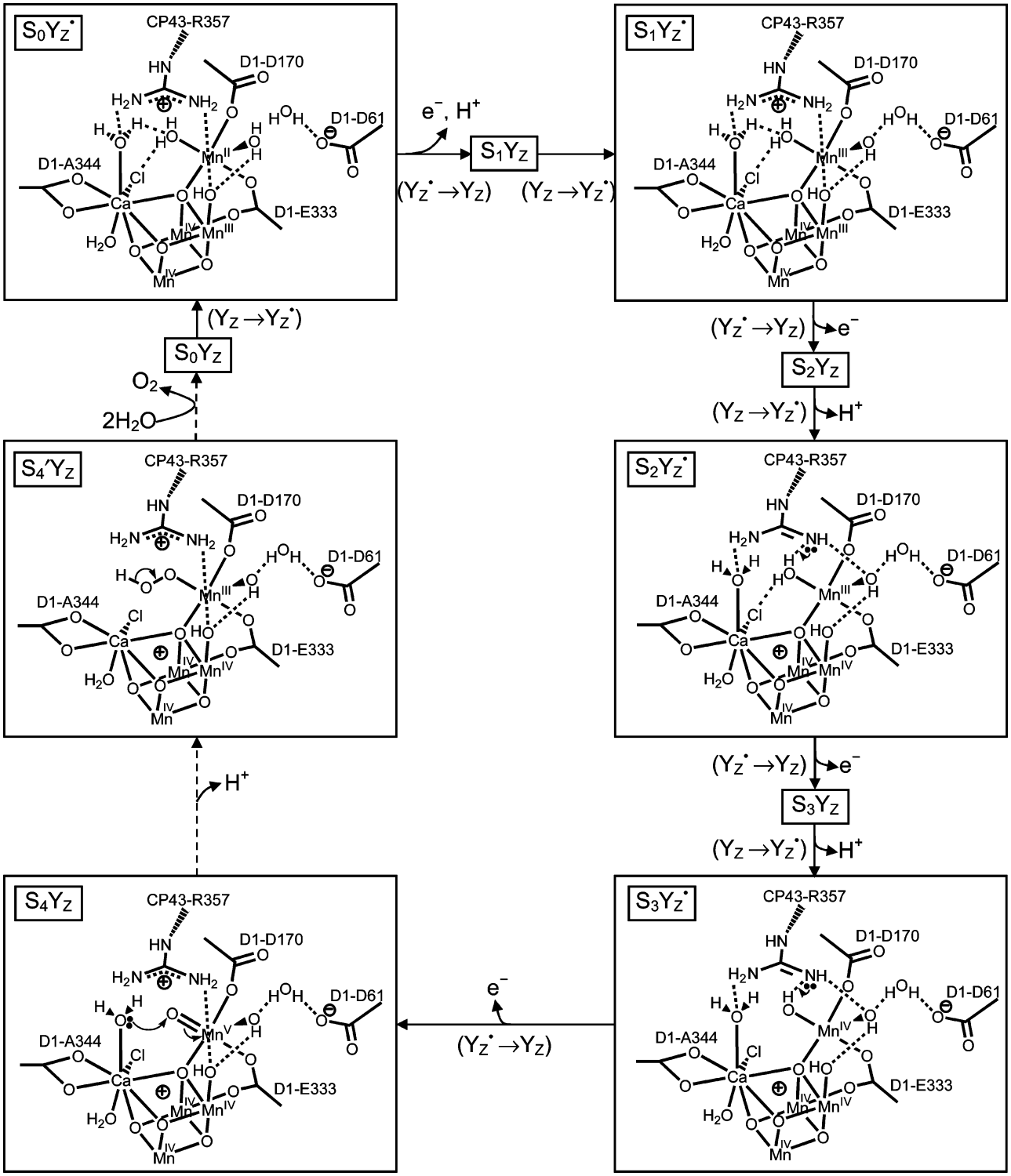

Figure 19. Proposed structure-based mechanism of water splitting in the OEC. The structure is based upon the crystallographic model of Ferreira et al.[53] with additions and alterations derived from computational modeling.[189] Hydrogen bonds (dashed lines) organize proton transfer in the latter half of the cycle from the Mn-bound substrate water to D1-Asp61 via CP43-Arg357. We have labeled S-states according to the oxidation state of the hydrated OEC metal−oxo cluster, so that our $S_3Y_Z^{\bullet}$ state following arginine deprotonation corresponds to the S_4 state of ref 29. Reprinted with permission of the Royal Society of Chemistry on behalf of the European Society for Photobiology and the European Photochemistry Association from ref 189. Copyright 2005 Royal Society of Chemistry.

site-directed mutant of *Azotobacter vinelandii* ferredoxin I, in which histidine replaces phenylalanine ca. 6 Å away from the [3Fe−4S] cluster.[431] Whereas in the wild-type protein the $[3Fe-4S]^{+/0}$ couple is accompanied by direct (de)-protonation of the cluster, in the mutant the acid/base chemistry occurs at the histidine imidazole via a through-space electrostatic effect.[431]

7.2. Proposed S-State Cycle

We present in Figure 19 our proposed S-state cycle.[382] This is essentially an application of our previous mechanistic proposal[79] to the 3.5 Å resolution X-ray crystal structure of the OEC,[53] with the modified proton-transfer pathway described above. The details of solvation, metal ligation, and

the hydrogen-bonding network around the "active face" of the cluster are based on molecular mechanics calculations performed upon the crystallographic structure.[189,381] Besides directing the addition of water, hydroxide, and chloride to the OEC, these calculations indicate two minor changes in amino acid ligation: the binding of Ca^{2+} by the D1 carboxylate terminus, and the bridging of Mn(4) and Mn(2) by D1-Glu333.[189,381] These ligations are reflections of overall energetic considerations in the S_1 state but are irrelevant to our mechanistic proposal. Our structural models comprise seven or eight metal-ligating waters or hydroxides (not all shown in Figure 19), standing in contradiction to the ca. three coupled waters detected by deuteron ESEEM experiments on the S_0, S_1, and S_2 states.[119] However, it should be noted (as in section 3.2.4) that the overall deuteron modulation depth observed in these experiments is comparable with that seen in fully hydrated $[Mn(D_2O)_6]^{2+}$ ions.[432] This qualitatively indicates that numerous exchangeable hydrogens, probably belonging to numerous waters or hydroxides, are close to the OEC. It is possible that these exchangeable hydrogens are not from waters directly ligated to the OEC. If so, then other ligands are required to complete the coordination of all of the metal ions. These could be supplied by bridging μ, η^2 carboxylate ligands, as suggested by Loll et al.,[52] in place of some of the terminal carboxylate ligands in our models. In addition, there could be non-proteinaceous ligands, such as chloride or possibly carbonate/bicarbonate, not seen by X-ray crystallography at the current resolution.

The changing redox state of Y_Z, which is alternately reduced by the cluster and oxidized by P_{680}^+, is indicated in Figure 19 alongside the reaction arrows. We have drawn the S_{0-3} states in the $S_nY_Z^\bullet$ state so that the $Y_Z^\bullet$ radical is shown poised to oxidize the cluster. The transiently stable S_4 state never coexists with the $Y_Z^\bullet$ radical and so is shown in the S_4Y_Z state. We hypothesize that the two Mn ions on the bottom face of the cuboidal cluster are not redox-active and remain in the +4 oxidation state throughout the cycle. Mn(3) and Mn(4) change their oxidation states as described previously. We have chosen to show a II, III, IV, IV Mn_4 oxidation assignment for S_0 in Figure 19 because this assignment was used in our earlier publications, although, as explained in section 4.2, a III, III, III, IV assignment is perhaps more likely. Recent ^{55}Mn pulse ENDOR experiments appear to favor the latter.[65] Again, the choice has only an incidental bearing upon our proposed mechanism (see below). If it is confirmed that the Mn ion ligated by D1-Asp170 (Mn(4)) does not change its oxidation state up to the S_3 state, as indicated by the FTIR experiments discussed in section 3.4,[186] then Mn(3) is the next most likely candidate for substrate water binding and oxidation to a high oxidation state, being close to Ca on the "active face" of the OEC. However, as things stand, structural factors make Mn(4) the more likely ion: its proximity to D1-Asp61, seemingly the start of the proton-exit channel, provides a direct escape route for protons. This easy proton loss upon oxidation should reduce the reduction potential of Mn(4), making this center the most easily oxidized of all the manganese ions.

If we take the III, III, III, IV assignment for S_0, then calculations indicate that the $S_0 \rightarrow S_1$ transition involves the oxidation of Mn(2) from the +3 to the +4 formal oxidation state.[188] At the same time, a proton is lost from a Mn(3)-ligating water through hydrogen-bonded waters via D1-Asp61.[188] The hydrogen-bonded connection between these two species is short enough that the PCET reaction is able to occur in the absence of a normal hydrogen-bonded network around the rest of the OEC (a situation perhaps characteristic of Cl^- depletion or acetate inhibition) and even in the absence of a normally constructed cluster (Ca^{2+} depletion). The second oxidation of the cluster, to reach the S_2Y_Z state, involves ET only, so the cluster develops a positive charge. This reaction occurs particularly easily because it involves no proton transfer at all. Oxidation of Y_Z to reach the $S_2Y_Z^\bullet$ state is swiftly followed by deprotonation of CP43-Arg357, activating it as a catalytic base and allowing concerted, bifurcated ETPT to take place in the next two cluster oxidations. In both the $S_2 \rightarrow S_3$ and the $S_3 \rightarrow S_4$ steps, Y_Z accepts an electron from Mn(4), while neutral arginine abstracts a proton from the metal's bound substrate water. This water is held in a precise orientation within the hydrogen-bond network by the calcium-bound chloride ion. Metal-bound chloride and bromide are both hydrogen-bond acceptors with similar properties, whereas fluoride is markedly different in this respect,[433,434] tallying perhaps with its inhibitory effect in the OEC. It is worth noting that the oxidation of the substrate-water-binding manganese in the $S_2 \rightarrow S_3$ transition is broadly compatible with the observation by Wydrzynski and co-workers that this step retards the exchange with bulk of the fast-exchanging substrate water 3-fold,[435] if one assigns the fast-exchanging water to the Mn(4)-bound water and the slow-exchanging water to the calcium-bound water.[85] Although the $S_2 \rightarrow S_3$ transition has been shown by EXAFS to involve significant changes in the structure of the OEC,[144,145] we are not sufficiently confident of the nature of this rearrangement to include it in our figure. However, following Dau and co-workers,[144] we might hypothesize that a new μ-oxo bridge is formed between Mn(3) and Mn(4) in the $S_2 \rightarrow S_3$ step, creating a new 2.7−2.8 Å Mn···Mn distance. This might be prompted by the oxidation of Mn(4) from the Jahn−Teller stabilized, five-coordinate Mn^{III} state to the six-coordinate Mn^{IV} oxidation state.[144]

By the $S_3 \rightarrow S_4$ step, the dangler Mn(4) is in the form of Mn^V═O. The subsequent $S_4 \rightarrow S_4'$ transition is the crucial O−O bond-forming step and involves the attack by a calcium-bound water ligand upon the electrophilic Mn^V═O oxo group. The nearby D1-Gln165 residue may play a role in this reaction by accepting a hydrogen bond from the calcium-bound substrate water as it nucleophilically attacks the Mn^V═O group. If it does play such a role, it appears that it is not absolutely required, since the D1-Q165A mutant has been found to be photoautotrophic.[167] A peroxo intermediate is formed at Mn(4), which is concomitantly reduced from Mn^V to Mn^{III}. The arginine side chain remains protonated, because Y_Z stays reduced until the formation of S_0 and so does not exert any electrostatic effect on CP43-Arg357. We assume therefore that the proton that is lost in the spontaneous $S_4 \rightarrow S_4'$ step moves to bulk without the intercession of any specific base. Finally, the unstable Mn^{III}-bound peroxo intermediate S_4' decays to produce dioxygen, and the OEC is reset to the S_0 state. If Mn(4) in this step is reduced all the way to weakly acidic Mn^{II}, it is plausible that the proton lost from the peroxo intermediate simply moves to the Mn(4) hydroxo ligand next to D1-Asp61, reforming the metal's nonsubstrate water ligand.

8. Tests of Mechanistic Hypotheses

The water-splitting chemistry of PSII is complicated, and there is much work to be done to discover which of the

proposed mechanisms described in this review lies closest to the truth. Structural studies hold the greatest promise in this regard. Oriented EXAFS measurements, crystallography performed under conditions that minimize radiation damage, and computational modeling ought to yield an unambiguous structure of the OEC in the not-too-distant future. A second question concerns the location of oxidizing power within the OEC and how this relates to the locations of amino acid and other ligands (particularly substrate water ligands). For instance, is it really the dangler Mn that accumulates most of the oxidizing power, as we suggest? Having established more precisely the coordination environment of the OEC in a well-defined oxidation state, it should be possible to assign changes in spectroscopic signals more reliably to alterations in the oxidation state and coordination environment of a particular metal atom. Magnetic resonance, X-ray, Raman, and IR spectroscopies all have a part to play in this effort, as well as high-level computational modeling. Evidence arguing against the oxidation of the dangler manganese comes from the FTIR spectroscopic experiments of Debus and co-workers, who find that the vibrational frequencies of D1-Asp170 (a ligand of Mn(4) in both the 3.5 Å[53] and the 3.0 Å[52] resolution structures) are unaffected by changes in S-state up to the S_3 state.[186] FTIR spectroscopy also indicates that the C-terminal carboxyl of D1-Ala344 does not ligate Ca^{2+},[177,178] whereas both the 3.5 Å and the 3.0 Å resolution structures imply that it might. Furthermore, if the carboxyl terminus does not ligate calcium, it is not clear what does: D1-Glu189, assigned as the most likely calcium ligand in the 3.0 Å resolution structure, has been found in mutational studies probably not to play this role.[436] Resolving these contradictions will be important in future efforts to determine both the structure and mechanism of the OEC. Finally, it is crucial to elucidate the movements of protons around the OEC as the S-state cycle progresses. Which species are involved in accepting protons from the catalytic water? This question is tied to the issue of charge distribution in and around the OEC. It seems to be increasingly likely that the development of positive charge at Y_Z/D1-His190 is linked to the expulsion of a proton from the vicinity of the OEC, at least in the $S_3 \rightarrow S_4 \rightarrow S_0$ transition.[29,301] Careful spectroscopic studies should help to establish whether this proton is really coming from CP43-Arg357, activating it as a catalytic base as we suggest, or whether this role is played by other species such as manganese ligand oxides.[134]

9. Conclusions

To understand the water-splitting chemistry of PSII, researchers have sought insights from a great number of different sorts of experiments, which have been directed both at the protein and at model metal complexes. Such is the complexity of the process that it continues to evade satisfactory description, although substantial progress has been made. Ever more sophisticated spectroscopic techniques (notably EPR, FTIR, and XAS, as well as time-resolved mass spectrometry) have been deployed against the OEC, yielding for the first time detailed information in a variety of S-states. The recent crystallographic studies have made it possible to propose and to test more detailed mechanistic proposals than have previously been tenable. Higher resolution and more definitive crystal structures of the OEC, obtained in different stages of the catalytic cycle, are eagerly awaited, along with further spectroscopic, biochemical and computational studies. The development of increasingly active and well-characterized model complexes will complement these investigations, as well as advancing efforts directed toward the development of artificial water-splitting photocatalysts.

10. List of Abbreviations

ENDOR	electron−nuclear double resonance
EPR	electron paramagnetic resonance
ESEEM	electron spin−echo envelope modulation
ET	electron transfer
EXAFS	extended X-ray absorption fine structure
FTIR	Fourier transform infrared
IMPDH	inosine 5′-monophosphate dehydrogenase
OEC	oxygen-evolving complex of photosystem II
P_{680}	primary electron donor of photosystem II
PCET	proton-coupled electron transfer
PL	polysaccharide lyase
PSII	photosystem II
Q_A	quinone A of photosystem II
Q_B	quinone B of photosystem II
SHE	standard hydrogen electrode
UV/vis	ultraviolet/visible
XAS	X-ray absorption spectroscopy
XANES	X-ray absorption near-edge structure
Y_Z	tyrosine Z of photosystem II

11. Acknowledgments

This work was supported by National Institutes of Health Grant GM32715.

12. References

(1) Wild, M.; Gilgen, H.; Roesch, A.; Ohmura, A.; Long, C. N.; Dutton, E. G.; Forgan, B.; Kallis, A.; Russak, V.; Tsvetkov, A. *Science* **2005**, *308*, 847.
(2) *Report of the International Energy Agency: Monthly Electricity Survey*; May 2005, International Energy Agency, 2005.
(3) Blankenship, R. E. *Molecular Mechanisms of Photosynthesis*; Blackwell Science: Oxford, U.K., 2002.
(4) Renger, G.; Holzwarth, A. R. In *Photosystem II: The Light-Driven Water:Plastoquinone Oxidoreductase*; Wydrzynski, T. J., Satoh, K., Eds.; Advances in Photosynthesis and Respiration 22; Springer: Dordrecht, The Netherlands, 2005; p 139.
(5) Diner, B. A.; Rappaport, F. *Annu. Rev. Plant Biol.* **2002**, *53*, 551.
(6) Barber, J. In *Encyclopedia of Biological Chemistry*; Lennarz, W. J., Lane, M. D., Eds.; Elsevier: Oxford, U.K., 2004; Vol. 3, p 367.
(7) Green, B. R.; Gantt, E. In *Photosystem II: The Light-Driven Water: Plastoquinone Oxidoreductase*; Wydrzynski, T. J., Satoh, K., Eds.; Advances in Photosynthesis and Respiration 22; Springer: Dordrecht, The Netherlands, 2005; p 23.
(8) Eaton-Rye, J. J.; Putnam-Evans, C. In *Photosystem II: The Light-Driven Water:Plastoquinone* Oxidoreductase; Wydrzynski, T. J., Satoh, K., Eds.; Advances in Photosynthesis and Respiration 22; Springer: Dordrecht, The Netherlands, 2005; p 45.
(9) Bricker, T. M.; Burnap, R. L. In *Photosystem II: The Light-Driven Water:Plastoquinone Oxidoreductase*; Wydrzynski, T. J., Satoh, K., Eds.; Advances in Photosynthesis and Respiration 22; Springer: Dordrecht, The Netherlands, 2005; p 95.
(10) Thornton, L. E.; Roose, J. L.; Pakrasi, H. B.; Ikeuchi, M. In *Photosystem II: The Light-Driven* Water:Plastoquinone Oxidoreductase; Wydrzynski, T. J., Satoh, K., Eds.; Advances in Photosynthesis and Respiration 22; Springer: Dordrecht, The Netherlands, 2005; p 121.
(11) Nixon, P. J.; Sarcina, M.; Diner, B. A. In *Photosystem II: The Light-Driven Water:Plastoquinone Oxidoreductase*; Wydrzynski, T. J., Satoh, K., Eds.; Advances in Photosynthesis and Respiration 22; Springer: Dordrecht, The Netherlands, 2005; p 71.
(12) Chow, W. S.; Aro, E. M. In *Photosystem II: The Light-Driven Water: Plastoquinone Oxidoreductase*; Wydrzynski, T. J., Satoh, K., Eds.; Advances in Photosynthesis and Respiration 22; Springer: Dordrecht, The Netherlands, 2005; p 627.
(13) Dismukes, G. C.; Ananyev, G.; Watt, R. In *Photosystem II: The Light-Driven Water:Plastoquinone Oxidoreductase*; Wydrzynski, T. J., Satoh, K., Eds.; Advances in Photosynthesis and Respiration 22; Springer: Dordrecht, The Netherlands, 2005; p 609.

(14) Baena-Gonzalez, E.; Aro, E. M. *Philos. Trans. R. Soc. London, Ser. B: Biol. Sci.* **2002**, *357*, 1451.
(15) Kanervo, E.; Aro, E. M. In *Encyclopedia of Biological Chemistry*; Lennarz, W. J., Lane, M. D., Eds.; Elsevier: Oxford, U.K., 2004; Vol. 3, p 363.
(16) Andersson, B.; Aro, E. M. In *Regulation of Photosynthesis*; Aro, E. M., Andersson, B., Eds.; Advances in Photosynthesis and Respiration 11; Kluwer Academic Publishers: Dordrecht, The Netherlands, 2001; p 377.
(17) Ruttinger, W.; Dismukes, G. C. *Chem. Rev.* **1997**, *97*, 1.
(18) Magnuson, A.; Styring, S.; Hammarström, L. In *Photosystem II: The Light-Driven Water:Plastoquinone Oxidoreductase*; Wydrzynski, T. J., Satoh, K., Eds.; Advances in Photosynthesis and Respiration 22; Springer: Dordrecht, The Netherlands, 2005; p 753.
(19) *Photosystem II: The Light-Driven Water:Plastoquinone Oxidoreductase*; Wydrzynski, T. J.; Satoh, K., Eds.; Advances in Photosynthesis and Respiration 22; Springer: Dordrecht, The Netherlands, 2005.
(20) Hillier, W.; Messinger, J. In *Photosystem II: The Light-Driven Water: Plastoquinone Oxidoreductase*; Wydrzynski, T. J., Satoh, K., Eds.; Advances in Photosynthesis and Respiration 22; Springer: Dordrecht, The Netherlands, 2005; p 567.
(21) Special issue dedicated to James Barber. *Photochem. Photobiol. Sci.* **2005**, *4* (12), 916−1096; Nield, J., Nixon, P. J., Eds.
(22) Special issue: Biophysical Studies of Photosystem II and Related Model Systems. *Phys. Chem. Chem. Phys*. **2004**, *6* (20), 1−4911; Messinger, J., Lubitz, W., Eds.
(23) Special issue dedicated to Mel Klein. *Biochim. Biophys. Acta* **2001**, *1503* (1−2), 1−259; Nugent, J. H. A., Ed.
(24) Special issue dedicated to Jerry Babcock. *Biochim. Biophys. Acta* **2004**, *1655* (12), 1−413; Tommos, C., Brzezinksi, P., Ehrenberg, A., Eds.
(25) Grabolle, M.; Dau, H. *Biochim. Biophys. Acta* **2005**, *1708*, 209.
(26) Rappaport, F.; Guergova-Kuras, M.; Nixon, P. J.; Diner, B. A.; Lavergne, J. *Biochemistry* **2002**, *41*, 8518.
(27) de Wijn, R.; van Gorkom, H. J. *Biochim. Biophys. Acta* **2002**, *1553*, 302.
(28) Kok, B.; Forbush, B.; McGloin, M. *Photochem. Photobiol.* **1970**, *11*, 457.
(29) Haumann, M.; Liebisch, P.; Muller, C.; Barra, M.; Grabolle, M.; Dau, H. *Science* **2005**, *310*, 1019.
(30) Clausen, J.; Junge, W. *Nature (London)* **2004**, *430*, 480.
(31) Penner-Hahn, J. E.; Yocum, C. F. *Science* **2006**, *312*, 1470.
(32) Dau, H.; Haumann, M. *Science* **2006**, *312*, 1471.
(33) Junge, W.; Clausen, J. *Science* **2006**, *312*, 1470.
(34) Diner, B. A.; Britt, R. D. In *Photosystem II: The Light-Driven Water: Plastoquinone Oxidoreductase*; Wydrzynski, T. J., Satoh, K., Eds.; Advances in Photosynthesis and Respiration 22; Springer: Dordrecht, The Netherlands, 2005; p 207.
(35) Debus, R. J.; Barry, B. A.; Sithole, I.; Babcock, G. T.; McIntosh, L. *Biochemistry* **1988**, *27*, 9071.
(36) Metz, J. G.; Nixon, P. J.; Rögner, M.; Brudvig, G. W.; Diner, B. A. *Biochemistry* **1989**, *28*, 6960.
(37) Debus, R. J.; Barry, B. A.; Babcock, G. T.; McIntosh, L. *Proc. Natl. Acad. Sci. U.S.A.* **1988**, *85*, 427.
(38) Vermaas, W. F. J.; Rutherford, A. W.; Hansson, Ö. *Proc. Natl. Acad. Sci. U.S.A.* **1988**, *85*, 8477.
(39) Renger, G. *Biochim. Biophys. Acta* **2004**, *1655*, 195.
(40) Renger, G. *Biochim. Biophys. Acta* **2001**, *1503*, 210.
(41) Renger, G.; Bittner, T.; Messinger, J. *Biochem. Soc. Trans.* **1994**, *22*, 318.
(42) Deisenhofer, J.; Epp, O.; Miki, K.; Huber, R.; Michel, H. *Nature (London)* **1985**, *318*, 618.
(43) Deisenhofer, J.; Epp, O.; Sinning, I.; Michel, H. *J. Mol. Biol.* **1995**, *246*, 429.
(44) Baxter, R. H. G.; Seagle, B. L.; Ponomarenko, N.; Norris, J. R. *Acta Crystallogr., Sect D: Biol. Crystallogr.* **2005**, *61*, 605.
(45) Nogi, T.; Fathir, I.; Kobayashi, M.; Nozawa, T.; Miki, K. *Proc. Natl. Acad. Sci. U.S.A.* **2000**, *97*, 13561.
(46) Nanba, O.; Satoh, K. *Proc. Natl. Acad. Sci. U.S.A.* **1987**, *84*, 109.
(47) Michel, H.; Deisenhofer, J. *Biochemistry* **1988**, *27*, 1.
(48) Yachandra, V. K. In *Photosystem II: The Light-Driven Water: Plastoquinone Oxidoreductase*; Wydrzynski, T. J., Satoh, K., Eds.; Advances in Photosynthesis and Respiration 22; Springer-Verlag: Dordrecht, The Netherlands, 2005; p 235.
(49) Bittl, R.; Kawamori, A. In *Photosystem II: The Light-Driven Water: Plastoquinone Oxidoreductase*; Wydrzynski, T. J., Satoh, K., Eds.; Advances in Photosynthesis and Respiration 22; Springer: Dordrecht, The Netherlands, 2005; p 389.
(50) Åhrling, K. A.; Pace, R. J.; Evans, M. C. W. In *Photosystem II: The Light-Driven Water:Plastoquinone Oxidoreductase*; Wydrzynski, T. J., Satoh, K., Eds.; Advances in Photosynthesis and Respiration 22; Springer: Dordrecht, The Netherlands, 2005; p 285.
(51) Noguchi, T.; Berthomieu, C. In *Photosystem II: The Light-Driven Water:Plastoquinone Oxidoreductase*; Wydrzynski, T. J., Satoh, K., Eds.; Advances in Photosynthesis and Respiration 22; Springer: Dordrecht, The Netherlands, 2005; p 367.
(52) Loll, B.; Kern, J.; Saenger, W.; Zouni, A.; Biesiadka, J. *Nature (London)* **2005**, *438*, 1040.
(53) Ferreira, K. N.; Iverson, T. M.; Maghlaoui, K.; Barber, J.; Iwata, S. *Science* **2004**, *303*, 1831.
(54) Biesiadka, J.; Loll, B.; Kern, J.; Irrgang, K. D.; Zouni, A. *Phys. Chem. Chem. Phys.* **2004**, *6*, 4733.
(55) Kamiya, N.; Shen, J. R. *Proc. Natl. Acad. Sci. U.S.A.* **2003**, *100*, 98.
(56) Zouni, A.; Witt, H. T.; Kern, J.; Fromme, P.; Krauss, N.; Saenger, W.; Orth, P. *Nature (London)* **2001**, *409*, 739.
(57) Cheniae, G. M.; Martin, I. F. *Biochim. Biophys. Acta* **1970**, *197*, 219.
(58) Sauer, K. *Acc. Chem. Res.* **1980**, *13*, 249.
(59) Yocum, C. F.; Yerkes, C. T.; Blankenship, R. E.; Sharp, R. R.; Babcock, G. T. *Proc. Natl. Acad. Sci. U.S.A.* **1981**, *78*, 7507.
(60) Dismukes, G. C.; Siderer, Y. *Proc. Natl. Acad. Sci. U.S.A.* **1981**, *78*, 274.
(61) de Paula, J. C.; Beck, W. F.; Brudvig, G. W. *J. Am. Chem. Soc.* **1986**, *108*, 4002.
(62) Hasegawa, K.; Ono, T. A.; Inoue, Y.; Kusunoki, M. *Chem. Phys. Lett.* **1999**, *300*, 9.
(63) Zheng, M.; Dismukes, G. C. *Inorg. Chem.* **1996**, *35*, 3307.
(64) Peloquin, J. M.; Campbell, K. A.; Randall, D. W.; Evanchik, M. A.; Pecoraro, V. L.; Armstrong, W. H.; Britt, R. D. *J. Am. Chem. Soc.* **2000**, *122*, 10926.
(65) Kulik, L. V.; Epel, B.; Lubitz, W.; Messinger, J. *J. Am. Chem. Soc.* **2005**, *127*, 2392.
(66) Britt, R. D.; Peloquin, J. M.; Campbell, K. A. *Annu. Rev. Biophys. Biomol. Struct.* **2000**, *29*, 463.
(67) Randall, D. W.; Sturgeon, B. E.; Ball, J. A.; Lorigan, G. A.; Chan, M. K.; Klein, M. P.; Armstrong, W. H.; Britt, R. D. *J. Am. Chem. Soc.* **1995**, *117*, 11780.
(68) Ghanotakis, D. F.; Babcock, G. T.; Yocum, C. F. *FEBS Lett.* **1984**, *167*, 127.
(69) Han, K.; Katoh, S. *Plant Cell Physiol.* **1993**, *34*, 585.
(70) Ädelroth, P.; Lindberg, K.; Andreásson, L. E. *Biochemistry* **1995**, *34*, 9021.
(71) Boussac, A.; Rutherford, A. W. *FEBS Lett.* **1988**, *236*, 432.
(72) Boussac, A.; Zimmermann, J. L.; Rutherford, A. W. *Biochemistry* **1989**, *28*, 8984.
(73) Sivaraja, M.; Tso, J.; Dismukes, G. C. *Biochemistry* **1989**, *28*, 9459.
(74) Ono, T. A.; Inoue, Y. *Arch. Biochem. Biophys.* **1989**, *275*, 440.
(75) Cinco, R. M.; Holman, K. L. M.; Robblee, J. H.; Yano, J.; Pizarro, S. A.; Bellacchio, E.; Sauer, K.; Yachandra, V. K. *Biochemistry* **2002**, *41*, 12928.
(76) Cinco, R. M.; Robblee, J. H.; Rompel, A.; Fernandez, C.; Yachandra, V. K.; Sauer, K.; Klein, M. P. *J. Phys. Chem. B* **1998**, *102*, 8248.
(77) Kim, S. H.; Gregor, W.; Peloquin, J. M.; Brynda, M.; Britt, R. D. *J. Am. Chem. Soc.* **2004**, *126*, 7228.
(78) Pecoraro, V. L.; Baldwin, M. J.; Caudle, M. T.; Hsieh, W. Y.; Law, N. A. *Pure Appl. Chem.* **1998**, *70*, 925.
(79) Vrettos, J. S.; Limburg, J.; Brudvig, G. W. *Biochim. Biophys. Acta* **2001**, *1503*, 229.
(80) Rutherford, A. W. *Trends Biochem. Sci.* **1989**, *14*, 227.
(81) Limburg, J.; Szalai, V. A.; Brudvig, G. W. *J. Chem. Soc., Dalton Trans.* **1999**, 1353.
(82) Riggs-Gelasco, P. J.; Mei, R.; Ghanotakis, D. F.; Yocum, C. F.; Penner-Hahn, J. E. *J. Am. Chem. Soc.* **1996**, *118*, 2400.
(83) Yachandra, V. K.; Sauer, K.; Klein, M. P. *Chem. Rev.* **1996**, *96*, 2927.
(84) Haumann, M.; Junge, W. *Biochim. Biophys. Acta* **1999**, *1411*, 121.
(85) Hendry, G.; Wydrzynski, T. *Biochemistry* **2003**, *42*, 6209.
(86) van Gorkom, H. J.; Yocum, C. F. In *Photosystem II: The Light-Driven Water:Plastoquinone* Oxidoreductase; Wydrzynski, T. J., Satoh, K., Eds.; Advances in Photosynthesis and Respiration 22; Springer: Dordrecht, The Netherlands, 2005; p 307.
(87) Hallahan, B. J.; Nugent, J. H. A.; Warden, J. T.; Evans, M. C. W. *Biochemistry* **1992**, *31*, 4562.
(88) Gilchrist, M. L.; Ball, J. A.; Randall, D. W.; Britt, R. D. *Proc. Natl. Acad. Sci. U.S.A.* **1995**, *92*, 9545.
(89) Lydakis-Simantiris, N.; Dorlet, P.; Ghanotakis, D. F.; Babcock, G. T. *Biochemistry* **1998**, *37*, 6427.
(90) Andreásson, L. E.; Vass, I.; Styring, S. *Biochim. Biophys. Acta* **1995**, *1230*, 155.
(91) Boussac, A.; Setif, P.; Rutherford, A. W. *Biochemistry* **1992**, *31*, 1224.
(92) Styring, S.; Feyziyev, Y.; Mamedov, F.; Hillier, W.; Babcock, G. T. *Biochemistry* **2003**, *42*, 6185.
(93) Homann, P. H. *Photosynth. Res.* **2002**, *73*, 169.
(94) Yocum, C. F. In *Manganese Redox Enzymes*; Pecoraro, V. L., Ed.; VCH: New York, 1992; p 71.

(95) Izawa, S.; Heath, R. L.; Hind, G. *Biochim. Biophys. Acta* **1969**, *180*, 388.
(96) Wincencjusz, H.; van Gorkom, H. J.; Yocum, C. F. *Biochemistry* **1997**, *36*, 3663.
(97) Wincencjusz, H.; Yocum, C. F.; van Gorkom, H. J. *Biochemistry* **1998**, *37*, 8595.
(98) Hasegawa, K.; Kimura, Y.; Ono, T. A. *Biochemistry* **2002**, *41*, 13839.
(99) Hasegawa, K.; Kimura, Y.; Ono, T. *Biophys. J.* **2004**, *86*, 1042.
(100) Lindberg, K.; Andreásson, L. E. *Biochemistry* **1996**, *35*, 14259.
(101) Kühne, H.; Szalai, V. A.; Brudvig, G. W. *Biochemistry* **1999**, *38*, 6604.
(102) Force, D. A.; Randall, D. W.; Britt, R. D. *Biochemistry* **1997**, *36*, 12062.
(103) Yu, H.; Aznar, C. P.; Xu, X.; Britt, R. D. *Biochemistry* **2005**, *44*, 12022.
(104) Baumgarten, M.; Philo, J. S.; Dismukes, G. C. *Biochemistry* **1990**, *29*, 10814.
(105) Ono, T.; Zimmermann, J. L.; Inoue, Y.; Rutherford, A. W. *Biochim. Biophys. Acta* **1986**, *851*, 193.
(106) Ono, T.; Conjeaud, H.; Gleiter, H.; Inoue, Y.; Mathis, P. *FEBS Lett.* **1986**, *203*, 215.
(107) Itoh, S.; Yerkes, C. T.; Koike, H.; Robinson, H. H.; Crofts, A. R. *Biochim. Biophys. Acta* **1984**, *766*, 612.
(108) Theg, S. M.; Jursinic, P. A.; Homann, P. H. *Biochim. Biophys. Acta* **1984**, *766*, 636.
(109) Olesen, K.; Andreásson, L. E. *Biochemistry* **2003**, *42*, 2025.
(110) Sandusky, P. O.; Yocum, C. F. *Biochim. Biophys. Acta* **1984**, *766*, 603.
(111) Kelley, P. M.; Izawa, S. *Biochim. Biophys. Acta* **1978**, *502*, 198.
(112) Ono, T. A.; Nakayama, H.; Gleiter, H.; Inoue, Y.; Kawamori, A. *Arch. Biochem. Biophys.* **1987**, *256*, 618.
(113) Homann, P. H. *Plant Physiol.* **1988**, *88*, 194.
(114) Sinclair, J. *Biochim. Biophys. Acta* **1984**, *764*, 247.
(115) Wincencjusz, H.; Yocum, C. F.; van Gorkom, H. J. *Biochemistry* **1999**, *38*, 3719.
(116) Turconi, S.; MacLachlan, D. J.; Bratt, P. J.; Nugent, J. H. A.; Evans, M. C. W. *Biochemistry* **1997**, *36*, 879.
(117) Evans, M. C. W.; Nugent, J. H. A.; Ball, R. J.; Muhiuddin, I.; Pace, R. J. *Biochemistry* **2004**, *43*, 989.
(118) Evans, M. C. W.; Rich, A. M.; Nugent, J. H. A. *FEBS Lett.* **2000**, *477*, 113.
(119) Britt, R. D.; Campbell, K. A.; Peloquin, J. M.; Gilchrist, M. L.; Aznar, C. P.; Dicus, M. M.; Robblee, J.; Messinger, J. *Biochim. Biophys. Acta* **2004**, *1655*, 158.
(120) Beck, W. F.; Brudvig, G. W. *Biochemistry* **1986**, *25*, 6479.
(121) Beck, W. F.; de Paula, J. C.; Brudvig, G. W. *J. Am. Chem. Soc.* **1986**, *108*, 4018.
(122) Force, D. A.; Randall, D. W.; Lorigan, G. A.; Clemens, K. L.; Britt, R. D. *J. Am. Chem. Soc.* **1998**, *120*, 13321.
(123) Evans, M. C. W.; Ball, R. J.; Nugent, J. H. A. *FEBS Lett.* **2005**, *579*, 3081.
(124) Randall, D. W.; Gelasco, A.; Caudle, M. T.; Pecoraro, V. L.; Britt, R. D. *J. Am. Chem. Soc.* **1997**, *119*, 4481.
(125) Cua, A.; Stewart, D. H.; Reifler, M. J.; Brudvig, G. W.; Bocian, D. F. *J. Am. Chem. Soc.* **2000**, *122*, 2069.
(126) Noguchi, T.; Sugiura, M. *Biochemistry* **2000**, *39*, 10943.
(127) Noguchi, T.; Sugiura, M. *Biochemistry* **2002**, *41*, 15706.
(128) Kimura, Y.; Ishii, A.; Yamanari, T.; Ono, T.-A. *Biochemistry* **2005**, *44*, 7613.
(129) Burda, K.; Bader, K. P.; Schmid, G. H. *FEBS Lett.* **2001**, *491*, 81.
(130) Burda, K.; Bader, K. P.; Schmid, G. H. *Biochim. Biophys. Acta* **2003**, *1557*, 77.
(131) Sauer, K.; Yano, J.; Yachandra, V. K. *Photosynth. Res.* **2005**, *85*, 73.
(132) Dau, H.; Liebisch, P.; Haumann, M. *Anal. Bioanal. Chem.* **2003**, *376*, 562.
(133) Penner-Hahn, J. E. *Struct. Bonding (Berlin)* **1998**, *90*, 1.
(134) Dau, H.; Iuzzolino, L.; Dittmer, J. *Biochim. Biophys. Acta* **2001**, *1503*, 24.
(135) DeRose, V. J.; Mukerji, I.; Latimer, M. J.; Yachandra, V. K.; Sauer, K.; Klein, M. P. *J. Am. Chem. Soc.* **1994**, *116*, 5239.
(136) Yano, J.; Pushkar, Y.; Glatzel, P.; Lewis, A.; Sauer, K.; Messinger, J.; Bergmann, U.; Yachandra, V. K. *J. Am. Chem. Soc.* **2005**, *127*, 14974.
(137) Cinco, R. M.; Robblee, J. H.; Messinger, J.; Fernandez, C.; Holman, K. L. M.; Sauer, K.; Yachandra, V. K. *Biochemistry* **2004**, *43*, 13271.
(138) Latimer, M. J.; DeRose, V. J.; Mukerji, I.; Yachandra, V. K.; Sauer, K.; Klein, M. P. *Biochemistry* **1995**, *34*, 10898.
(139) Yachandra, V. K.; Guiles, R. D.; McDermott, A.; Britt, R. D.; Dexheimer, S. L.; Sauer, K.; Klein, M. P. *Biochim. Biophys. Acta* **1986**, *850*, 324.
(140) Kirby, J. A.; Robertson, A. S.; Smith, J. P.; Thompson, A. C.; Cooper, S. R.; Klein, M. P. *J. Am. Chem. Soc.* **1981**, *103*, 5529.
(141) Pecoraro, V. L.; Hsieh, W. Y. In *Manganese and its Role in Biological Processes*; Sigel, A., Sigel, H., Eds.; Metal Ions in Biological Systems, Vol. 37; Marcel Dekker: New York, 2000; p 429.
(142) Yachandra, V. K.; Guiles, R. D.; McDermott, A. E.; Cole, J. L.; Britt, R. D.; Dexheimer, S. L.; Sauer, K.; Klein, M. P. *Biochemistry* **1987**, *26*, 5974.
(143) Robblee, J. H.; Messinger, J.; Cinco, R. M.; McFarlane, K. L.; Fernandez, C.; Pizarro, S. A.; Sauer, K.; Yachandra, V. K. *J. Am. Chem. Soc.* **2002**, *124*, 7459.
(144) Haumann, M.; Muller, C.; Liebisch, P.; Iuzzolino, L.; Dittmer, J.; Grabolle, M.; Neisius, T.; Meyer-Klaucke, W.; Dau, H. *Biochemistry* **2005**, *44*, 1894.
(145) Liang, W. C.; Roelofs, T. A.; Cinco, R. M.; Rompel, A.; Latimer, M. J.; Yu, W. O.; Sauer, K.; Klein, M. P.; Yachandra, V. K. *J. Am. Chem. Soc.* **2000**, *122*, 3399.
(146) Messinger, J.; Wacker, U.; Renger, G. *Biochemistry* **1991**, *30*, 7852.
(147) Casey, J. L.; Sauer, K. *Biochim. Biophys. Acta* **1984**, *767*, 21.
(148) Beck, W. F.; Brudvig, G. W. *Chem. Scr.* **1988**, *28A*, 93.
(149) Szalai, V. A.; Brudvig, G. W. *Biochemistry* **1996**, *35*, 1946.
(150) Szalai, V. A.; Kühne, H.; Lakshmi, K. V.; Brudvig, G. W. *Biochemistry* **1998**, *37*, 13594.
(151) Szalai, V. A.; Brudvig, G. W. *Biochemistry* **1996**, *35*, 15080.
(152) Tang, X. S.; Randall, D. W.; Force, D. A.; Diner, B. A.; Britt, R. D. *J. Am. Chem. Soc.* **1996**, *118*, 7638.
(153) Maclachlan, D. J.; Nugent, J. H. A. *Biochemistry* **1993**, *32*, 9772.
(154) Karge, M.; Irrgang, K. D.; Renger, G. *Biochemistry* **1997**, *36*, 8904.
(155) Renger, G.; Hanssum, B. *FEBS Lett.* **1992**, *299*, 28.
(156) Renger, G.; Christen, G.; Karge, M.; Eckert, H. J.; Irrgang, K. D. *J. Biol. Inorg. Chem.* **1998**, *3*, 360.
(157) Haumann, M.; Bogershausen, O.; Cherepanov, D.; Ahlbrink, R.; Junge, W. *Photosynth. Res.* **1997**, *51*, 193.
(158) Lydakis-Simantiris, N.; Ghanotakis, D. F.; Babcock, G. T. *Biochim. Biophys. Acta* **1997**, *1322*, 129.
(159) Hasegawa, K.; Ono, T.; Inoue, T.; Kusunoki, M. *Bull. Chem. Soc. Jpn.* **1999**, *72*, 1013.
(160) Kulik, L.; Epel, B.; Messinger, J.; Lubitz, W. *Photosynth. Res.* **2005**, *84*, 347.
(161) Charlot, M. F.; Boussac, A.; Blondin, G. *Biochim. Biophys. Acta* **2005**, *1708*, 120.
(162) Carrell, T. G.; Tyryshkin, A. M.; Dismukes, G. C. *J. Biol. Inorg. Chem.* **2002**, *7*, 2.
(163) Dorlet, P.; Di Valentin, M.; Babcock, G. T.; McCracken, J. L. *J. Phys. Chem. B* **1998**, *102*, 8239.
(164) Lakshmi, K. V.; Eaton, S. S.; Eaton, G. R.; Frank, H. A.; Brudvig, G. W. *J. Phys. Chem. B* **1998**, *102*, 8327.
(165) Lakshmi, K. V.; Eaton, S. S.; Eaton, G. R.; Brudvig, G. W. *Biochemistry* **1999**, *38*, 12758.
(166) Peloquin, J. M.; Campbell, K. A.; Britt, R. D. *J. Am. Chem. Soc.* **1998**, *120*, 6840.
(167) Debus, R. J. In *Photosystem II: The Light-Driven Water:Plastoquinone Oxidoreductase*; Wydrzynski, T. J., Satoh, K., Eds.; Advances in Photosynthesis and Respiration 22; Springer: Dordrecht, The Netherlands, 2005; p 261.
(168) Debus, R. J. *Biochim. Biophys. Acta* **2001**, *1503*, 164.
(169) Diner, B. A. *Biochim. Biophys. Acta* **2001**, *1503*, 147.
(170) Tang, X. S.; Diner, B. A.; Larsen, B. S.; Gilchrist, M. L.; Lorigan, G. A.; Britt, R. D. *Proc. Natl. Acad. Sci. U.S.A.* **1994**, *91*, 704.
(171) Britt, R. D.; Tang, X. S.; Gilchrist, M. L.; Lorigan, G. A.; Larsen, B. S.; Diner, B. A. *Biochem. Soc. Trans.* **1994**, *22*, 343.
(172) Debus, R. J.; Campbell, K. A.; Gregor, W.; Li, Z. L.; Burnap, R. L.; Britt, R. D. *Biochemistry* **2001**, *40*, 3690.
(173) Debus, R. J.; Campbell, K. A.; Peloquin, J. M.; Pham, D. P.; Britt, R. D. *Biochemistry* **2000**, *39*, 470.
(174) Guy, R. D.; Fogel, M. L.; Berry, J. A. *Plant Physiol.* **1993**, *101*, 37.
(175) Kimura, Y.; Mizusawa, N.; Ishii, A.; Ono, T. A. *Biochemistry* **2005**, *44*, 16072.
(176) Nixon, P. J.; Trost, J. T.; Diner, B. A. *Biochemistry* **1992**, *31*, 10859.
(177) Kimura, Y.; Hasegawa, K.; Ono, T. *Biochemistry* **2002**, *41*, 5844.
(178) Strickler, M. A.; Walker, L. M.; Hillier, W.; Debus, R. J. *Biochemistry* **2005**, *44*, 8571.
(179) Chu, H.; Hillier, W.; Debus, R. J. *Biochemistry* **2004**, *43*, 3152.
(180) Kimura, Y.; Mizusawa, N.; Yamanari, T.; Ishii, A.; Ono, T. *J. Biol. Chem.* **2005**, *280*, 2078.
(181) Gascon, J. A.; Sproviero, E. M.; McEvoy, J. P.; Brudvig, G. W.; Batista, V. S., unpublished results.
(182) Nixon, P. J.; Diner, B. A. *Biochemistry* **1992**, *31*, 942.
(183) Campbell, K. A.; Force, D. A.; Nixon, P. J.; Dole, F.; Diner, B. A.; Britt, R. D. *J. Am. Chem. Soc.* **2000**, *122*, 3754.
(184) Debus, R. J.; Aznar, C.; Campbell, K. A.; Gregor, W.; Diner, B. A.; Britt, R. D. *Biochemistry* **2003**, *42*, 10600.
(185) Chu, H. A.; Debus, R. J.; Babcock, G. T. *Biochemistry* **2001**, *40*, 2312.

(186) Debus, R. J.; Strickler, M. A.; Walker, L. M.; Hillier, W. *Biochemistry* **2005**, *44*, 1367.
(187) Glatzel, P.; Bergmann, U.; Yano, J.; Visser, H.; Robblee, J. H.; Gu, W. W.; de Groot, F. M. F.; Christou, G.; Pecoraro, V. L.; Cramer, S. P.; Yachandra, V. K. *J. Am. Chem. Soc.* **2004**, *126*, 9946.
(188) Sproviero, E. M.; Gascon, J. A.; McEvoy, J. P.; Brudvig, G. W.; Batista, V. S. *J. Chem. Theory Comput.* **2006**, *2*, 1119.
(189) McEvoy, J. P.; Gascon, J. A.; Batista, V. S.; Brudvig, G. W. *Photochem. Photobiol. Sci.* **2005**, *4*, 940.
(190) Rhee, K. H.; Morriss, E. P.; Barber, J.; Kühlbrandt, W. *Nature (London)* **1998**, *396*, 283.
(191) Strickler, M. A.; Hillier, W.; Debus, R. J. *Biochemistry* **2006**, *45*, 8801.
(192) Yano, J.; Kern, J.; Irrgang, K. D.; Latimer, M. J.; Bergmann, U.; Glatzel, P.; Pushkar, Y.; Biesiadka, J.; Loll, B.; Sauer, K.; Messinger, J.; Zouni, A.; Yachandra, V. K. *Proc. Natl. Acad. Sci. U.S.A.* **2005**, *102*, 12047.
(193) Dau, H.; Liebisch, P.; Haumann, M. *Phys. Chem. Chem. Phys.* **2004**, *6*, 4781.
(194) Grabolle, M.; Haumann, M.; Muller, C.; Liebisch, P.; Dau, H. *J. Biol. Chem.* **2006**, *281*, 4580.
(195) van Rensen, J. J. S. *Photosynth. Res.* **2002**, *73*, 185.
(196) van Rensen, J. J. S.; Klimov, V. V. In *Photosystem II: The Light-Driven Water:Plastoquinone Oxidoreductase*; Wydrzynski, T. J., Satoh, K., Eds.; Advances in Photosynthesis and Respiration 22; Springer: Dordrecht, The Netherlands, 2005; p 329.
(197) Stemler, A. J. *Photosynth. Res.* **2002**, *73*, 177.
(198) Klimov, V. V.; Baranov, S. V. *Biochim. Biophys. Acta* **2001**, *1503*, 187.
(199) Hillier, W.; McConnell, I.; Badger, M. R.; Boussac, A.; Klimov, V. V.; Dismukes, G. C.; Wydrzynski, T. *Biochemistry* **2006**, *45*, 2094.
(200) Radmer, R.; Ollinger, O. *FEBS Lett.* **1980**, *110*, 57.
(201) Stemler, A.; Radmer, R. *Science* **1975**, *190*, 457.
(202) Clausen, J.; Beckmann, K.; Junge, W.; Messinger, J. *Plant Physiol.* **2005**, *139*, 1444.
(203) Allakhverdiev, S. I.; Yruela, I.; Picorel, R.; Klimov, V. V. *Proc. Natl. Acad. Sci. U.S.A.* **1997**, *94*, 5050.
(204) Baranov, S. V.; Tyryshkin, A. M.; Katz, D.; Dismukes, G. C.; Ananyev, G. M.; Klimov, V. V. *Biochemistry* **2004**, *43*, 2070.
(205) Brudvig, G. W.; Crabtree, R. H. *Proc. Natl. Acad. Sci. U.S.A.* **1986**, *83*, 4586.
(206) Mukhopadhyay, S.; Mandal, S. K.; Bhaduri, S.; Armstrong, W. H. *Chem. Rev.* **2004**, *104*, 3981.
(207) Mishra, A.; Wernsdorfer, W.; Abboud, K. A.; Christou, G. *Chem. Commun.* **2005**, 54.
(208) Lundberg, M.; Siegbahn, P. E. M. *Phys. Chem. Chem. Phys.* **2004**, *6*, 4772.
(209) Sproviero, E. M.; Gascon, J. A.; McEvoy, J. P.; Brudvig, G. W.; Batista, V. S. *J. Inorg. Biochem.* **2006**, *100*, 786.
(210) Kohen, A.; Klinman, J. P. *Chem. Biol.* **1999**, *6*, R191.
(211) Rappaport, F.; Lavergne, J. *Biochim. Biophys. Acta* **2001**, *1503*, 246.
(212) Sharp, R. R. In *Manganese Redox Enzymes*; Pecoraro, V. L., Ed.; VCH: New York, 1992; p 177.
(213) Wydrzynski, T. J. *Photosynth. Res.* **2004**, *80*, 125.
(214) Bovet, J. M.; Park, E. J.; Sharp, R. R. *Photosynth. Res.* **1993**, *38*, 347.
(215) Dekker: J. P. In *Manganese Redox Enzymes*; Pecoraro, V. L., Ed.; VCH: New York, 1992; p 85.
(216) de Paula, J. C.; Brudvig, G. W. *J. Am. Chem. Soc.* **1985**, *107*, 2643.
(217) Zimmermann, J. L.; Rutherford, A. W. *Biochemistry* **1986**, *25*, 4609.
(218) Haddy, A.; Lakshmi, K. V.; Brudvig, G. W.; Frank, H. A. *Biophys. J.* **2004**, *87*, 2885.
(219) Cotton, F. A.; Wilkinson, G. *Advanced Inorganic Chemistry*, 6th ed.; Wiley-Interscience: New York, 1999.
(220) Thorp, H. H. *Inorg. Chem.* **1992**, *31*, 1585.
(221) Riggs, P. J.; Mei, R.; Yocum, C. F.; Penner-Hahn, J. E. *J. Am. Chem. Soc.* **1992**, *114*, 10650.
(222) Bergmann, U.; Grush, M. M.; Horne, C. R.; DeMarois, P.; Penner-Hahn, J. E.; Yocum, C. F.; Wright, D. W.; Dube, C. E.; Armstrong, W. H.; Christou, G.; Eppley, H. J.; Cramer, S. P. *J. Phys. Chem. B* **1998**, *102*, 8350.
(223) Messinger, J.; Robblee, J. H.; Bergmann, U.; Fernandez, C.; Glatzel, P.; Visser, H.; Cinco, R. M.; McFarlane, K. L.; Bellacchio, E.; Pizarro, S. A.; Cramer, S. P.; Sauer, K.; Klein, M. P.; Yachandra, V. K. *J. Am. Chem. Soc.* **2001**, *123*, 7804.
(224) Pizarro, S. A.; Glatzel, P.; Visser, H.; Robblee, J. H.; Christou, G.; Bergmann, U.; Yachandra, V. K. *Phys. Chem. Chem. Phys.* **2004**, *6*, 4864.
(225) Zheng, M.; Khangulov, S. V.; Dismukes, G. C.; Barynin, V. V. *Inorg. Chem.* **1994**, *33*, 382.
(226) Kuntzleman, T.; Yocum, C. F. *Biochemistry* **2005**, *44*, 2129.
(227) Riggs-Gelasco, P. J.; Mei, R.; Yocum, C. F.; Penner-Hahn, J. E. *J. Am. Chem. Soc.* **1996**, *118*, 2387.
(228) Messinger, J.; Seaton, G.; Wydrzynski, T.; Wacker, U.; Renger, G. *Biochemistry* **1997**, *36*, 6862.
(229) Goodin, D. B.; Yachandra, V. K.; Britt, R. D.; Sauer, K.; Klein, M. P. *Biochim. Biophys. Acta* **1984**, *767*, 209.
(230) Dekker: J. P.; van Gorkom, H. J.; Brok, M.; Ouwehand, L. *Biochim. Biophys. Acta* **1984**, *764*, 301.
(231) Cole, J.; Yachandra, V. K.; Guiles, R. D.; McDermott, A. E.; Britt, R. D.; Dexheimer, S. L.; Sauer, K.; Klein, M. P. *Biochim. Biophys. Acta* **1987**, *890*, 395.
(232) Kusunoki, M.; Ono, T.; Matsushita, T.; Oyanagi, H.; Inoue, Y. *J. Biochem.* **1990**, *108*, 560.
(233) Ono, T.; Noguchi, T.; Inoue, Y.; Kusunoki, M.; Matsushita, T.; Oyanagi, H. *Science* **1992**, *258*, 1335.
(234) Roelofs, T. A.; Liang, W. C.; Latimer, M. J.; Cinco, R. M.; Rompel, A.; Andrews, J. C.; Sauer, K.; Yachandra, V. K.; Klein, M. P. *Proc. Natl. Acad. Sci. U.S.A.* **1996**, *93*, 3335.
(235) Iuzzolino, L.; Dittmer, J.; Dorner, W.; Meyer-Klaucke, W.; Dau, H. *Biochemistry* **1998**, *37*, 17112.
(236) Robblee, J. H.; Cinco, R. M.; Yachandra, V. K. *Biochim. Biophys. Acta* **2001**, *1503*, 7.
(237) Guiles, R. D.; Yachandra, V. K.; McDermott, A. E.; Cole, J. L.; Dexheimer, S. L.; Britt, R. D.; Sauer, K.; Klein, M. P. *Biochemistry* **1990**, *29*, 486.
(238) Lavergne, J.; Junge, W. *Photosynth. Res.* **1993**, *38*, 279.
(239) Haumann, M.; Junge, W. In *Oxygenic Photosynthesis: The Light Reactions*; Ort, D. R., Yocum, C. F., Eds.; Advances in Photosynthesis, Vol. 4; Kluwer Academic Publishers: Dordrecht, The Netherlands, 1996; p 165.
(240) Haumann, M.; Hundelt, M.; Jahns, P.; Chroni, S.; Bogershausen, O.; Ghanotakis, D.; Junge, W. *FEBS Lett.* **1997**, *410*, 243.
(241) Schlodder, E.; Witt, H. T. *J. Biol. Chem.* **1999**, *274*, 30387.
(242) Saygin, Ö.; Witt, H. T. *FEBS Lett.* **1985**, *187*, 224.
(243) Saygin, Ö.; Witt, H. T. *FEBS Lett.* **1984**, *176*, 83.
(244) Rappaport, F.; Lavergne, J. *Biochemistry* **1991**, *30*, 10004.
(245) Kretschmann, H.; Schlodder, E.; Witt, H. T. *Biochim. Biophys. Acta* **1996**, *1274*, 1.
(246) Damoder, R.; Dismukes, G. C. *FEBS Lett.* **1984**, *174*, 157.
(247) Geijer, P.; Deak, Z.; Styring, S. *Biochemistry* **2000**, *39*, 6763.
(248) Bernat, G.; Morvaridi, F.; Feyziyev, Y.; Styring, S. *Biochemistry* **2002**, *41*, 5830.
(249) Suzuki, H.; Sugiura, M.; Noguchi, T. *Biochemistry* **2005**, *44*, 1708.
(250) Tommos, C.; Hoganson, C. W.; Di Valentin, M.; Lydakis-Simantiris, N.; Dorlet, P.; Westphal, K.; Chu, H. A.; McCracken, J.; Babcock, G. T. *Curr. Opin. Chem. Biol.* **1998**, *2*, 244.
(251) Brettel, K.; Schlodder, E.; Witt, H. T. *Biochim. Biophys. Acta* **1984**, *766*, 403.
(252) Eckert, H. J.; Renger, G. *FEBS Lett.* **1988**, *236*, 425.
(253) Jeans, C.; Schilstra, M. J.; Klug, D. R. *Biochemistry* **2002**, *41*, 5015.
(254) Koike, H.; Hanssum, B.; Inoue, Y.; Renger, G. *Biochim. Biophys. Acta* **1987**, *893*, 524.
(255) Brudvig, G. W.; Casey, J. L.; Sauer, K. *Biochim. Biophys. Acta* **1983**, *723*, 366.
(256) Styring, S.; Rutherford, A. W. *Biochim. Biophys. Acta* **1988**, *933*, 378.
(257) Zhang, C. X.; Styring, S. *Biochemistry* **2003**, *42*, 8066.
(258) Jahns, P.; Junge, W. *Biochemistry* **1992**, *31*, 7398.
(259) Jahns, P.; Lavergne, J.; Rappaport, F.; Junge, W. *Biochim. Biophys. Acta* **1991**, *1057*, 313.
(260) Wang, S. Y.; Wemple, M. S.; Yoo, J.; Folting, K.; Huffman, J. C.; Hagen, K. S.; Hendrickson, D. N.; Christou, G. *Inorg. Chem.* **2000**, *39*, 1501.
(261) Gelasco, A.; Kirk, M. L.; Kampf, J. W.; Pecoraro, V. L. *Inorg. Chem.* **1997**, *36*, 1829.
(262) Lal, T. K.; Mukherjee, R. *Inorg. Chem.* **1998**, *37*, 2373.
(263) Krishtalik, L. I. *Biochim. Biophys. Acta* **1986**, *849*, 162.
(264) Krishtalik, L. I. *Bioelectrochem. Bioenerg.* **1990**, *23*, 249.
(265) Hoganson, C. W.; Babcock, G. T. *Science* **1997**, *277*, 1953.
(266) Blomberg, M. R. A.; Siegbahn, P. E. M.; Styring, S.; Babcock, G. T.; Akermark, B.; Korall, P. *J. Am. Chem. Soc.* **1997**, *119*, 8285.
(267) Hoganson, C. W.; Lydakis-Simantiris, N.; Tang, X. S.; Tommos, C.; Warncke, K.; Babcock, G. T.; Diner, B. A.; McCracken, J.; Styring, S. *Photosynth. Res.* **1995**, *46*, 177.
(268) Tommos, C.; Babcock, G. T. *Acc. Chem. Res.* **1998**, *31*, 18.
(269) Force, D. A.; Randall, D. W.; Britt, R. D.; Tang, X. S.; Diner, B. A. *J. Am. Chem. Soc.* **1995**, *117*, 12643.
(270) Diner, B. A.; Force, D. A.; Randall, D. W.; Britt, R. D. *Biochemistry* **1998**, *37*, 17931.
(271) Tang, X. S.; Zheng, M.; Chisholm, D. A.; Dismukes, G. C.; Diner, B. A. *Biochemistry* **1996**, *35*, 1475.
(272) Tommos, C.; Tang, X. S.; Warncke, K.; Hoganson, C. W.; Styring, S.; McCracken, J.; Diner, B. A.; Babcock, G. T. *J. Am. Chem. Soc.* **1995**, *117*, 10325.
(273) Un, S.; Tang, X. S.; Diner, B. A. *Biochemistry* **1996**, *35*, 679.

(274) Tommos, C.; McCracken, J.; Styring, S.; Babcock, G. T. *J. Am. Chem. Soc.* **1998**, *120*, 10441.
(275) Ahlbrink, R.; Haumann, M.; Cherepanov, D.; Bogershausen, O.; Mulkidjanian, A.; Junge, W. *Biochemistry* **1998**, *37*, 1131.
(276) Lide, D. R. *Handbook of Chemistry and Physics*, 77th ed.; CRC Press: Boca Raton, FL, 1996.
(277) Baldwin, M. J.; Pecoraro, V. L. *J. Am. Chem. Soc.* **1996**, *118*, 11325.
(278) Tommos, C.; Babcock, G. T. *Biochim. Biophys. Acta* **2000**, *1458*, 199.
(279) Kühne, H.; Brudvig, G. W. *J. Phys. Chem. B* **2002**, *106*, 8189.
(280) Hays, A. M. A.; Vassiliev, I. R.; Golbeck, J. H.; Debus, R. J. *Biochemistry* **1998**, *37*, 11352.
(281) Mamedov, F.; Sayre, R. T.; Styring, S. *Biochemistry* **1998**, *37*, 14245.
(282) Candeias, L. P.; Turconi, S.; Nugent, J. H. A. *Biochim. Biophys. Acta* **1998**, *1363*, 1.
(283) Nugent, J. H. A.; Rich, A. M.; Evans, M. C. W. *Biochim. Biophys. Acta* **2001**, *1503*, 138.
(284) Diner, B. A.; Bautista, J. A.; Nixon, P. J.; Berthomieu, C.; Hienerwadel, R.; Britt, R. D.; Vermaas, W. F. J.; Chisholm, D. A. *Phys. Chem. Chem. Phys.* **2004**, *6*, 4844.
(285) Schilstra, M. J.; Rappaport, F.; Nugent, J. H. A.; Barnett, C. J.; Klug, D. R. *Biochemistry* **1998**, *37*, 3974.
(286) Christen, G.; Seeliger, A.; Renger, G. *Biochemistry* **1999**, *38*, 6082.
(287) Christen, G.; Renger, G. *Biochemistry* **1999**, *38*, 2068.
(288) Berthomieu, C.; Hienerwadel, R. *Biochim. Biophys. Acta* **2005**, *1707*, 51.
(289) Noguchi, T.; Inoue, Y.; Tang, X. S. *Biochemistry* **1997**, *36*, 14705.
(290) Berthomieu, C.; Hienerwadel, R.; Boussac, A.; Breton, J.; Diner, B. A. *Biochemistry* **1998**, *37*, 10547.
(291) Haumann, M.; Mulkidjanian, A.; Junge, W. *Biochemistry* **1999**, *38*, 1258.
(292) Jeans, C.; Schilstra, M. J.; Ray, N.; Husain, S.; Minagawa, J.; Nugent, J. H. A.; Klug, D. R. *Biochemistry* **2002**, *41*, 15754.
(293) Diner, B. A.; Nixon, P. J. In *Photosynthesis: Mechanisms and Effects*; Garab, G., Ed.; Kluwer Academic Publishers: Dordrecht, The Netherlands, 1998; Vol. 2; p 1177.
(294) Zhang, C. X.; Boussac, A.; Rutherford, A. W. *Biochemistry* **2004**, *43*, 13787.
(295) Tang, X. S.; Chisholm, D. A.; Dismukes, G. C.; Brudvig, G. W.; Diner, B. A. *Biochemistry* **1993**, *32*, 13742.
(296) Faller, P.; Goussias, C.; Rutherford, A. W.; Un, S. *Proc. Natl. Acad. Sci. U.S.A.* **2003**, *100*, 8732.
(297) Faller, P.; Rutherford, A. W.; Debus, R. J. *Biochemistry* **2002**, *41*, 12914.
(298) Babcock, G. T.; Barry, B. A.; Debus, R. J.; Hoganson, C. W.; Atamian, M.; McIntosh, L.; Sithole, I.; Yocum, C. F. *Biochemistry* **1989**, *28*, 9557.
(299) Frey, P. A. In *Encyclopedia of Biological Chemistry*; Lennarz, W., Lane, M., Eds.; Elsevier: Oxford, U.K., 2004; Vol. 2, p 594.
(300) Rappaport, F.; Lavergne, J. *Biochemistry* **1997**, *36*, 15294.
(301) Rappaport, F.; Blanchard-Desce, M.; Lavergne, J. *Biochim. Biophys. Acta* **1994**, *1184*, 178.
(302) Junge, W.; Haumann, M.; Ahlbrink, R.; Mulkidjanian, A.; Clausen, J. *Philos. Trans. R. Soc. London, Ser. B: Biol. Sci.* **2002**, *357*, 1407.
(303) Ioannidis, N.; Nugent, J. H. A.; Petrouleas, V. *Biochemistry* **2002**, *41*, 9589.
(304) Petrouleas, V.; Koulougliotis, D.; Ioannidis, N. *Biochemistry* **2005**, *44*, 6723.
(305) Nugent, J. H. A.; Ball, R. J.; Evans, M. C. W. *Biochim. Biophys. Acta* **2004**, *1655*, 217.
(306) Geijer, P.; Peterson, S.; Ahrling, K. A.; Deak, Z.; Styring, S. *Biochim. Biophys. Acta* **2001**, *1503*, 83.
(307) Geijer, P.; Morvaridi, F.; Styring, S. *Biochemistry* **2001**, *40*, 10881.
(308) Su, J. H.; Havelius, K. G. V.; Mamedov, F.; Ho, F. M.; Styring, S. *Biochemistry* **2006**, *45*, 7617.
(309) Renger, G. *FEBS Lett.* **1977**, *81*, 223.
(310) Velthuys, B. R. *Annu. Rev. Plant Physiol. Plant Mol. Biol.* **1980**, *31*, 545.
(311) Vincent, J. B.; Christou, G. *Inorg. Chim. Acta* **1987**, *136*, L41.
(312) Pecoraro, V. L. *Photochem. Photobiol.* **1988**, *48*, 249.
(313) Renger, G. *Chem. Scr.* **1988**, *28A*, 105.
(314) Homann, P. H. *Plant Physiol.* **1988**, *88*, 1.
(315) Brudvig, G. W.; Thorp, H. H.; Crabtree, R. H. *Acc. Chem. Res.* **1991**, *24*, 311.
(316) Brudvig, G. W.; Beck, W. F.; de Paula, J. C. *Annu. Rev. Biophys. Biophys. Chem.* **1989**, *18*, 25.
(317) Vrettos, J. S.; Brudvig, G. W. In *Comprehensive Coordination Chemistry II: From Biology to Nanotechnology*; McCleverty, J. A., Meyer, T. J., Eds.; Elsevier: Amsterdam, 2003; Vol. 8, p 507.
(318) Ananyev, G. M.; Zaltsman, L.; Vasko, C.; Dismukes, G. C. *Biochim. Biophys. Acta* **2001**, *1503*, 52.
(319) Barber, J. *Biochim. Biophys. Acta* **2004**, *1655*, 123.
(320) Dismukes, G. C.; Zheng, M.; Hutchins, R.; Philo, J. S. *Biochem. Soc. Trans.* **1994**, *22*, 323.
(321) Messinger, J. *Biochim. Biophys. Acta* **2000**, *1459*, 481.
(322) Siegbahn, P. E. M. *Inorg. Chem.* **2000**, *39*, 2923.
(323) Fromme, P.; Kern, J.; Loll, B.; Biesiadka, J.; Saenger, W.; Witt, H. T.; Krauss, N.; Zouni, A. *Philos. Trans. R. Soc. London, Ser. B: Biol. Sci.* **2002**, *357*, 1337.
(324) Goussias, C.; Boussac, A.; Rutherford, A. W. *Philos. Trans. R. Soc. London, Ser. B: Biol. Sci.* **2002**, *357*, 1369.
(325) Sauer, K.; Yachandra, V. K. *Proc. Natl. Acad. Sci. U.S.A.* **2002**, *99*, 8631.
(326) Tommos, C. *Philos. Trans. R. Soc. London, Ser. B: Biol. Sci.* **2002**, *357*, 1383.
(327) Halfen, J. A.; Mahapatra, S.; Wilkinson, E. C.; Kaderli, S.; Young, V. G.; Que, L.; Zuberbuhler, A. D.; Tolman, W. B. *Science* **1996**, *271*, 1397.
(328) Tolman, W. B. *Acc. Chem. Res.* **1997**, *30*, 227.
(329) Lewis, E. A.; Tolman, W. B. *Chem. Rev.* **2004**, *104*, 1047.
(330) Yachandra, V. K. *Philos. Trans. R. Soc. London, Ser. B: Biol. Sci.* **2002**, *357*, 1347.
(331) Messinger, J.; Robblee, J. H.; Fernandez, C.; Cinco, R. M.; Visser, H.; Bergmann, U.; Glatzel, P.; Cramer, S. P.; Campbell, K. A.; Peloquin, J. M.; Britt, R. D.; Sauer, K.; Yachandra, V. K.; Klein, M. L. In *Photosynthesis: Mechanisms and Effects*; Garab, G., Ed.; Kluwer Academic Publishers: Dordrecht, The Netherlands, 1998; Vol. 2, p 1279.
(332) Sauer, K.; Yachandra, V. K. *Biochim. Biophys. Acta* **2004**, *1655*, 140.
(333) Yachandra, V. K.; DeRose, V. J.; Latimer, M. J.; Mukerji, I.; Sauer, K.; Klein, M. P. *Science* **1993**, *260*, 675.
(334) Messinger, J. *Phys. Chem. Chem. Phys.* **2004**, *6*, 4764.
(335) Siegbahn, P. E. M.; Blomberg, M. R. A. *Philos. Trans. R. Soc. London, Ser. A* **2005**, *363*, 847.
(336) Messinger, J.; Badger, M.; Wydrzynski, T. *Proc. Natl. Acad. Sci. U.S.A.* **1995**, *92*, 3209.
(337) Dau, H.; Iuzzolino, L.; Dittmer, J.; Dorner, W.; Meyer-Klaucke, W. In *Photosynthesis: Mechanism and* Effects; Garab, G., Ed.; Kluwer Academic Publishers: Dordrecht, The Netherlands, 1998; Vol. 2, p 1327.
(338) Ruettinger, W. F.; Yagi, M.; Wolf, K.; Bernasek, S.; Dismukes, G. C. *J. Am. Chem. Soc.* **2000**, *122*, 10353.
(339) Proserpio, D. M.; Hoffmann, R.; Dismukes, G. C. *J. Am. Chem. Soc.* **1992**, *114*, 4374.
(340) Micklitz, W.; Bott, S. G.; Bentsen, J. G.; Lippard, S. J. *J. Am. Chem. Soc.* **1989**, *111*, 372.
(341) Manev, V.; Ilchev, N.; Nassalevska, A. *J. Power Sources* **1989**, *25*, 167.
(342) Yagi, M.; Wolf, K. V.; Baesjou, P. J.; Bernasek, S. L.; Dismukes, G. C. *Angew. Chem., Int. Ed.* **2001**, *40*, 2925.
(343) Carrell, T. G.; Cohen, S.; Dismukes, G. C. *J. Mol. Catal. A: Chem.* **2002**, *187*, 3.
(344) Groves, J. T.; Lee, J. B.; Marla, S. S. *J. Am. Chem. Soc.* **1997**, *119*, 6269.
(345) Zhang, R.; Newcomb, M. *J. Am. Chem. Soc.* **2003**, *125*, 12418.
(346) Ruettinger, W. F.; Dismukes, G. C. *Inorg. Chem.* **2000**, *39*, 1021.
(347) Maneiro, M.; Ruettinger, W. F.; Bourles, E.; McLendon, G. L.; Dismukes, G. C. *Proc. Natl. Acad. Sci. U.S.A.* **2003**, *100*, 3707.
(348) Carrell, T. G.; Bourles, E.; Lin, M.; Dismukes, G. C. *Inorg. Chem.* **2003**, *42*, 2849.
(349) Shimazaki, Y.; Nagano, T.; Takesue, H.; Ye, B. H.; Tani, F.; Naruta, Y. *Angew. Chem., Int. Ed.* **2004**, *43*, 98.
(350) Zhang, R.; Horner, J. H.; Newcomb, M. *J. Am. Chem. Soc.* **2005**, *127*, 6573.
(351) Meunier, B. *Chem. Rev.* **1992**, *92*, 1411.
(352) Watanabe, Y.; Fujii, H. *Struct. Bonding (Berlin)* **2000**, *97*, 61.
(353) Workman, J. M.; Powell, R. D.; Procyk, A. D.; Collins, T. J.; Bocian, D. F. *Inorg. Chem.* **1992**, *31*, 1548.
(354) Collins, T. J.; Gordon-Wylie, S. W. *J. Am. Chem. Soc.* **1989**, *111*, 4511.
(355) Collins, T. J.; Powell, R. D.; Slebodnick, C.; Uffelman, E. S. *J. Am. Chem. Soc.* **1990**, *112*, 899.
(356) MacDonnell, F. M.; Fackler, N. L. P.; Stern, C.; O'Halloran, T. V. *J. Am. Chem. Soc.* **1994**, *116*, 7431.
(357) Miller, C. G.; Gordon-Wylie, S. W.; Horwitz, C. P.; Strazisar, S. A.; Peraino, D. K.; Clark, G. R.; Weintraub, S. T.; Collins, T. J. *J. Am. Chem. Soc.* **1998**, *120*, 11540.
(358) Limburg, J.; Vrettos, J. S.; Liable-Sands, L. M.; Rheingold, A. L.; Crabtree, R. H.; Brudvig, G. W. *Science* **1999**, *283*, 1524.
(359) Limburg, J.; Vrettos, J. S.; Chen, H. Y.; de Paula, J. C.; Crabtree, R. H.; Brudvig, G. W. *J. Am. Chem. Soc.* **2001**, *123*, 423.
(360) Gersten, S. W.; Samuels, G. J.; Meyer, T. J. *J. Am. Chem. Soc.* **1982**, *104*, 4029.
(361) Hurst, J. K. *Coord. Chem. Rev.* **2005**, *249*, 313.

(362) Binstead, R. A.; Chronister, C. W.; Ni, J. F.; Hartshorn, C. M.; Meyer, T. J. *J. Am. Chem. Soc.* **2000**, *122*, 8464.
(363) Hurst, J. K.; Zhou, J. Z.; Lei, Y. B. *Inorg. Chem.* **1992**, *31*, 1010.
(364) Hendry, G.; Wydrzynski, T. *Biochemistry* **2002**, *41*, 13328.
(365) Hillier, W.; Wydrzynski, T. *Biochim. Biophys. Acta* **2001**, *1503*, 197.
(366) Wydrzynski, T.; Huggins, B. J.; Jursinic, P. A. *Biochim. Biophys. Acta* **1985**, *809*, 125.
(367) Kuzek, D.; Pace, R. J. *Biochim. Biophys. Acta* **2001**, *1503*, 123.
(368) Pace, R. J.; Åhrling, K. A. *Biochim. Biophys. Acta* **2004**, *1655*, 172.
(369) Razeghifard, M. R.; Pace, R. J. *Biochemistry* **1999**, *38*, 1252.
(370) Clausen, J.; Debus, R. J.; Junge, W. *Biochim. Biophys. Acta* **2004**, *1655*, 184.
(371) Richens, D. T. *The Chemistry of Aqua Ions*; John Wiley and Sons: Chichester, U.K., 1997.
(372) *Lange's Handbook of Chemistry*, 15th ed.; Dean, J. A., Ed.; McGraw-Hill: New York, 1999.
(373) Tagore, R.; Chen, H.; Crabtree, R. H.; Brudvig, G. W. *J. Am. Chem. Soc.* **2006**, *128*, 9457.
(374) Vrettos, J. S.; Stone, D. A.; Brudvig, G. W. *Biochemistry* **2001**, *40*, 7937.
(375) Boussac, A.; Rappaport, F.; Carrier, P.; Verbavatz, J.; Gobin, R.; Kirilovsky, D.; Rutherford, A. W.; Sugiura, M. *J. Biol. Chem.* **2004**, *279*, 22809.
(376) Pistorius, E. K. *Eur. J. Biochem.* **1983**, *135*, 217.
(377) Vander Meulen, K. A.; Hobson, A.; Yocum, C. F. *Biochim. Biophys. Acta* **2004**, *1655*, 179.
(378) Waggoner, C. M.; Pecoraro, V.; Yocum, C. F. *FEBS Lett.* **1989**, *244*, 237.
(379) Ono, T. *J. Inorg. Biochem.* **2000**, *82*, 85.
(380) Bakou, A.; Buser, C.; Dandulakis, G.; Brudvig, G.; Ghanotakis, D. F. *Biochim. Biophys. Acta* **1992**, *1099*, 131.
(381) McEvoy, J. P.; Gascon, J. A.; Sproviero, E. M.; Batista, V. S.; Brudvig, G. W. In *Photosynthesis: Fundamental Aspects to Global Perspectives*; Bruce, D., van der Est, A., Eds.; Allen Press: Lawrence, KS, 2005; Vol. 1, p 278.
(382) McEvoy, J. P.; Brudvig, G. W. *Phys. Chem. Chem. Phys.* **2004**, *6*, 4754.
(383) Vass, I.; Styring, S. *Biochemistry* **1991**, *30*, 830.
(384) Hoganson, C. W.; Tommos, C. *Biochim. Biophys. Acta* **2004**, *1655*, 116.
(385) Bricker, T. M. *Photosynth. Res.* **1990**, *24*, 1.
(386) Knoepfle, N.; Bricker, T. M.; Putnam-Evans, C. *Biochemistry* **1999**, *38*, 1582.
(387) Lavergne, J.; Blanchard-Desce, M.; Rappaport, F. In *Research in Photosynthesis*; Murata, N., Ed.; Kluwer Academic Publishers: Dordrecht, The Netherlands, 1992; Vol. 2, p 273.
(388) Voet, D.; Voet, J. G. *Biochemistry*, 2nd ed.; Wiley: New York, 1995.
(389) Guillén Schlippe, Y. V.; Hedstrom, L. *Arch. Biochem. Biophys.* **2005**, *433*, 266.
(390) Doherty, M. K.; Pealing, S. L.; Miles, C. S.; Moysey, R.; Taylor, P.; Walkinshaw, M. D.; Reid, G. A.; Chapman, S. K. *Biochemistry* **2000**, *39*, 10695.
(391) Mowat, C. G.; Moysey, R.; Miles, C. S.; Leys, D.; Doherty, M. K.; Taylor, P.; Walkinshaw, M. D.; Reid, G. A.; Chapman, S. K. *Biochemistry* **2001**, *40*, 12292.
(392) Taylor, P.; Pealing, S. L.; Reid, G. A.; Chapman, S. K.; Walkinshaw, M. D. *Nat. Struct. Biol.* **1999**, *6*, 1108.
(393) Horsefield, R.; Iwata, S.; Byrne, B. *Curr. Protein Pept. Sci.* **2004**, *5*, 107.
(394) Turner, K. L.; Doherty, M. K.; Heering, H. A.; Armstrong, F. A.; Reid, G. A.; Chapman, S. K. *Biochemistry* **1999**, *38*, 3302.
(395) Berthold, D. A.; Babcock, G. T.; Yocum, C. F. *FEBS Lett.* **1981**, *134*, 231.
(396) Lee, C.; Brudvig, G. W. *J. Chin. Chem. Soc.* **2004**, *51*, 1221.
(397) Mowat, C. G.; Pankhurst, K. L.; Miles, C. S.; Leys, D.; Walkinshaw, M. D.; Reid, G. A.; Chapman, S. K. *Biochemistry* **2002**, *41*, 11990.
(398) Messner, K. R.; Imlay, J. A. *J. Biol. Chem.* **2002**, *277*, 42563.
(399) Tedeschi, G.; Negri, A.; Mortarino, M.; Ceciliani, F.; Simonic, T.; Faotto, L.; Ronchi, S. *Eur. J. Biochem.* **1996**, *239*, 427.
(400) Bossi, R. T.; Negri, A.; Tedeschi, G.; Mattevi, A. *Biochemistry* **2002**, *41*, 3018.
(401) Tedeschi, G.; Ronchi, S.; Simonic, T.; Treu, C.; Mattevi, A.; Negri, A. *Biochemistry* **2001**, *40*, 4738.
(402) Charnock, S. J.; Brown, I. E.; Turkenburg, J. P.; Black, G. W.; Davies, G. J. *Proc. Natl. Acad. Sci. U.S.A.* **2002**, *99*, 12067.
(403) Tardy, F.; Nasser, W.; Robert-Baudouy, J.; Hugouvieux-Cotte-Pattat, N. *J. Bacteriol.* **1997**, *179*, 2503.
(404) Sanchez-Torres, P.; Visser, J.; Benen, J. A. E. *Biochem. J.* **2003**, *370*, 331.
(405) Herron, S. R.; Scavetta, R. D.; Garrett, M.; Legner, M.; Jurnak, F. *J. Biol. Chem.* **2003**, *278*, 12271.
(406) Herron, S. R.; Benen, J. A. E.; Scavetta, R. D.; Visser, J.; Jurnak, F. *Proc. Natl. Acad. Sci. U.S.A.* **2000**, *97*, 8762.
(407) Scavetta, R. D.; Herron, S. R.; Hotchkiss, A. T.; Kita, N.; Keen, N. T.; Benen, J. A. E.; Kester, H. C. M.; Visser, J.; Jurnak, F. *Plant Cell* **1999**, *11*, 1081.
(408) Guillén Schlippe, Y. V.; Hedstrom, L. *Biochemistry* **2005**, *44*, 11700.
(409) Guillén Schlippe, Y. V.; Riera, T. V.; Seyedsayamdost, M. R.; Hedstrom, L. *Biochemistry* **2004**, *43*, 4511.
(410) Markham, G. D.; Bock, C. L.; Schalk-Hihi, C. *Biochemistry* **1999**, *38*, 4433.
(411) Gan, L.; Seyedsayamdost, M. R.; Shuto, S.; Matsuda, A.; Petsko, G. A.; Hedstrom, L. *Biochemistry* **2003**, *42*, 857.
(412) Sundararaju, B.; Antson, A. A.; Phillips, R. S.; Demidkina, T. V.; Barbolina, M. V.; Gollnick, P.; Dodson, G. G.; Wilson, K. S. *Biochemistry* **1997**, *36*, 6502.
(413) Faleev, N. G.; Axenova, O. V.; Demidkina, T. V.; Phillips, R. S. *Biochim. Biophys. Acta* **2003**, *1647*, 260.
(414) Kiick, D. M.; Phillips, R. S. *Biochemistry* **1988**, *27*, 7333.
(415) Poulos, T. L.; Kraut, J. *J. Biol. Chem.* **1980**, *255*, 8199.
(416) Smith, A. T.; Sanders, S. A.; Greschik, H.; Thorneley, R. N. F.; Burke, J. F.; Bray, R. C. *Biochem. Soc. Trans.* **1992**, *20*, 340.
(417) Vitello, L. B.; Erman, J. E.; Miller, M. A.; Wang, J.; Kraut, J. *Biochemistry* **1993**, *32*, 9807.
(418) Howes, B. D.; Rodriguez-Lopez, J. N.; Smith, A. T.; Smulevich, G. *Biochemistry* **1997**, *36*, 1532.
(419) Rodriguez-Lopez, J. N.; Lowe, D. J.; Hernandez-Ruiz, J.; Hiner, A. N. P.; Garcia-Canovas, F.; Thorneley, R. N. F. *J. Am. Chem. Soc.* **2001**, *123*, 11838.
(420) Meunier, B.; Bernadou, J. *Struct. Bonding (Berlin)* **2000**, *97*, 1.
(421) Filizola, M.; Loew, G. H. *J. Am. Chem. Soc.* **2000**, *122*, 18.
(422) Loo, S.; Erman, J. E. *Biochemistry* **1975**, *14*, 3467.
(423) Nissum, M.; Schiodt, C. B.; Welinder, K. G. *Biochim. Biophys. Acta* **2001**, *1545*, 339.
(424) Gajhede, M.; Schuller, D. J.; Henriksen, A.; Smith, A. T.; Poulos, T. L. *Nat. Struct. Biol.* **1997**, *4*, 1032.
(425) Xiao, Y. W.; Hutson, M. S.; Belenky, M.; Herzfeld, J.; Braiman, M. S. *Biochemistry* **2004**, *43*, 12809.
(426) Garczarek, F.; Brown, L. S.; Lanyi, J. K.; Gerwert, K. *Proc. Natl. Acad. Sci. U.S.A.* **2005**, *102*, 3633.
(427) Melo, A.; Ramos, M. J. *Chem. Phys. Lett.* **1995**, *245*, 498.
(428) Mehler, E. L.; Fuxreiter, M.; Simon, I.; Garcia-Moreno, E. B. *Proteins* **2002**, *48*, 283.
(429) Ishikita, H.; Saenger, W.; Loll, B.; Biesiadka, J.; Knapp, E. W. *Biochemistry* **2006**, *45*, 2063.
(430) Ishikita, H.; Knapp, E. W. *Biophys. J.* **2006**, *90*, 3886.
(431) Chen, K. S.; Bonagura, C. A.; Tilley, G. J.; McEvoy, J. P.; Jung, Y. S.; Armstrong, F. A.; Stout, C. D.; Burgess, B. K. *Nat. Struct. Biol.* **2002**, *9*, 188.
(432) Hoogstraten, C. G.; Britt, R. D. *RNA* **2002**, *8*, 252.
(433) Aullon, G.; Bellamy, D.; Brammer, L.; Bruton, E. A.; Orpen, A. G. *Chem. Commun.* **1998**, 653.
(434) Brammer, L.; Bruton, E. A.; Sherwood, P. *New J. Chem.* **1999**, *23*, 965.
(435) Hillier, W.; Wydrzynski, T. *Phys. Chem. Chem. Phys.* **2004**, *6*, 4882.
(436) Chu, H. A.; Nguyen, A. P.; Debus, R. J. *Biochemistry* **1995**, *34*, 5839.
(437) Pourbaix, M. *Atlas of Electrochemical Equilibria*; Pergamon Press: Oxford, U.K., 1966.
(438) Wood, P. M. *Biochem. J.* **1988**, *253*, 287.
(439) Koppenol, W. H.; Liebman, J. F. *J. Phys. Chem.* **1984**, *88*, 99.
(440) Hillier, W.; Wydrzynski, T. *Biochemistry* **2000**, *39*, 4399.
(441) Helman, Y.; Barkan, E.; Eisenstadt, D.; Luz, B.; Kaplan, A. *Plant Physiol.* **2005**, *138*, 2292.
(442) Haumann, M.; Junge, W. *Biochemistry* **1994**, *33*, 864.
(443) Atkinson, G.; Emara, M. M.; Fernande, R. *J. Phys. Chem.* **1974**, *78*, 1913.

CR0204294